Fall 2010

Control of the protein and lipid content of the plasma membrane by ATP-binding cassette transporter proteins in S. Cerevisiae

Soraya Sarah Johnson
University of Iowa

CONTROL OF THE PROTEIN AND LIPID CONTENT OF THE PLASMA MEMBRANE BY ATP-BINDING CASSETTE TRANSPORTER PROTEINS IN S. CEREVISIAE

by

Soraya Sarah Johnson

An Abstract

Of a thesis submitted in partial fulfillment
of the requirements for the Doctor of
Philosophy degree in Molecular and Cellular Biology
in the Graduate College of
The University of Iowa

December 2010

Thesis Supervisor: Professor W. Scott Moye-Rowley

ABSTRACT

Pdr5 and Yor1 are two ATP-binding cassette transporters regulated by the pleiotropic drug resistance (PDR) network in the yeast *Saccharomyces cerevisiae*. Recent work demonstrated that a *pdr5Δ yor1* strain confers remarkable resistance to a sphingolipid intermediate, phytosphingosine (PHS), which was surprising as loss of these transporters normally leads to elevated drug sensitivity.

PHS is toxic to the cell at high levels due to mislocalization of nutrient permeases, such as the high affinity tryptophan transporter, Tat2. Although the above study suggested that this resistance was due to increased expression of Rsb1, a known mediator of PHS tolerance, this was not reproducible in our hands and we sought to identify other determinants for this phenotype. The work presented here demonstrates that the *pdr5Δ yor1* strain exhibits delayed turnover of Tat2 and an increase in tryptophan uptake, which we postulate is due to changes in asymmetric phospholipid distribution of the plasma membrane, resulting in decreased endocytosis. Conversely, cells lacking Rsb1 showed a decrease in tryptophan import and increased Tat2 turnover, independent of endogenous PHS levels. Rsb1 has a predicted 7 transmembrane (7TM) topology, which argues against the idea that Rsb1 functions directly in PHS transport, as there are currently no known transporters with this topology. These data suggest that Rsb1 and Pdr5/Yor1 function in regulation of endocytosis of Tat2, and possibly other membrane proteins.

I discovered that *pdr5Δ yor1* strains were also highly tolerant of the sphingolipid biosynthesis inhibitor, Aureobasidin A (AbA). AbA represents a novel phenotype for *pdr5Δ yor1* strains and was used as a tool to find genes that are involved in the response to loss of Pdr5 and Yor1. Ethyl methanesulfonate

mutagenesis of the *pdr5Δ yor1* strain and a candidate gene approach were alternative methods used to identify mediators of AbA tolerance in this strain. These approaches revealed several genes, including Gda1, Mss4, and Ypk1 that are important for AbA tolerance in the *pdr5Δ yor1* strain. Many of these determinants play a role in cell wall integrity, suggesting that loss of Pdr5 and Yor1 may lead to activated cell wall integrity pathways resulting in altered cell wall structure.

Abstract Approved: _____
Thesis Supervisor

_____
Title and Department

_____
Date

CONTROL OF THE PROTEIN AND LIPID CONTENT OF THE PLASMA MEMBRANE BY ATP-BINDING CASSETTE TRANSPORTER PROTEINS IN S. CEREVISIAE

by

Soraya Sarah Johnson

A thesis submitted in partial fulfillment
of the requirements for the Doctor of
Philosophy degree in Molecular and Cellular Biology
in the Graduate College of
The University of Iowa

December 2010

Thesis Supervisor: Professor W. Scott Moye-Rowley

Graduate College
The University of Iowa
Iowa City, Iowa

CERTIFICATE OF APPROVAL

_____

PH.D. THESIS

_____

This is to certify that the Ph.D. thesis of

Soraya Sarah Johnson

has been approved by the Examining Committee
for the thesis requirement for the Doctor of Philosophy
degree in Molecular and Cellular Biology at the December 2010
graduation.

Thesis Committee:_____
W. Scott Moye-Rowley, Thesis Supervisor

_____
Adam Dupuy

_____
Robert Piper

_____
Dawn Quelle

_____
Mark Stamnes

To Bryon, Tresina, Mom, Dad, and Grandma

ACKNOWLEDGMENTS

I would like to thank Dr. Scott Moye-Rowley for his advice and guidance, and especially for his confidence in my ability to complete this venture. I would also like to thank the members of my thesis committee: Dr. Adam Dupuy, Dr. Rob Piper, Dr. Dawn Quelle, and Dr. Mark Stamnes for their helpful advice, discussions, and encouragement, as well as use of equipment and reagents.

I would also like to thank Dr. Pamela Hanson for her many contributions to my projects, especially for the work described in Chapter 2, as well as for numerous constructive discussions. I thank Sarah Brice and Dr. L. Ashley Cowart at the Medical University of South Carolina for their important contribution to the work in Chapter 2 as well. Thank you to Dr. Robert C. Dickson at the University of Kentucky for countless explanations and advice regarding sphingolipid analysis. I also thank Dr. Jan Fassler for her insightful suggestions and use of equipment.

Thank you to the current and former members of the Moye-Rowley lab with whom I have had the pleasure to work: Dr. Sneh Panwar, Dr.Kailash Gulshan, Dr. Puja Shahi, Dr. Sanjoy Paul, Dr. Raman Manoharlal, Sarah Bergeron, Stella Lee, and Jen Schmidt. I also thank my dear friends, Dr. Alok Shah, Dr. Audrey Dickey, and David Marion for their moral support and many good times had through the years of graduate school.

TABLE OF CONTENTS

LIST OF TABLES

LIST OF FIGURES

LIST OF ABBREVIATIONS

2μm	high-copy plasmid, contains 2μm circle
7 TM	7 transmembrane
AbA	Aureobasidin A
ABC	ATP-binding cassette
Aur1	Aureobasidin A resistance 1
Bst1	bypass of sec thirteen 1
Bul1/2	binds ubiquitin ligase 1 or 2
CEN	low-copy plasmid, centromere-containing
Csg2	calcium sensitive growth
CSM	complete supplement media
Cyc8	aka Ssn6 cytochrome c 8
Dpl1	dihydrosphingosine phosphate lyase 1
DRM	detergent-resistant membrane
eGFP	enhanced green fluorescent protein
EMS	ethyl methanesulfonate
Exo70	exocyst 70
Fpk1/2	FliPase kinase 1 or 2
Gap1	general amino acid permease
Gda1	guanosine diphosphatase
Gln3	glutamine metabolism
GPCR	G-protein coupled receptor
GPI	glycophosphatidylinositol
HePC	hexadecylphosphocholine
HPLC	high performance liquid chromatography
IPC	inositolphosphorylceramide

LCB	long chain base
LCBP	long chain base phosphate
$M(IP)_2C$	mannose di-inositolphosphorylceramide
MDR	multidrug resistance
MIPC	mannose inositolphosphorylceramide
Mss4	multicopy suppressor of stt4 mutation
Myr	myriocin
NBD	N-[7-(4-nitrobenzo-2-oxa-1,3-diazole)]
PC	phosphatidylcholine
PCR	polymerase chain reaction
PDR	pleiotropic drug resistance
Pdr1	pleiotropic drug resisitance 1
Pdr3	pleiotropic drug resistance 3
Pdr5	pleiotropic drug resistance 5
PDRE	pleiotropic drug resistance element
PE	phosphatidylethanolamine
PHS	phytosphingosine
$PI_{4,5}P_2$	phosphoinositide 4,5-bisphosphate
PI_4P	phosphoinositide 4-phosphate
Pkc1	protein kinase c
Pkh1/2	Pkb-activating kinase homologue 1 or 2
PM	plasma membrane
Pma1	plasma membrane ATPase 1
Rsb1	resistance to sphingoid base 1
SC	synthetic complete
SDS	sodium dodecyl sulfate
SDS-PAGE	SDS polyacrylamide gel electrophoresis

Sec3	secretory 3
Sfk1	suppressor of four kinase 1
Sjl1	synaptojanin-like 1
Stt4	staurosporine and temperature sensitive 4
TAP	tandem affinity purification
Tat2	tryptophan amino acid transporter 2
TLC	thin layer chromatography
Trp	tryptophan
Ure2	ureidosuccinate transport
Vph1	vacuolar pH 1
WT	wild-type
Yor1	yeast oligomycin resistance 1
YPD	yeast peptone dextrose
Ypk1/2	yeast protein kinase 1 or 2
Yrr1	yeast reveromycin resistance 1

CHAPTER I

INTRODUCTION

Multidrug resistance (MDR) is a common phenomenon that is conserved across species and is a major problem in the clinical arena. It is defined as the acquisition of tolerance to a diverse range of compounds, which have different intracellular sites of action. MDR is a particular problem in many types of mammalian cancers, which are able to evade the array of chemotherapeutic agents currently available for treatment. Furthermore, many opportunistic fungal pathogens, such as *Candida glabrata,* exhibit a high intrinsic resistance to several anti-fungal agents (1). Both of these phenomena are typically due to over-expression of ATP-binding cassette (ABC) transporter proteins, such as MDR1, which was the first ABC transporter identified in mammalian cells (2). ABC transporters consist of two sets of multiple transmembrane domains and two nucleotide binding domains, which allow for binding and hydrolysis of ATP, thus creating energy for outward movement of toxins. In the yeast, *Saccharomyces cerevisiae*, multidrug resistance is referred to as pleiotropic drug resistance (PDR).

The Pleiotropic Drug Resistance (PDR) Network

The baker's yeast, *S. cerevisiae*, has a very well understood network of proteins that function together in drug resistance, making it a great model organism in which to elucidate the physiological roles of this pathway. The PDR network is comprised of two major transcription factors and several ABC transporters. More recent studies have suggested that this network also includes several genes involved in the control of an important class of membrane lipids called sphingolipids (Figure 1).

There are two major PDR transcription factors, Pdr1 and Pdr3 which confer resistance to a broad range of compounds by up-regulating transcription of ABC transporters. Pdr1 and Pdr3 are zinc cluster transcription factors that share 33% identity (3). These factors bind to regions in the promoter of target genes known as pleiotropic drug response elements (PDREs). Pdr3 is present at a much lower intracellular concentration than Pdr1, however, its own promoter contains a PDRE, allowing it to be auto-regulated. A few of the known genes that are regulated by these factors include several ABC transporters, such as Pdr5 and Yor1, a 7 transmembrane receptor-like protein, Rsb1, as well as multiple genes involved in sphingolipid biosynthesis (3-5). Interestingly, ABC transporters are typically localized to lipid rafts or detergent-resistant membrane fractions, which are comprised mostly of sphingolipids and sterols (6). This led to the idea that by regulating sphingolipid metabolism, the PDR network is controlling not only the expression of ABC transporters but also the environment in which these proteins function.

ATP-binding Cassette (ABC) Transporters

ABC transporters are most commonly known to function in efflux of toxic compounds from the cell. The PDR network is comprised of many ABC transporters, two examples of which are Pdr5 and Yor1. Pdr5 is the major ABC transporter influencing drug resistance in the yeast, *Saccharomyces cerevisiae*. It was initially identified in a high copy screen for genes involved in resistance to multiple drugs, including cycloheximide (7). It is known to confer resistance to a myriad of compounds, including the anti-fungal fluconazole as well as several others (8-11). Yor1 (*Y*east *o*ligomycin *r*esistance) was first identified for its role in resistance to the mitochondrial ATPase inhibitor, Oligomycin (12). More recent

work also suggested that Yor1 is involved in tolerance to a sphingolipid biosynthesis inhibitor, Aureobasidin A (AbA) (13).

Interestingly, Pdr5 and Yor1 not only have functions in drug efflux, but also in movement of phospholipids. Both of these proteins function in “flop” or outward movement of phosphatidylcholine (PC) and phosphatidylethanolamine (PE) between the inner and outer leaflets of the plasma membrane (14). Movement of phospholipids by ABC transporters is conserved across species. Bacteria utilize ABC transporters in “flip-flop” movement of lipoproteins across the lipid bilayer (15). Multiple examples of this are also present in mammalian cells, including ABCB4, which is important in secretion of PC into bile, while ABCA4 is an ABC transporter found in the retina, which has been shown to move PE derivatives. Defects in ABCA4 function have been linked with macular degeneration (15). This conservation of function is suggestive of a physiological role in maintenance of lipid homeostasis.

While Pdr5 and Yor1 effect outward movement of PE and PC, there are also P-type ATPases, designated as DNF (*D*rs2 *N*eo1 *F*amily) proteins, in yeast that function in the reverse reaction, moving these phospholipids from the outer to the inner leaflet of the plasma membrane. These proteins are not transcriptionally regulated by the PDR pathway. However, DNF protein activity was recently demonstrated to be influenced by changes in complex sphingolipids (16). This suggests that there may be indirect control of flippases via PDR regulation of sphingolipid biosynthesis. Since plasma membrane asymmetry is tightly regulated, it is conceivable that alteration of Pdr5 and Yor1 may disturb important cellular processes that depend on the composition of the membrane.

Sphingolipid Biosynthesis and Functions

Sphingolipids are important players in membrane structure as well as intracellular signaling and formation of detergent-resistant membrane (DRM) fractions or lipid rafts. Lipid rafts and DRMs are important not only in delivery of certain proteins to the plasma membrane, but they are also required for appropriate endocytosis of proteins that are localized at these sites (17,18). Aberrant sphingolipid metabolism is associated with multiple diseases, including several types of cancer, heart disease, diabetes, and Alzheimer disease, making it crucial to better understand how these lipids are regulated (19).

Sphingolipids in yeast are first constructed by the condensation of serine and palmitoyl CoA by Lcb1/Lcb2 to make 3-ketodihydrosphingosine (Fig. 2) (20). This is then reduced by Tsc10 to make dihydrosphingosine (DHS), the first long chain base in the pathway (21). DHS is hydroxylated to form phytosphingosine (PHS), another bioactive sphingolipid intermediate (22). Both DHS and PHS can take two different routes after being synthesized. They can either be amide-linked to a very long chain fatty acid to form ceramides or they can be phosphorylated to form long chain base phosphates (LCBPs) (23,24). The long chain base phosphates are broken down by Dpl1, the long chain base phosphate lyase, into ethanolamine phosphate and fatty aldehydes (25). Ceramides are linked to an inositol phosphate to form inositol phosphorylceramide (IPC) by the IPC synthase complex containing Aur1 and Kei1 (26,27). IPC is modified by addition of mannose in the Golgi by Csg1, Csh1 and Csg2 to form mannose inositolphosphorylceramide (MIPC) (28,29). MIPC can be further modified to form $M(IP)_2C$ with addition of another inositol phosphate by Ipt1 (30). A simplified diagram of the sphingolipid biosynthesis pathway is depicted in Figure 2.

Long Chain Bases (LCBs) and Complex Sphingolipids

The long chain bases, DHS and PHS, as well as their phosphorylated derivatives function in intracellular signaling in addition to their role in formation of sphingolipids. Intracellular levels of these important lipids are tightly controlled by multiple mechanisms. Dpl1, as mentioned above, will break down phosphorylated derivatives of PHS and DHS. Another protein, Rsb1 (*R*esistance to *s*phingoid *b*ase) was cloned based on its ability to bypass the PHS sensitivity of a *dpl1Δ* strain when over-expressed (31). Loss of Rsb1 shows an increased sensitivity to exogenously added PHS. Further analysis indicated efflux of long chain bases from the cell was increased when Rsb1 was over-expressed and decreased when it was deleted (31). These data were interpreted to mean that Rsb1 functions as a transporter or translocase for long chain bases, suggesting further regulation of these lipid levels. Although it is clear that Rsb1 serves an important role in PHS tolerance, my work has indicated a novel mechanism for the action of Rsb1 during PHS stress and will be discussed further in Chapter 2.

PHS is toxic to cells, in part, because it causes nutrient transporters to mislocalize, moving to the vacuole rather than to their functionally relevant site at the plasma membrane (32,33). This is especially significant for auxotrophic strains, which require the presence of these nutrient permeases for viability. A majority of common laboratory strains contain multiple nutrient auxotrophies and therefore rely on nutrient transport for viability. Tryptophan auxotrophy is linked to the most pronounced PHS sensitivity, likely due to the fact that there is only one high affinity tryptophan permease in *S. cerevisiae*, Tat2 (34). Any defects in this single route for tryptophan uptake will cause cells to starve for this amino acid.

PHS has also been demonstrated to activate kinases involved in regulation of the heat stress response, actin cytoskeletal organization, exocytosis

and endocytosis. PHS was shown to activate the serine/threonine kinases Pkh1 and Pkh2 (*P*kb-activating *k*inase *h*omologue), which in turn activate Ypk1 (*Y*east *p*rotein *k*inase) (35). Other evidence suggested that PHS may also be able to activate Ypk1 and its homologue, Ypk2 directly (35). Much of the earlier work on PHS and Ypk1/2 activation could not distinguish between PHS or another sphingolipid as being the regulating lipid and was unable to determine whether the lipid itself was directly activating Ypk1 or if this was an indirect effect via Pkh1/2 (35). Recent work from the Thorner lab indicated that changes in the complex sphingolipid, MIPC, was partially responsible for indirect negative regulation of Ypk1 (16). MIPC activates another pair of kinases, Fpk1 and Fpk2, which activate the DNF phospholipid flippases, but also will inactivate Ypk1. Ypk1 is involved in many pathways, including cell wall integrity and sphingolipid-mediated signaling pathways as well as receptor-mediated endocytosis (36,37). Figure 3 depicts Ypk1 regulation discussed above. Many interactions between complex sphingolipids and other cellular pathways have recently been elucidated, suggesting that there are more intricate functions of these lipids than was previously appreciated.

Complex sphingolipids comprise approximately 30% of the plasma membrane lipids and are important in formation of detergent-resistant membrane fractions as well as in cell signaling (19). While some information is known about transcriptional regulation of the enzymes involved in this part of the sphingolipid pathway, much more has been elucidated regarding post-translational regulation. Csg2 (*C*alcium *s*ensitive *g*rowth), which is part of the complex responsible for making MIPC, is also regulated by calcium levels (28). High levels of calcium in the cell accelerate the conversion of IPC to MIPC (38). The reason for this is unknown, however it is speculated that either IPC becomes toxic under these conditions or that MIPC becomes rate limiting (38). Interestingly, a mutation in

Mss4, the PI_4P 5-kinase, was demonstrated to bypass the calcium sensitivity of a *csg2Δ* strain (39). The product of Mss4, $PI_{4,5}P_2$ is a key signaling molecule. Multiple cellular processes, including actin cytoskeleton reorganization, cell wall integrity, exocytosis, and complex sphingolipid metabolism are regulated by downstream effectors of $PI_{4,5}P_2$ (39-42). The adapter proteins, Slm1 and Slm2 are important intermediates in $PI_{4,5}P_2$ signaling. When activated (phosphorylated) the Slm proteins are involved in negative regulation of not only calcineurin, which is important in calcium signaling and regulation of Csg1 and Csg2, but also Isc1, a protein which functions in conversion of IPC to ceramide (Figure 4) (38). The above data suggest that the key to these interactions may be to maintain the amount of IPC in the cell, as accumulation of this sphingolipid is thought to be toxic at high levels. Intriguingly, other data argue that appropriate levels of MIPC are crucial for Mss4 localization and function (43). Loss of Csg2 (and therefore loss of the mannosylated sphingolipids) showed mislocalization and decreased activity of Mss4. These data taken together argue that there is cross talk between sphingolipids and phosphoinositides.

Interactions between the PDR Network and Sphingolipids

Although it is well established that the PDR network is involved in the cell's tolerance to a multitude of toxic compounds, this does not seem an adequate explanation for the physiological role of this pathway in the organism. As discussed above, some ABC transporters have functions in movement of phospholipids, suggesting a role in lipid homeostasis. To further contribute to this hypothesis, there have been several links made between players in the PDR network and proteins involved in sphingolipid biosynthesis and homeostasis. A microarray experiment conducted in the Goffeau lab indicated that IPT1 (the last

enzyme in sphingolipid biosynthesis) was up-regulated in a strain that contained a hyperactive form of the Pdr1 transcription factor (44). IPT1 contains a PDRE in its promoter region and is regulated by Pdr1 and Pdr3. This was the first indication that the PDR network might also regulate sphingolipids. Further analyses revealed several other genes involved in *de novo* sphingolipid biosynthesis that contained PDREs in their promoters: LCB2, SUR2, and LAC1 (Figure 5) (45). Additional evidence of links between the PDR network and sphingolipids came from a surprising discovery that loss of the ABC transporters, Pdr5 and Yor1, created an increased tolerance to high levels of the sphingolipid intermediate, phytosphingosine (PHS) (4). This resistance was attributed to up-regulation of Rsb1 because it is also PDR-regulated and was known to confer resistance to PHS, suggesting a possible feedback loop in the PDR network (4). These data provided more evidence of an alternative role for this pathway, beyond drug resistance.

The work presented in the following chapters focuses on elucidating the function of Rsb1, as well as an explanation for the observed increase in PHS tolerance of the *pdr5Δ yor1* strain. The prevailing theory for the PHS tolerance of a *pdr5Δ yor1* strain was an increase in expression of Rsb1 (4). However, while we saw the same resistance phenotype of the double mutant strain, we did not see increased Rsb1 expression (46). This led us to re-examine why this *pdr5Δ yor1* strain was resistant to PHS. The first hypothesis was that the tryptophan transporter, Tat2, was stabilized in this strain, due to changes in endocytosis resulting from altered plasma membrane phospholipid content.

It was also possible that another gene, possibly a transporter, was induced in this strain and was responsible for removal of PHS. An EMS screen was initiated to determine other players in PHS tolerance. However, PHS was too leaky to be used as a screening agent and alternative compounds that effect

sphingolipids were tested. Here I made the novel discovery that the *pdr5Δ yor1* strain is also robustly resistant to a drug called Aureobasidin A (AbA). AbA is a potent inhibitor of Aur1, a subunit of the IPC synthase complex (Figure 2). The EMS screen was done using AbA to determine novel mediators of resistance to this compound and candidates were cross-tested on PHS, as it was possible determinants for PHS and AbA tolerance could be the same. The following chapters will address these ideas in more detail.

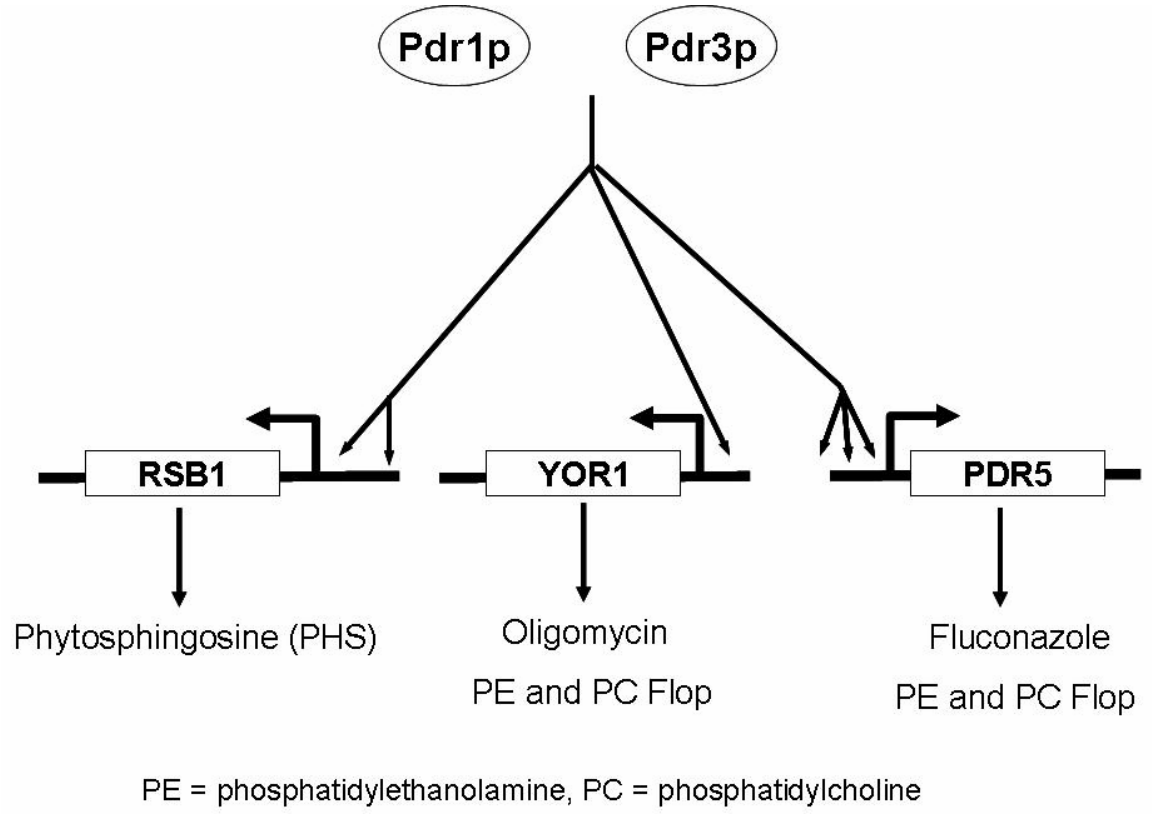

Figure 1. Diagram of the pleiotropic drug resistance (PDR) network. Pdr1 and Pdr3 are the two major transcription factors which bind to PDR response elements (PDREs) in the promoters of target genes, thereby increasing expression. Pdr5 (right) and Yor1 (middle) are localized to the plasma membrane and function in efflux of fluconazole and oligomycin, respectively. Both are also involved in outward movement of phosphatidylethanolamine (PE) and phosphatidylcholine (PC) between the inner and outer leaflets of the plasma membrane. Rsb1 (left) is also a plasma membrane localized protein, which functions in tolerance to the sphingolipid intermediate, phytosphingosine (PHS).

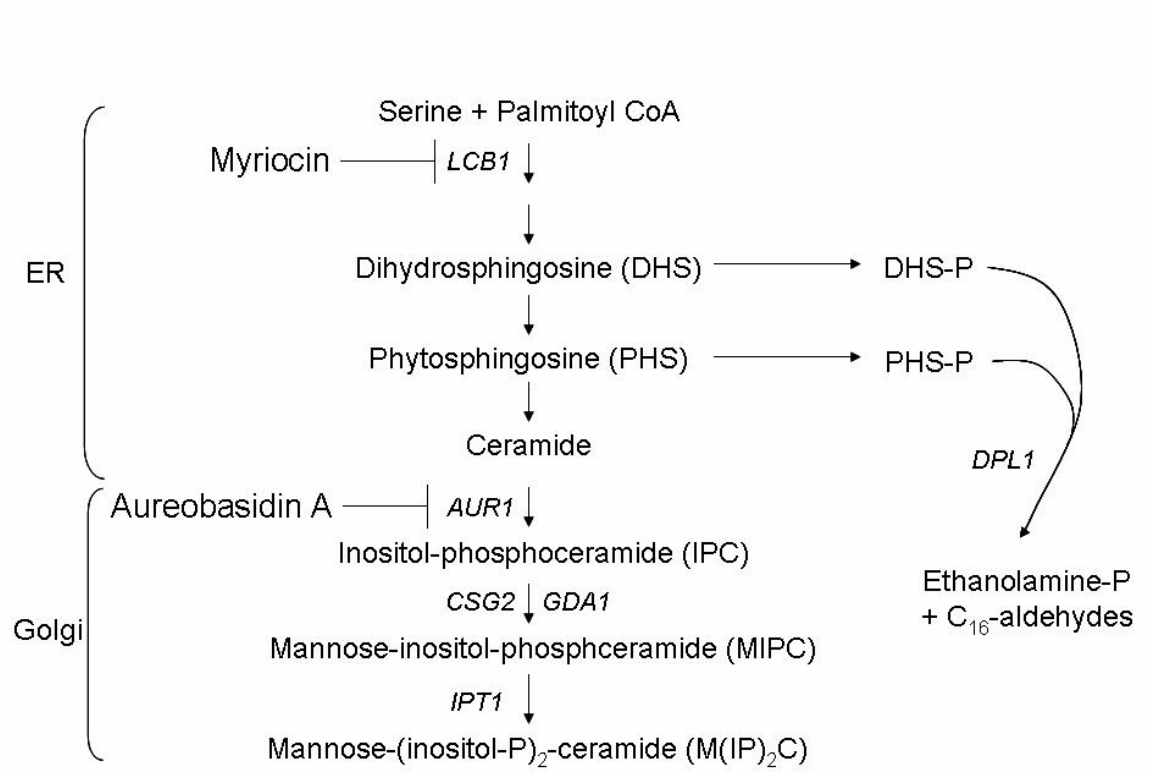

Figure 2. A simplified diagram of the sphingolipid biosynthesis pathway. The first step of *de novo* sphingolipid synthesis through the formation of ceramide occurs in the ER, while the complex sphingolipids are made and modified in the Golgi. Myriocin is an inhibitor of serine palmitoyl transferase and blocks synthesis from the first step. Aureobasidin A is an inhibitor of Aur1 (part of the IPC synthase complex).

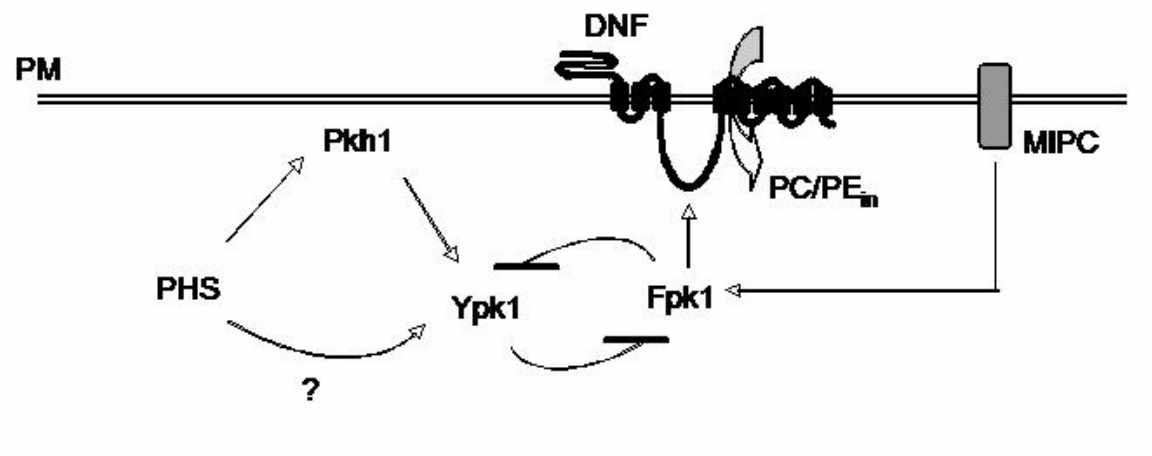

Figure 3. Ypk1 regulation. PHS is thought to activate Ypk1 either directly or via Pkh1. Ypk1 can also be inactivated by the Fpk1 kinase, which itself is inactivated by Ypk1, suggesting some sort of feedback loop. The complex sphingolipid, MIPC, has been shown to activate Fpk1, thereby stimulating flippase activity and decreasing Ypk1 activation.

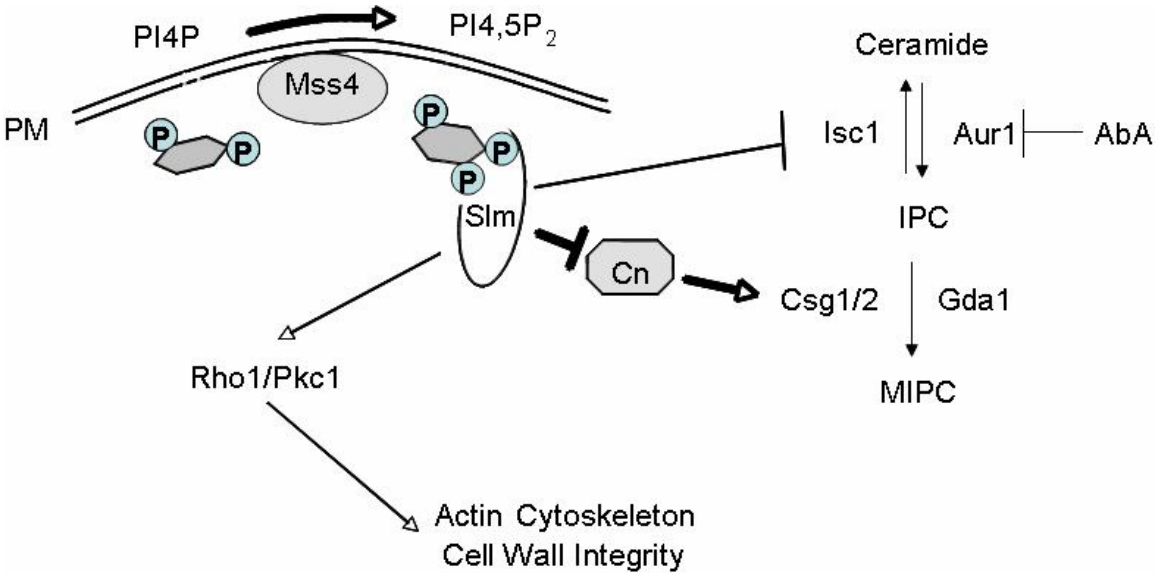

Figure 4. Mss4/ $PI_{4,5}P_2$ interactions with sphingolipid biosynthesis. The product of Mss4, $PI_{4,5}P_2$, interacts with the adapter proteins Slm1/2. The Slm proteins have been indicated to negatively regulate both calcineurin (Cn) and Isc1, a protein involved in complex sphingolipid catabolism. Calcineurin, in the presence of calcium, will activate the Csg1 and Csg2 proteins to stimulate production of MIPC. The activity of this downstream pathway is thought to modulate levels of IPC. Mss4 is also involved in other signaling pathways, including those that regulate actin cytoskeleton organization and cell wall integrity.

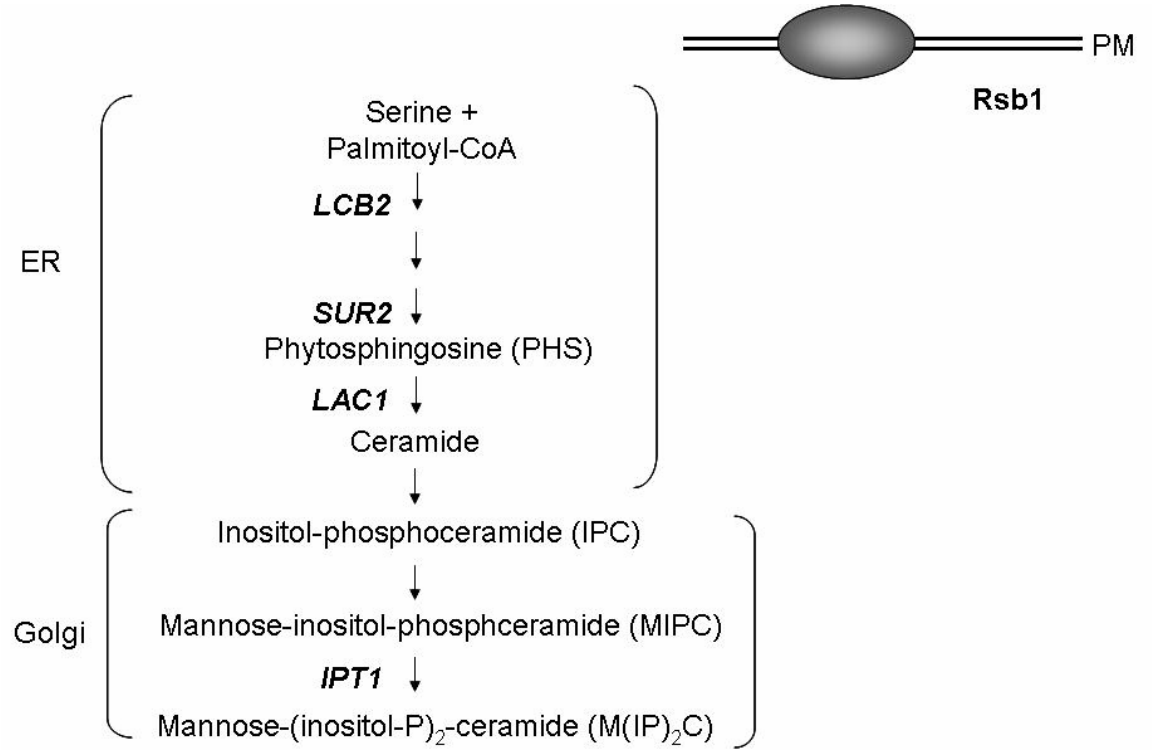

Figure 5. Interactions between the PDR network and sphingolipids. Several genes in the sphingolipid biosynthesis pathway indicated in **BOLD** type (LCB1, SUR2, LAC1, and IPT1) contain PDREs in their promoters and are regulated by the Pdr1 and Pdr3 transcription factors. Rsb1, a plasma membrane localized 7 TM receptor-like protein is also regulated by Pdr1 and Pdr3, and is important in tolerance of excess phytosphingosine (PHS), amongst other compounds.

CHAPTER II

REGULATION OF NUTRIENT PERMEASE ENDOCYTOSIS BY ABC TRANSPORTERS AND A SEVEN TRANSMEMBRANE RECEPTOR-LIKE PROTEIN, RSB1

Introduction

Sphingolipids represent one of the major components of the eukaryotic plasma membrane. Biosynthesis of these lipids proceeds through production of ceramide that is formed from the linkage of a long chain base (LCB) with a very long chain fatty acid. In the yeast *Saccharomyces cerevisiae*, one of the two LCBs produced *in vivo* is referred to as phytosphingosine (PHS) (See (47,48) for reviews). PHS is required for sphingolipid production but also has regulatory properties in terms of subcellular localization of proteins. Elevated levels of PHS cause mislocalization of nutrient permeases from the plasma membrane to the vacuole where these proteins are degraded (32,33). Regulation of PHS levels in the cell is tightly controlled and important to ensure normal metabolism.

One of the best described routes of PHS degradation is provided by the LCB-phosphate lyase Dpl1 (25). This enzyme breaks LCBPs into an aldehyde and ethanolamine phosphate limiting accumulation of LCBs *in vivo*. Strains lacking Dpl1 are hypersensitive to PHS. This phenotype was exploited to identify an integral membrane protein designated Rsb1 that suppressed the PHS hypersensitivity of a *dpl1Δ* strain (31). Evidence was presented that elevated levels of Rsb1 led to increased LCB efflux in cells. More recent work demonstrated that loss of the multidrug transporters Pdr5 and Yor1 from cells led to a strong increase in PHS tolerance (4). This increase was argued to be a

result of increased *RSB1* gene expression with accompanying elevation in Rsb1-mediated LCB transport activity.

Inspection of the predicted topology of Rsb1 suggests an alternative view to the idea that this membrane protein directly acts on PHS levels in cells. Rsb1 is predicted to have 7 transmembrane domains making it a potential member of the family of 7 transmembrane receptor (7 TM) proteins or G-protein-coupled receptors (recently reviewed in (49)). These membrane receptor proteins are well-known to serve as transducers of various signals but no examples are yet described in which these proteins possess a transporter activity. Rsb1 is localized to the plasma membrane and contains two N-linked glycosylation sites in its amino-terminus consistent with the topology expected for a 7 TM receptor protein (46).

Work from several labs has demonstrated that increased function of the high-affinity tryptophan transporter Tat2 influences PHS resistance (32,33,50). Since Rsb1 resembles a 7 TM receptor protein, we hypothesized that Rsb1 might influence Tat2 activity which in turn would stimulate PHS resistance. Screening *rsb1Δ* strains for phenotypes in addition to their already described PHS sensitivity revealed that these mutants are also sensitive to detergents and a lysophospholipid analogue. Direct measurements of LCB levels in these strains demonstrated that no Rsb1-dependent change in these sphingolipid intermediates was seen. Finally, *rsb1Δ* cells produced lower levels of plasma membrane-localized tryptophan transport activity. These data are consistent with the view that Rsb1 regulates Tat2 activity rather than levels of intracellular LCBs.

Strains lacking the plasma membrane ATP-binding cassette transporters Pdr5 and Yor1 were also hyper-resistant to the same compounds to which *rsb1Δ* strains were hypersensitive. The *pdr5Δ yor1* strains degraded Tat2 more slowly and maintained higher levels of this permease on the plasma membrane than did

wild-type strains. These findings suggest that endocytosis in *pdr5Δ yor1* strains is slowed compared to wild-type cells. Measuring endocytosis using the fluorescent FM4-64 dye demonstrated that bulk endocytosis is slowed in *pdr5Δ yor1* strains. We interpret these data to implicate Rsb1 and Pdr5/Yor1 as modulators of Tat2 endocytosis.

Experimental Procedures

Yeast strains and Media

The genotypes of yeast strains used in this study are listed in Table 1. Yeast transformations were performed using the lithium acetate procedure (51). Cells were grown in YPD (1% yeast extract, 2% peptone, 2% glucose) under non-selective conditions or appropriate SC media under selective conditions. Hexadecylphosphocholine (HePC) resistance, SDS, and low tryptophan tolerance was assessed by spot test assays on plates containing different concentrations of HePC (Avanti Polar Lipids, Inc), SDS, or tryptophan, respectively. PHS resistance was also determined by spot test assays on plates containing varying concentrations of PHS (Avanti Polar Lipids, Inc) as well as NP-40 as described previously (46).

To introduce the *rsb1Δ* allele, the rsb1::NatMX4 cassette containing 500bp flanking sequence, was removed by digestion from the TOPO 2.1 vector (pSLP2) and transformed into the *pdr5Δ yor1* strain and selected on nourseothricin (200 μg/ml). Primers *Rsb1* forward 5'-GACAGTGCGGCAATTGATAT-3' and Nat reverse primer –5'-ACACTGGTGCGGTACCGGTAA-3' were used.

SRY149, SRY150, and SRY156 were constructed by amplifying the *bul1::KanMX4* cassette from the BY4742 Open Biosystems strain with the forward primer 5'-GCGCCAGCGGCACTGGCGGT-3' and reverse primer 5'-GCATGCGAGATTTAATCGTT-3' and transforming SEY6210 wild-type, *rsb1Δ*,

and *pdr5Δ yor1* strains. These were selected on G-418 (150 μg/ml). These deletions were confirmed by PCR using the primers *Bul1* forward 5'-GCGTATCTGGCACTGGTCAA-3' with internal Kan B reverse primer 5'-CTGCAGCGAGGAGCCGTAAT-3' and the *Bul1* reverse primer 5'-TGGCAATGCAGCGTAATAAC-3' with the internal Kan C forward primer 5'-TGATTTTGATGACGAGCGTAAT-3'.

Plasmids

The *Tat2*-containing plasmid pSR74 was constructed by recombination of *TAT2* into the pRS316 plasmid containing the *CUP1* promoter, *MVB12*, and a 3x HA C-terminal tag (provided by Robert Piper), which was digested with EcoR1 and BglII to remove *MVB12*. *Tat2* was amplified with forward primer 5'-tagaagtcatcgaaatagatattaagaaaaacaaactgtaacgaattcataTGACCGAAGACTTTATTTC-3' and reverse primer 5'-gcccgcatagtcaggaacatcgtatgggtaaaagatgcggcccagatctttACACCAGAAATGGAACTGTC-3'. This amplicon was transformed into SEY6210 wild-type cells along with the digested MVB12 plasmid and selected on CSM –URA media. Plasmids were isolated and confirmed by digestion and sequencing. This plasmid was called pSR71. To facilitate microscopic visualization of Tat2, eGFP was inserted into this plasmid between *TAT2* and the 3xHA tag as a single C-terminal eGFP tag. eGFP was amplified from a previously constructed *Tat2*-GFP plasmid with forward primer 5'-cctagattcccgtccatggtacgtga gacagttccatttctggtgtaaagatcccTCTAAAGGTGAAGAATTATT-3' and reverse primer 5'-agggatagcccgcatagtcaggaacatcgtatgggtaaaagatgcggcccagatctttTTTGTCAATTCATCCATAC-3'. This amplicon was transformed into wild-type yeast with pSR71 plasmid digested with BglII (a unique site is present between the ORF and 3xHA tag) and recombinants were

selected on CSM –URA media. Plasmids were isolated using standard procedures and confirmed by digestion and sequencing.

To construct pSR86, pSLP8 was digested with PflF1 and Sma1 to gap the plasmid and the *RSB1* ORF from amino acids 41-334 was amplified with primers *Rsb1* forward 5'-TCATTTGGGGTATACTACTG-3' and *Rsb1* reverse 5'-tagtcaggaacatcgtatgggtaaaagatgttaattaacccggggatccgTTCAACATCGTCAGTATGTG-3' (lower case 50bp of 3xHA tag and upper case 20bp of *RSB1* ORF starting at amino acid 334). The PCR product and gapped plasmid were transformed into SEY6210 *rsb1Δ* and selected for gap repair on CSM –URA. Plasmids were isolated and electroporated into *E. coli*. Plasmids isolated from bacteria were confirmed by digestion and sequencing.

To construct pSR87, pSLP8 was digested with PflF1 and Sma1 to gap the plasmid and the *RSB1* ORF from amino acids 41-359 was amplified with primers *Rsb1* forward 5'-TCATTTGGGGTATACTACTG-3' and *Rsb1* reverse 5'-tagtcaggaacatcgtatgggtaaaagatgttaattaacccggggatccgCGGGTATTTCATGCTTGCTT-3' (lower case 50bp of 3xHA tag and upper case 20bp of *RSB1* ORF starting at amino acid 359). The PCR product and gapped plasmid were transformed into SEY6210 *rsb1Δ* and selected for gap repair on CSM –URA. Plasmids were isolated using standard procedures and electroporated into *E. coli*. Plasmids isolated from bacteria were confirmed by digestion and sequencing.

Tryptophan Transport Assays

Cells were cultured overnight in 10 ml of CSM+40μg/ml trp and diluted to OD_{600} of 0.25 in 30 ml of CSM + 40 μg/ml trp. Cells were grown to an OD_{600} 0.5-1.0 and 15 OD equivalents were harvested. Cells were washed in 2 ml 10 mM sodium citrate, pH 4.5 and resuspended in 4.5 ml assay buffer (10 mM sodium

citrate, pH 4.5, plus 2% glucose) at A_{600} ~3. Tritiated tryptophan was added at 2 μCi/ml, samples were mixed and 1ml samples were transferred to a 0.45-μm Durapore membrane filter (Millipore) which was equilibrated with 1-2 mls 10 mM sodium citrate. Filter was washed six times with 1 ml wash buffer (10 mM sodium citrate, pH 4.5, plus 2 mM tryptophan) per wash. Washed filter was transferred to a scintillation vial and allowed to air dry overnight. Procedure was repeated at ten minute intervals after addition of radiolabeled tryptophan. Liquid scintillation counting was used for quantification and values were expressed as counts per minute (cpm) per A_{600}. Tritiated tryptophan was from American Radiolabeled Chemicals, Inc.

Sphingoid base measurements

Yeast were grown to mid-log phase in YPD media and harvested by centrifugation. Frozen pellets were resuspended in water and sphingolipids were extracted by the method of Bligh and Dyer (52)), followed by mild alkaline hydrolysis. Extracts were derivatized with *o*-pthalaldialdehyde and resolved by HPLC as described (53) using C17 sphingosine as an internal standard.

Western analysis

For analysis of the Rsb1 truncation mutants, cells were grown to an A_{600} of 0.8-1 in CSM –URA and whole cell extracts were prepared using the TWIRL buffer (8M urea, 5% SDS, 10% glycerol, 50 mM Tris pH 6.8) extraction method. Briefly, 2 OD units of cells were resuspended in 60 μl of TWIRL buffer and vortexed for 1 minute with glass beads at 4°C and centrifuged for 5 minutes at 12k rpm at 4°C. Samples were electrophoresed on SDS-PAGE, transferred to nitrocellulose, and probed using monoclonal anti-HA antibody (1:1000) (Covance). The membrane was stripped and re-probed for the plasma membrane H+ ATPase, Pma1 (Invitrogen).

Cycloheximide Chase Assay

SEY6210 wild-type and SEY6210 *pdr5Δ yor1* strains were transformed with either pRS316 or pSR74. Overnight cultures were sub-cultured to an A_{600} of 0.15 and allowed to grow to an A_{600} of approximately 0.4-0.5. 2 OD units of cells were taken for time 0 and 75 μg/ml cycloheximide was added to each culture. Cells were grown for an additional 4 hours with samples taken at each 1 hour interval. At each time point, 2 OD units of cells were centrifuged, washed once with sterile water and frozen at -20°C until all samples were ready. Whole cell extracts were prepared by the TWIRL method (as described above). Proteins were electrophoresed on SDS-PAGE, transferred to nitrocellulose, and probed with anti-HA antibody.

Fluorescence Microscopy

GFP: Strains (same as for cycloheximide chase) transformed with pSR74 or empty vector control were grown overnight in CSM –URA, sub-cultured to an A_{600} of 0.15 in CSM –URA, then shifted to media containing 4 μg/ml tryptophan to starve the cells. After 6 hours of growth in low tryptophan conditions, a 500μl sample was harvested, washed in water, and resuspended in SC azide buffer. Cells were visualized for GFP fluorescence and Nomarski optics using an Olympus (Tokyo, Japan) BX-60 microscope with a 100X oil objective. Images were captured using a Hamamatsu (Shizuoka, Japan) ORCA charge-coupled device camera.

FM 4-64 Chase Analysis: Overnight cultures were diluted to an A_{600} of 0.15 in 5 ml of YPD and grown to an A_{600} of 0.8-1.0. Cultures were harvested and resuspended at 20 OD units/ml in YPD. These samples were chilled on ice for 20 minutes. FM 4-64 dye was added to these chilled samples, which were then rotated at 4°C for 45 minutes. Samples were washed with cold water and

resuspended at 10 OD units/ml in pre-warmed YPD and kept at 30°C. At indicated time points, samples were harvested, washed in cold SC-Azide buffer and visualized as described above for GFP analysis. Pixel quantification was done using Image J. The number of pixels per area in vacuoles and whole cells were calculated using Image J, analyzed, and expressed as a percentage of pixels in the vacuole and as compared to the whole cell.

Results

Rsb1 was first isolated and characterized on the basis of its effect on resistance to the long chain base (LCB) phytosphingosine (PHS) (31). Interestingly, this initial observation has been expanded to demonstrate that PHS resistance was strongly induced in a strain lacking the genes encoding the plasma membrane ATP-binding cassette (ABC) transporters Pdr5 and Yor1 (4). While much of the study of Rsb1 has focused on its importance in PHS tolerance given the hypothesis that this protein may act as a LCB translocase (31), we wondered if this protein might have a less direct action on the phenotype of PHS resistance. Work from other labs has indicated that the sensitivity to PHS phenotype may be due to an effect on trafficking of the high affinity tryptophan permease, Tat2, to the vacuole instead of the plasma membrane (32,33). Briefly, high level PHS diverts Tat2 to the vacuole, leading to a deficit in tryptophan uptake in these cells. Since many laboratory *Saccharomyces cerevisiae* strains are tryptophan auxotrophs, diverting the tryptophan transporter away from its functionally relevant site at the plasma membrane leads to starvation for this aromatic amino acid.

Along with PHS, many other compounds and conditions have been found to act in large part through an effect on tryptophan transport. For example, resistance to regimens of high pressure, rapamycin treatment and quinine

exposure are all limited by the ability to normally transport tryptophan into the cell (54-56). Importantly, PHS resistance of a Trp+ strain is much greater than a Trp- strain (33), again placing tryptophan transport at the center of many different stresses. While on sabbatical, Dr. Pamela Hanson screened a collection of different compounds to evaluate their ability to influence cell growth by potentially interfering with tryptophan transport to test if the effects of PHS were specific to this sphingolipid precursor or if many different compounds could phenocopy this behavior. Our standard laboratory wild-type strain was transformed with low-copy-number plasmids containing either the *URA3* or *TRP1* genes. Transformants were then compared for the ability to grow on medium containing the compounds indicated in Figure 6. While many compounds were screened, data for two are presented here: the strong detergent SDS and hexadecylphosphocholine (HePC aka miltefosine (57)).

The Trp+ strain was better able to grow in the presence of these compounds than the Ura+ transformant. Since all these compounds behaved in a manner similar to PHS (less effective on Trp+ strains), we wanted to determine if mutants with known PHS phenotypes would behave similarly in response to challenge with these other compounds. Wild-type, *rsb1Δ*, *pdr5Δ yor1* and *pdr5Δ yor1 rsb1Δ* cells were grown to mid-log phase and placed on media containing various concentrations of PHS, SDS or HePC (Figure 7)

Loss of *RSB1* caused hypersensitivity to PHS while disruption of *PDR5* and *YOR1* led to pronounced PHS resistance as previously reported (4). The same relative behavior was seen when these strains were placed on media containing either HePC or SDS. Importantly, the effects of Rsb1 loss could be strongly suppressed by removal of Pdr5 and Yor1. This is most consistent with Rsb1 and Pdr5/Yor1 acting in different pathways to influence resistance.

To assess the likelihood that the different phenotypes seen for *rsb1Δ* and *pdr5Δ yor1* cells could be explained by an issue with tryptophan transport, I tested the ability of these same strains to grow on progressively limiting concentrations of tryptophan in the medium. Strains were grown as above but placed on minimal medium containing the indicated levels of tryptophan (Figure 7D).

At high levels of tryptophan, all strains grew equally. However, as the tryptophan concentration in the medium was reduced, *rsb1Δ* cells failed to grow at 10μg/ml, which was a concentration tolerated by the other strains. Further lowering the tryptophan concentration to 6μg/ml caused a major growth defect in wild-type cells while the *pdr5Δ yor1* strains, containing or lacking Rsb1, were not significantly inhibited. Strikingly, the phenotypic behavior of this set of strains was remarkably similar across these four different growth regimens. These data are consistent with the view that a major contributor to the phenotypes seen in strains lacking Rsb1 or Pdr5/Yor1 is caused by changes in tryptophan transport. To directly test this hypothesis, tryptophan uptake was measured in these same strains.

Changes in tryptophan transport correlate with the observed tryptophan sensitivity of *rsb1Δ* and *pdr5Δ yor1* strains

The data above suggests that *rsb1*Δ cells have less ability to take up tryptophan from the media, as they are unable to grow on low levels of exogenous tryptophan. To test this idea, wild-type and *rsb1*Δ strains were grown in minimal media to mid-log phase and tryptophan transport assays were performed. The *rsb1*Δ strain showed a decreased rate of transport at 0.012 relative tryptophan uptake per minute as compared to wild-type which had

relative tryptophan uptake per minute of 0.02 (Figure 8B). This same experiment was conducted with wild-type and *pdr5Δ yor1* strains since the above data also suggested that there is increased uptake of tryptophan in the *pdr5Δ yor1* strain. The *pdr5Δ yor1* strain showed a significant increase in transport with a relative tryptophan uptake per minute of 0.032 as compared to the wild-type which had a relative uptake per minute of 0.02 (Figure 8A). These data suggest that the *pdr5Δ yor1* strain may have increased levels of the high-affinity tryptophan transporter, Tat2, at the plasma membrane. These experiments support the view that Rsb1 acts as a positive regulator of tryptophan transport while Pdr5 and Yor1 serve as negative regulators of uptake of this amino acid. The tryptophan transport analyses were completed by Pamela Hanson.

PHS levels are not altered in the absence of Rsb1 or Pdr5 and Yor1

While the data above indicate that changes in tryptophan transport, in the absence of exogenously added PHS, may be sufficient to explain the phenotypes caused by loss of Rsb1 and Pdr5/Yor1, it is also possible that loss of these proteins influences endogenous PHS levels. For example, if *rsb1Δ* cells had an elevated intracellular PHS pool, then this in turn could cause mislocalization of Tat2 with the attendant effects on tryptophan transport. Similarly, loss of Pdr5 and Yor1 might lead to lowered intracellular PHS which could stimulate Tat2 delivery to the plasma membrane.

To directly assess this alternative possibility, Sarah Brice and Ashley Cowart at the Medical University of South Carolina measured levels of intracellular LCBs in these strains by HPLC as described above. Deletion of *RSB1* had no effect on constitutive levels of C18 or C20 phytosphingosine, or C18 dihydrosphingosine (C20 dihydrosphingosine was undetectable in this

background strain). Similarly, deletion of *PDR5* and *YOR1* did not affect sphingoid bases. These data argue strongly against a role for these genes in regulation of intracellular sphingoid base levels.

A role for Rsb1 in sphingoid base efflux from cells was previously suggested (31). Thus, while deletion of *RSB1* alone did not increase sphingoid bases, as would be expected given this former hypothesis, it might be possible that a role in regulating sphingoid base levels might be more easily detected under conditions which aberrantly increase sphingoid base levels. Thus, to better determine whether Rsb1 plays a role in regulating intracellular sphingoid bases, we utilized a strain deleted in the sphingoid base phosphate lyase, *DPL1*. Since this strain lacks a key enzyme in sphingolipid degradation, it accumulates high levels of long chain bases. This was confirmed in our hands (Figure 9). However, deletion of *RSB1* in this strain did not change phytosphingosine levels, and showed only a modest decrease in dihydrosphingosine levels. We conclude that regulation of endogenous sphingoid base levels does not seem to be a key role for Rsb1. The effect of Rsb1 on Tat2 and tryptophan transport most likely occurs through other mechanisms.

Turnover of Tat2 is decreased in the absence of Pdr5 and Yor1

Together, the data above support the view that Rsb1 and Pdr5/Yor1 regulate Tat2-mediated tryptophan transport activity. Tat2 regulation can occur at the transcriptional as well as post-translational level (58). To simplify analysis of Tat2 regulation, we constructed a gene fusion in which the *TAT2* coding sequences were placed under regulation of the well-studied *CUP1* promoter. *CUP1* transcription can be induced with the addition of copper to the medium, providing a means to study post-translational regulation of Tat2 without

interference from potential transcriptional regulatory inputs. Additionally, Tat2 sequences were fused to eGFP sequences which in turn contained a 3X HA epitope tag at the C-terminal end of the fusion protein. This hybrid protein allowed facile detection of subcellular distribution of Tat2 by fluorescence microscopy and efficient detection via the epitope tags. The chimeric Tat2 protein was functional for tryptophan transport as it was able to elevate PHS resistance and low tryptophan tolerance of wild-type cells when overproduced (Figure 10A).

Previous work has shown that Tat2 follows the typical itinerary of a plasma membrane nutrient permease (55,59). Under conditions of low substrate, in this case tryptophan, Tat2 is delivered to the plasma membrane where it acts to facilitate tryptophan transport. When tryptophan levels are high, Tat2 is targeted to the vacuole for degradation. To estimate if Tat2 delivery to the vacuole was slowed in a *pdr5Δ yor1* strain, I carried out a cycloheximide chase assay using the *CUP1*-driven Tat2-eGFP-3X HA protein. Transformants of wild-type or *pdr5Δ yor1* cells were grown to mid-log phase, 75 μg/ml of cycloheximide added and samples were removed at one hour intervals after addition of this translational inhibitor. Protein extracts were prepared and analyzed for loading by staining with Ponceau S and for levels of Tat2-eGFP-3X HA by Western blotting using an anti-HA epitope antibody (Figure 10B).

Levels of epitope-tagged Tat2 were detectable at higher levels in the *pdr5Δ yor1* background compared to wild-type cells. This stabilization was pronounced at the later time points in which Tat2 levels in wild-type were much reduced compared to those seen in the *pdr5Δ yor1* strain. Estimates of the $t_{1/2}$ carried out by quantification of Western data indicated an approximate half-life of 90 minutes for Tat2 turnover in wild-type cells with this increasing to 266 minutes

in *pdr5Δ yor1* cells. The percentage of Tat2 remaining over time for both wild-type and *pdr5Δ yor1* cells is shown in Figure 10C.

These data support the view that Tat2 is delayed in its arrival at the vacuole in *pdr5Δ yor1* cells. To determine if there is a change in Tat2 subcellular distribution in this mutant background, we examined localization of this nutrient permease using the covalently linked eGFP probe.

Plasma membrane localization of Tat2 is increased in the *pdr5Δ yor1* strain

The above data support the idea that Tat2 is stabilized at the plasma membrane in the absence of Pdr5 and Yor1, thereby explaining both the enhanced growth on low levels of tryptophan and increased Tat2 stability. To test this prediction, wild-type and *pdr5Δ yor1* strains were transformed with a plasmid expressing Tat2-eGFP-3X HA or empty vector control. Transformants were grown in minimal media containing a high level of tryptophan (>20 μg/ml) to mid-log phase. These cultures were then shifted to media containing a low concentration of tryptophan (4 μg/ml). Six hours after the shift, cells were washed and visualized for GFP fluorescence (Figure 11).

Figure 11 shows an increased amount of Tat2-GFP at the plasma membrane in the *pdr5Δ yor1* strain as compared to the wild-type strain. This analysis provides further evidence that loss of the plasma membrane ABC transporter Pdr5 and Yor1 inhibit the endocytosis of Tat2. To determine if this decrease in turnover was specific to Tat2 or a more general slowing of endocytosis, we used a well-characterized probe of yeast endocytosis, FM4-64 (60). Wild-type and *pdr5Δ yor1* strains were labeled with FM4-64 for 45 minutes at 4°C, excess dye removed by washing the cells and then chased with fresh media at 30°C for the indicated times. Distribution of the dye was assessed by

fluorescence microscopy (Figure 12). This same experiment was carried out in the *rsb1Δ* strain, though there was no detectable difference as compared to wild-type. I compared the intensity of fluorescence in the vacuoles compared to the entire cell through the use of Image J software (http://rsbweb.nih.gov/ij/). Pixels were quantified inside a circle corresponding to the vacuolar membrane and compared to the total fluorescence detected for a circle enclosing the cell to generate the vacuolar pixel fraction (Figure 12B).

Within 30 minutes, more than 40% of FM4-64 fluorescence was detectable on the vacuolar membrane of wild-type cells. In cells lacking Pdr5 and Yor1, only 24% of FM4-64 was found on the vacuolar membrane. These data provide evidence that these ABC transporter proteins are required for normal bulk endocytic rates, not only internalization of Tat2.

Interaction of Rsb1 and Pdr5/Yor1 with the ubiquitin ligase adaptor protein Bul1

Previous experiments have implicated the Rsp5 adaptor protein Bul1 in controlling the endocytosis of Tat2 and other nutrient permeases (61,62). Loss of Bul1 along with other Rsp5 adaptor proteins, known as arrestins (reviewed in (63)), led to a pronounced retention of Tat2 on the plasma membrane (64). To determine if Bul1 regulation of Tat2 endocytosis might interact with the effects of Pdr5/Yor1 and/or Rsb1 on Tat2 described above, the *BUL1* gene was deleted from these genetic backgrounds. Representative mutant strains were grown to mid-log phase and tested for the ability to tolerate PHS challenge by placing equal numbers of cells on medium containing various concentrations of this LCB. Plates were allowed to develop at 30°C and then photographed (Figure 13).

Loss of Bul1 caused a dramatic increase in PHS resistance. This effect has been seen before for both PHS resistance and also tolerance to the

immunosuppressant FTY720 (50). Combining a *bul1Δ* allele with the *pdr5Δ yor1* mutant background increased PHS resistance to a level greater than either starting mutant strain alone. This finding suggested that the effect of Bul1 and Pdr5/Yor1 define two separate pathways controlling activity of Tat2. Finally, the PHS sensitivity caused by the *rsb1Δ* allele could be fully suppressed by deleting *BUL1*. This result suggests that Rsb1 may act through Bul1 to inhibit Tat2 endocytosis.

Role of the C-terminus of Rsb1 in control of PHS resistance

Earlier models suggested that Rsb1 might act as a translocase or transporter (31). Our *in silico* analyses of Rsb1 provided a different possibility. Topological predictions by programs such as Griffin (http://griffin.cbrc.jp/) or RbDe (http://icb.med.cornell.edu/crt/RbDe/Rbde.xml) led to structural models for Rsb1 resembling the well-known 7 transmembrane (7 TM) receptor superfamily, most often associated with G-protein coupled receptor proteins (Figure 14A). Since there are no examples of 7 TM receptor proteins behaving as direct mediators of transport to our knowledge, we hypothesized that Rsb1 might carry out a regulatory role. Furthermore, 7 TM receptor proteins are known to often be regulated by modulation of their cell surface residence after ubiquitination on their cytoplasmic C-terminal domains.

To begin the structure-function analysis of Rsb1, I constructed two different C-terminal truncation mutant variants. Wild-type Rsb1, which contains 382 amino acids was shortened to either 360 or 335 amino acids. These proteins, termed Rsb1ΔC360 or Rsb1ΔC335, were expressed with a 3X HA epitope tag inserted at their new C-termini. Low-copy plasmids expressing each of these truncation mutants, along with wild-type and empty vector controls, were

transformed into a *rsb1Δ* strain. A wild-type yeast strain was transformed with the empty vector to serve as a control for the wild-type chromosomal copy of *RSB1*. Transformants were grown to mid-log phase, placed on medium containing various concentrations of PHS and analyzed by Western blotting using an anti-HA antibody (Figure 14).

Removal of the C-terminal 22 residues of Rsb1 to form the Rsb1ΔC360 protein reduced but did not eliminate function as this protein was still able to partially complement the PHS sensitivity of the *rsb1Δ* strain. Interestingly, the steady-state level of this mutant protein was significantly greater than that of the wild-type polypeptide. Rsb1ΔC360 exhibited both the glycosylated (>64 kD) and the unglycosylated species (~37 kD) that were present in elevated amounts compared to the wild-type protein. This same behavior was seen for the Rsb1ΔC335 mutant, although the glycosylated form of this mutant was less abundant than that of the Rsb1ΔC360 protein.

One possible function of Rsb1 is that of a G-protein coupled receptor as mentioned above. To test this idea, *GPA2*, one of two G-alpha subunit encoding genes in *S. cerevisiae*, was deleted in the wild-type strain and assessed for a phenotype on PHS. Loss of *GPA2* showed a slight elevation in PHS tolerance at 7.5μM as compared to wild-type (Figure 14D). This result suggests that Gpa2 may have a negative role in PHS resistance, which is inconsistent with the idea that it functions downstream of Rsb1. However it is possible that Rsb1 could act via Gpa1 or, more likely, it may function in G-protein independent signaling.

These data implicate the C-terminus of Rsb1 as a regulator of the steady-state levels of this protein. The increased levels of Rsb1 in mutants lacking the complete C-terminus are consistent with a role for this protein domain in the endocytosis and eventual turnover of this plasma membrane protein. Further work is required to substantiate this idea.

Discussion

The identification of Rsb1 as a determinant of PHS resistance led to the understandable focus on the role of this membrane protein as a potential transporter of this LCB. PHS is a naturally occurring intermediate in sphingolipid biosynthesis but can be toxic at high levels. An informative feature of this PHS toxicity is its dependence on tryptophan auxotrophy. Loss of tryptophan prototrophy dramatically increases the sensitivity to PHS (33). This type of dependence on tryptophan prototrophy has been noticed before for a range of phenotypes (reviewed in (65)) and led us to consider that there might be a relationship between Rsb1 and control of tryptophan transport, rather than directly on efflux of LCBs. We argue that Rsb1 serves a regulatory function in Tat2-dependent tryptophan uptake based on the findings reported here. First, *rsb1Δ* cells have a range of phenotypes other than PHS sensitivity. Second, loss of Rsb1 caused no detectable accumulation of PHS in cells. Third, the topology of Rsb1 is most consistent with the structure of a 7 TM receptor rather than a transporter. Strikingly, while the 7 TM receptor family of membrane proteins is one of the largest known in biology, no protein with this topology has been shown to serve as a transporter/translocase. Together, these observations are more consistent with a role for Rsb1 as a regulator of membrane dynamics rather than a direct determinant of lipid distribution.

Loss of the phospholipid floppase activities mediated by the ABC transporters Pdr5 and Yor1 at the plasma membrane was previously described to strongly elevate PHS tolerance (4). While previous experiments argued that this elevation proceeded exclusively through Rsb1, these studies used strains that lack the long chain base-phosphate lyase Dpl1. This enzyme plays a major role in degradation of LCB metabolites (25). Our analysis of the epistasis of Rsb1 and Pdr5/Yor1 indicates that, although Rsb1 is a key contributor to PHS

resistance, loss of Pdr5/Yor1 still increased PHS tolerance, even if the *rsb1Δ* allele was present (Figure 7). We interpret these observations to indicate that Rsb1 and Pdr5/Yor1 actions influence PHS tolerance via different pathways.

The demonstration that both Rsb1 and Pdr5/Yor1 activities modulate levels of Tat2 transport provides a simplifying theme for an important role of these proteins. We propose that Rsb1 inhibits endocytosis while Pdr5 and Yor1 enhance this process. The exquisite sensitivity of tryptophan auxotrophs to levels of Tat2 function, which has been commented on before (61), makes tryptophan transport a faithful reporter of the endocytic regulatory influences exerted by Rsb1 and Pdr5/Yor1. The finding that internalization of the FM4-64 dye probe is also delayed by loss of Pdr5 and Yor1 indicates that, while Tat2 provides a useful phenotype to follow here, the effects of these regulatory proteins extend beyond control of this tryptophan transporter.

Considering Rsb1 as a 7 TM receptor also influences models for the actions of the related gene products in *S. cerevisiae*. Three Rsb1 homologues are encoded by the *S. cerevisiae* genome. Pug1 is a Rsb1 homologue which has recently been found to influence uptake of heme derivatives (66). Pug1 is found at the plasma membrane and detected as a 60 kD protein in Western blots of SDS-PAGE; although predicted from its DNA sequence to encode a protein of 33 kD. This is similar to the observed behavior of Rsb1 and consistent with both of these related proteins serving as plasma membrane glycoproteins that regulate membrane transport processes. The other two Rsb1 homologues, Rta1 and Ylr046c, are more poorly characterized. Rta1 confers resistance to a sterol analogue (67) while no phenotypes have been associated with Ylr046c. An interesting feature of both *RTA1* and *YLR046c* is that these genes are transcriptional regulatory targets of the pleiotropic drug resistance network (reviewed in (68)). *RTA1* is a direct transcriptional target of Pdr1/Pdr3 while

YLR046c is controlled by the Yrr1/Yrm1 factors (69). No evidence is yet available suggesting that *PUG1* is a member of the Pdr network but the co-regulation of the other three members suggests an intimate association of these proteins with the response to drug challenges.

One of the defining features of the large family of 7 TM receptors is the signaling between these integral membrane receptors and downstream heterotrimeric G-proteins (reviewed in (70)). *S. cerevisiae* contains two α-subunit-encoding genes, *GPA1* and *GPA2*, which have been linked to signaling via the GPCR homologues Ste2/3 (see (71) for a review) or Gpr1 (recently reviewed in (72)). Ste2/3 represent the mating pheromone receptors in S. cerevisiae while Gpr1 is involved in glucose signaling. Disruption of *GPA2* has little effect on PHS resistance (Figure 14D). Recent analyses of downstream signaling from Ste2/3 have demonstrated a link between these pheromone-induced GPCRs and endosomal function that converges on the kinase Vps15 (73). However, since the effect of Gpa1 signaling is restricted to Vps15 (and its partner Vps34 (74)), and while many *VPS* genes are involved in endosomal function, we doubt that this pathway is involved in Rsb1 signaling, although this has yet to be determined.

Since no strong evidence can be derived from the literature that classical G-protein signaling is involved in downstream function of Rsb1, we hypothesize that this protein might act to control endocytosis through an arrestin-mediated mechanism. Arrestins act to deliver ubiquitin ligases to target membrane proteins (reviewed in (75)). The finding that loss of the Bul1 arrestin-like adapter protein both elevated PHS resistance alone and suppressed the PHS sensitivity of an *rsb1Δ* strain is consistent with Rsb1 acting upstream of this protein. We hypothesize that Rsb1 acts to antagonize Bul1 function and it is this antagonism that leads to the observed phenotypic effects caused by loss of Rsb1 or Bul1

respectively. The simplest interpretation of the interaction of Rsb1 and Bul1 is that these two proteins act in the same pathway. This is in contrast to the behavior of Rsb1, Bul1 and Pdr5/Yor1. Loss of Bul1 or Pdr5/Yor1 increased PHS tolerance but the triple mutant combination was more resistant to LCB exposure than either strain alone. This additive behavior is most consistent with Bul1 and Pdr5/Yor1 defining two separate pathways that act to control Tat2 plasma membrane localization.

G-protein independent signaling as a result of activation of 7 TM receptor proteins is emerging as an important theme in the downstream function of these regulatory proteins (76). 5-hydroxytryptamine receptors have been found to couple to the non-receptor tyrosine kinase Src (77) or calmodulin (78) and signal in a fashion that is G-protein independent. Interestingly, calmodulin binding acts to recruit β-arrestin proteins to the 5-hydroxytryptamine$_{2C}$ receptor (77). Earlier work on the β2-adrenergic receptor demonstrated that this 7 TM receptor protein could activate the ERK MAP kinase pathway even in the absence of normal levels of the Gα protein or β-arrestin (reviewed in (79)). Together, these data indicate that 7 TM receptor proteins can couple to a variety of downstream signaling systems other than the classical G-protein pathways. Identification of the regulators of Rsb1-dependent signaling will provide important new information on the links between lipid composition and regulation of endocytosis.

Table 1. Strains and plasmids used in this study

Strain	Genotype	Ref.
SEY6210	MATα *leu2-3,-112 ura3-52,lys2-801 trp1-901 his3-200 suc2-9 Mel-*	Scott Emr
SEY6210 Δpdr5 yor1	SEY6210 *pdr5::hisG yor1::hisG*	Moye-Rowley Lab Collection
SEY6210 Δrsb1	SEY6210 *rsb1::natMX4*	(46)
SRY5	SEY6210 *pdr5::hisG yor1::hisG rsb1:natMX4*	This study
SRY149	SEY6210 *bul1::kanMX4*	This study
SRY150	SEY6210 *rsb1::natmX4:bul1::kanMX4*	This study
SRY156	SEY6210 *pdr5::hisG:yor1::hisG:bul1::kanMX4*	This study
Plasmid	Plasmid Description	
pSLP8	pRS316-Rsb1-3xHA	(46)
pSR74	pRS316-Cup1-Tat2-GFP-3xHA	This study
pSR86	pRS316-Rsb1Δ335-382-3xHA	This study
pSR87	pRS316-Rsb1Δ360-383-3xHA	This study

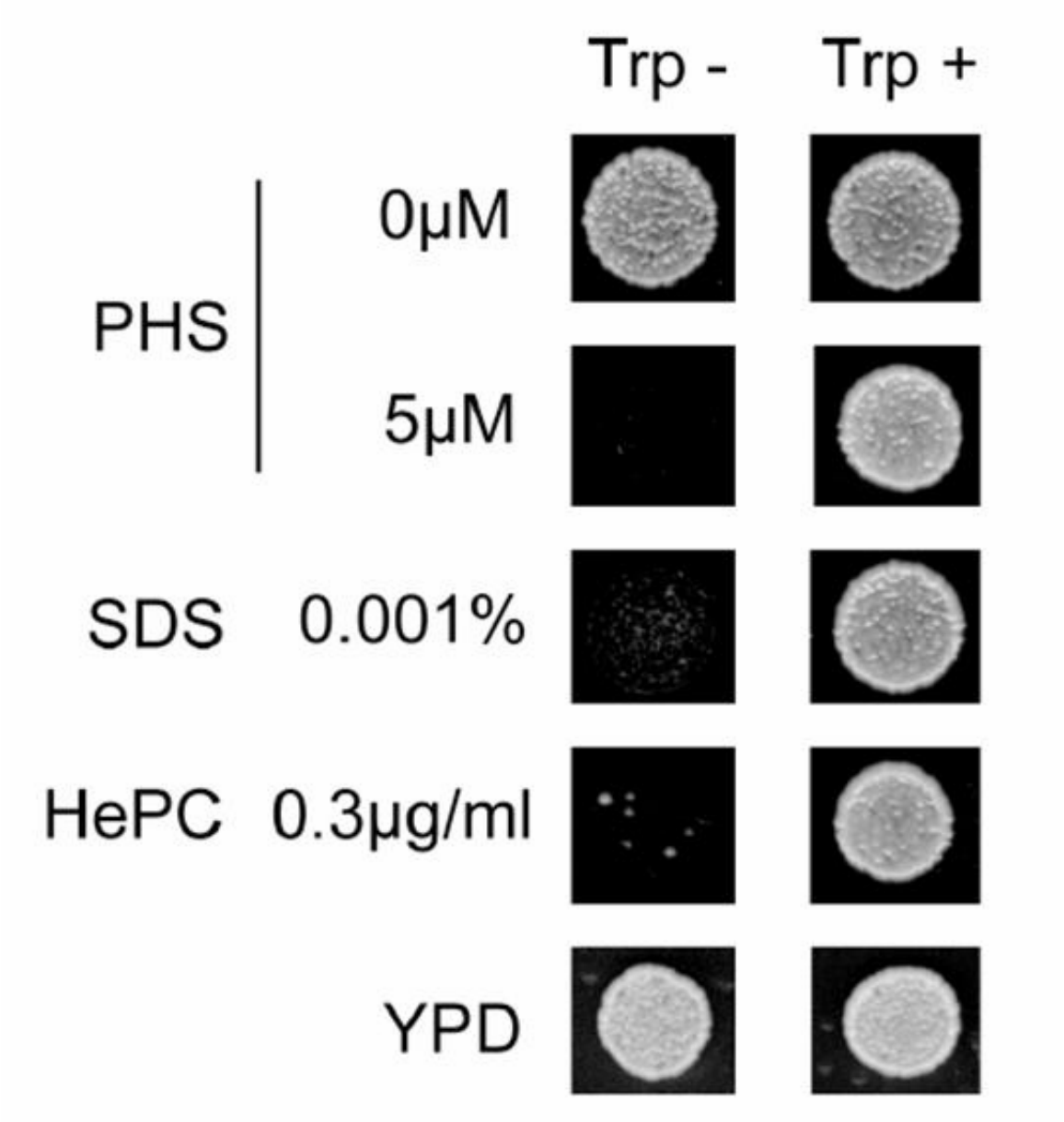

Figure 6. Multiple phenotypes are affected by tryptophan status. Wild-type cells transformed with either a low-copy *URA3* plasmid (pRS316) or a low-copy *TRP1* plasmid (pRS314) were grown in selective minimal media to mid-log phase and spotted onto YPD plates containing the indicated drug concentration or YPD alone. Trp + (pRS314) strains were more resistant to PHS, SDS, and HePC as compared to their Trp – (pRS316) counterparts, indicating that tryptophan status influences multiple phenotypes.

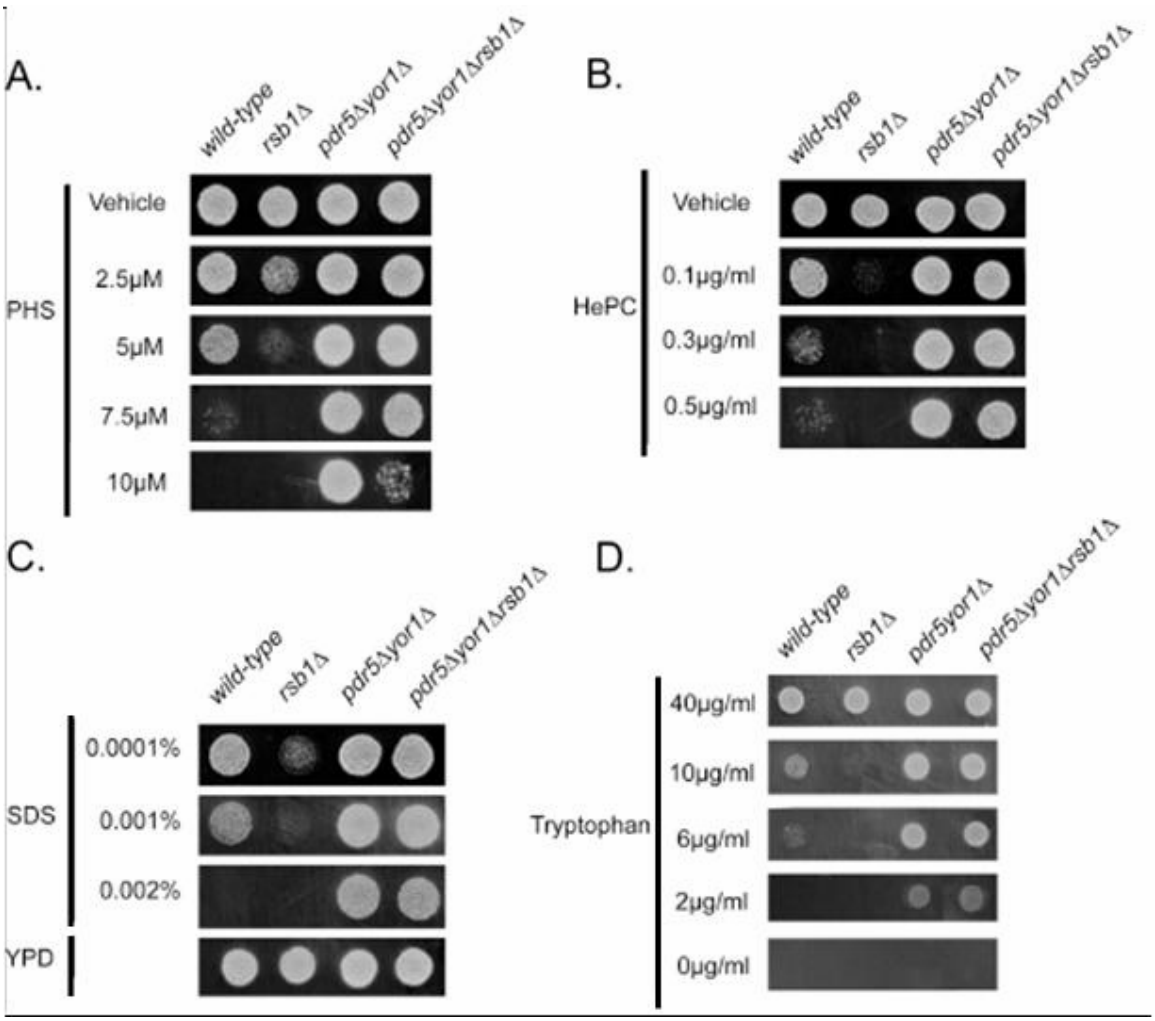

Figure 7. Bypass of *rsb1*Δ by *pdr5*Δ *yor1*. Wild-type and isogenic derivatives lacking the indicated genes were grown in YPD to mid-log phase and spotted onto YPD plates containing above indicated concentrations of PHS (A), HePC (B), SDS (C), or YPD alone. D. These same strains were spotted onto minimal media plates containing the indicated concentrations of tryptophan. Strains lacking Rsb1 are sensitive to all three compounds, whereas strains lacking both Pdr5 and Yor1 show increased resistance.

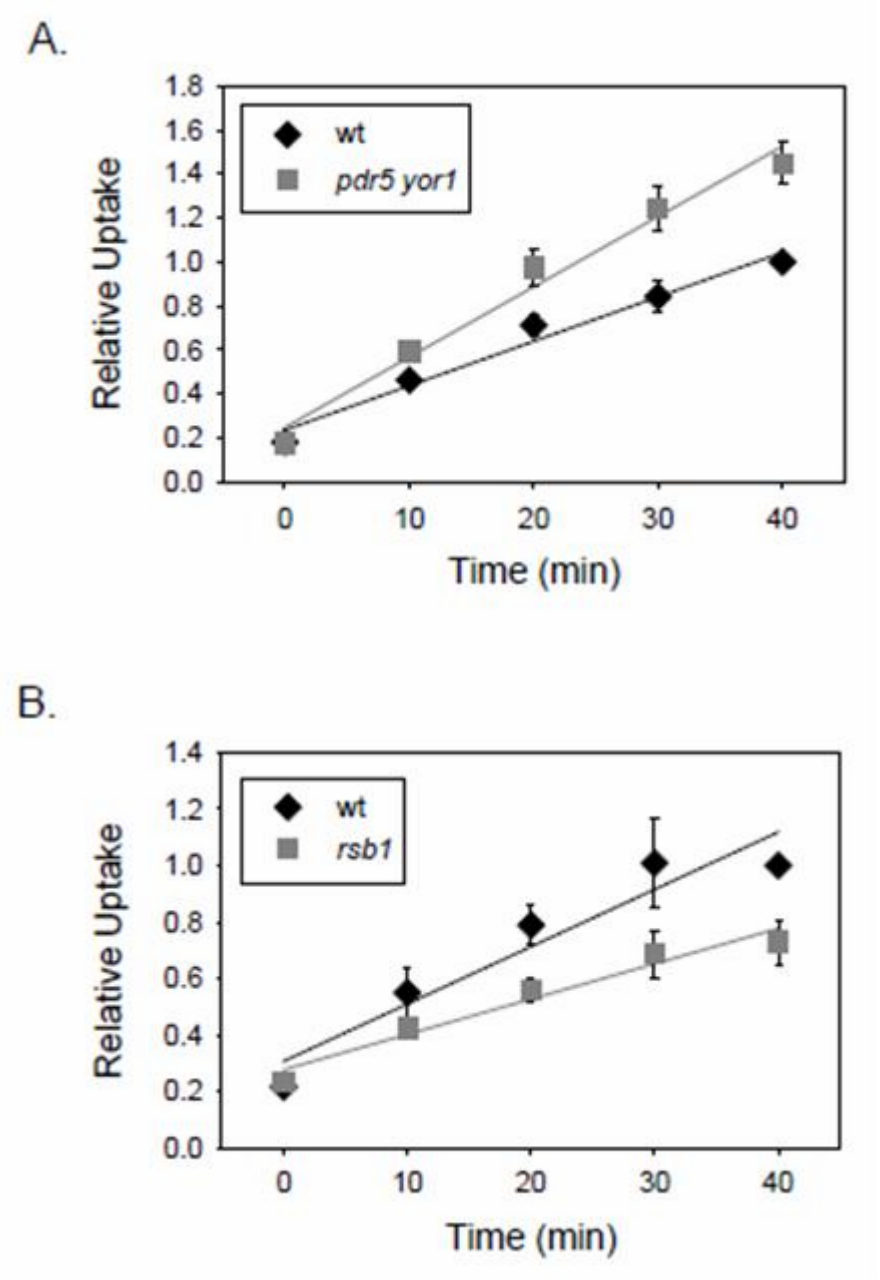

Figure 8 . Tryptophan uptake is increased in the *pdr5*Δ *yor1* strain and decreased in the *rsb1*Δ strain. A. Wild-type (indicated by closed diamonds) and *pdr5*Δ *yor1* (indicated by closed squares) strains were grown to mid-log phase and harvested. Cells were subjected to tryptophan uptake assays as described above. Samples were taken at 10 minute intervals for 40 minutes. B. Wild-type (closed diamonds) and *rsb1*Δ (closed squares) strains were grown and assayed as in A. Error bars represent standard error for three independent assays.

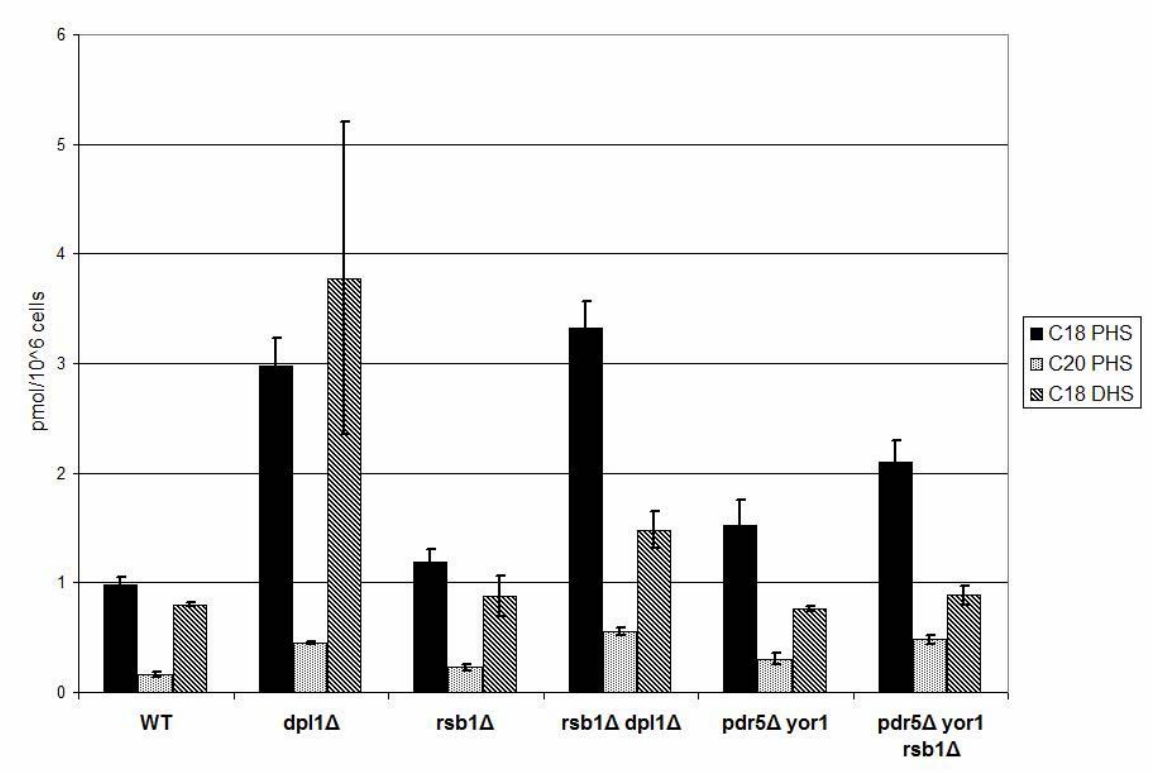

Figure 9. Endogenous PHS levels are not significantly elevated in either the absence of Rsb1 or the absence of Pdr5 and Yor1. Wild-type, *rsb1Δ, rsb1Δ dpl1Δ, dpl1Δ, pdr5Δ yor1*, and *pdr5Δ yor1 rsb1Δ* strains were grown to mid-log phase and processed for HPLC analysis. Long chain base levels are not significantly different in the absence of Rsb1 or in the absence of Pdr5 and Yor1 as compared to the wild-type strain.

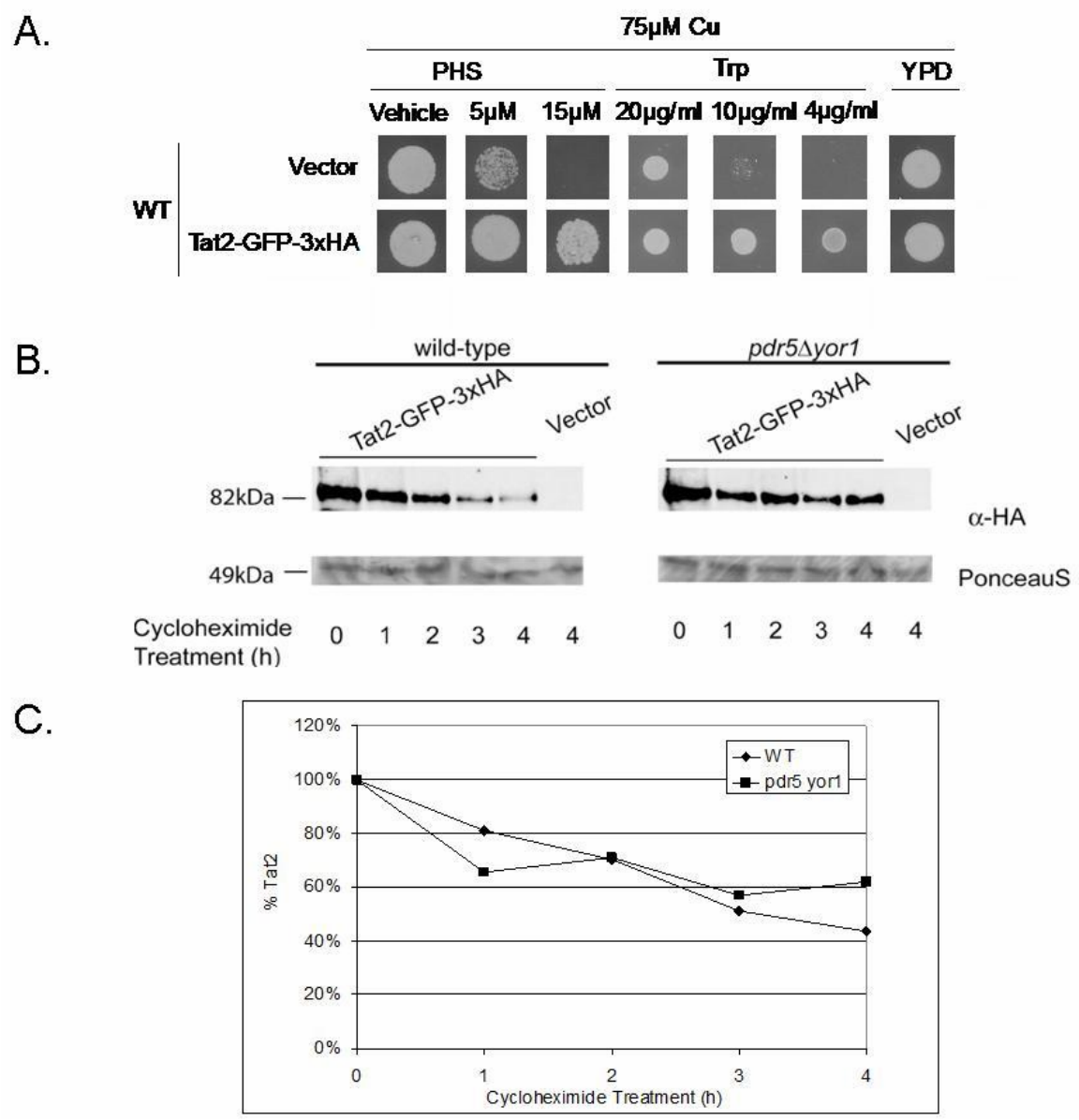

Figure 10. Tat2 is stabilized in the absence of Pdr5 and Yor1. A. Wild-type strain transformed with vector or pRS316-*CUP1*-Tat2-GFP-3xHA (pSR74) were grown to mid-log phase and spotted onto YPD plates containing varying concentrations of PHS or minimal media plates containing varying concenrtrations of tryptophan. B. Wild-type and *pdr5*Δ *yor1* strains were transformed with the same plasmids as in A. Transformants were grown to mid-log phase and time 0 sample was harvested. 75 μg/ml cycloheximide was added to the remaining cultures and samples were harvested at the times indicated above. Western blot analysis of whole cell proteins extracts was done as described in experimental procedures. C. Percentage of Tat2 remaining in wild-type and *pdr5*Δ *yor1* cells over time. Quantification was done using Image J and excel.

A.

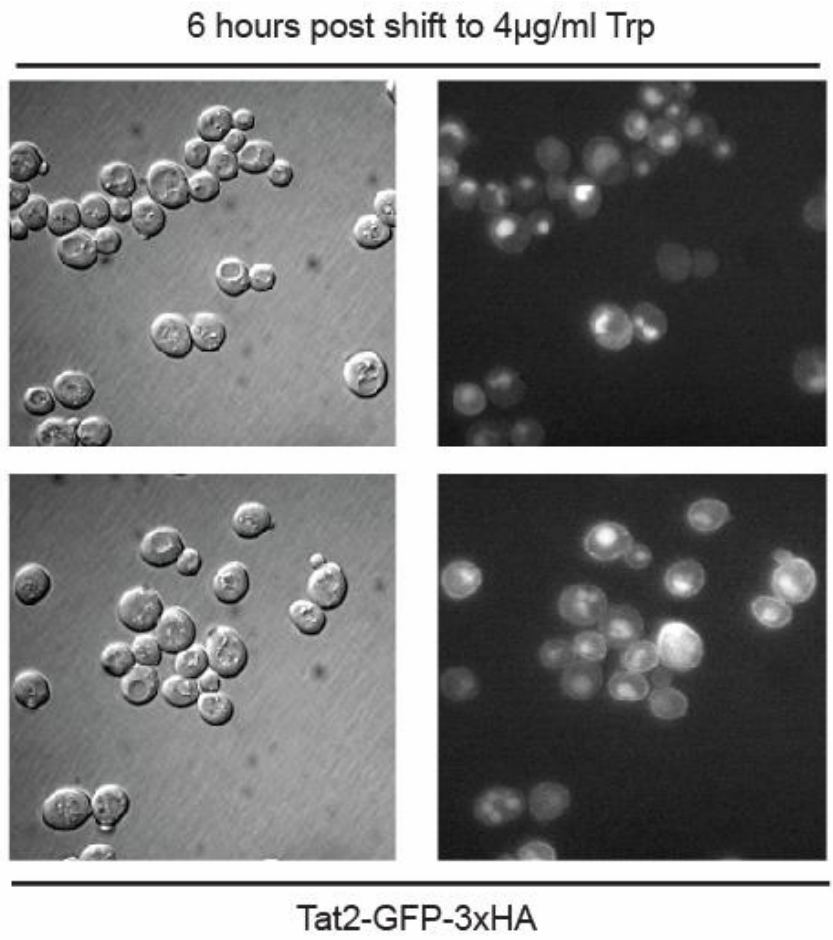

B.

	% Pixels in Vacuole
wild type	40.1% +/- 1.5%
pdr5Δyor1	33.8% +/- 1.9%

Figure 11. Tat2 is present at the plasma membrane longer in the absence of Pdr5 and Yor1. A. Wild-type and *pdr5Δ yor1* strains were transformed with pRS316-Cup1-Tat2-GFP-3xHA (pSR74) and transformants were grown overnight in CSM -URA media. These cultures were shifted to CSM –URA media containing 4 µg/ml tryptophan, grown for 6 hours, and visualized by Nomarski optics and fluorescence microscopy. B. Quantification was done using Image J and excel.

A.

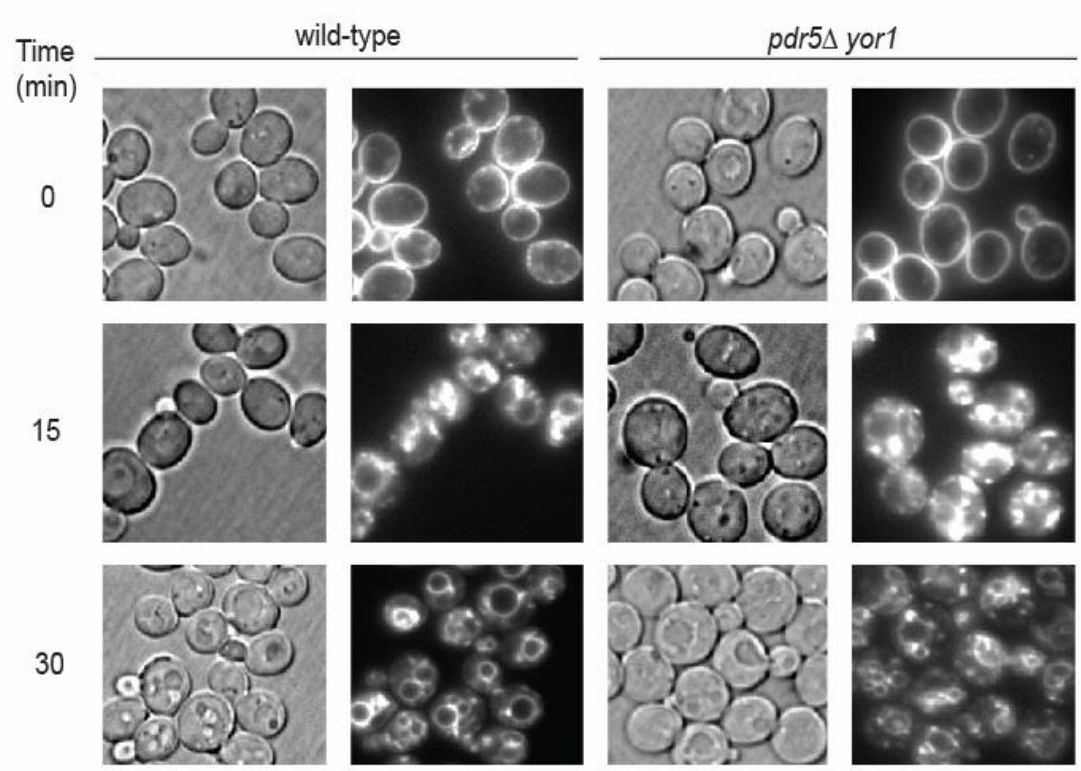

B.

% Pixels on Vacuolar Membrane		
	wild-type	*pdr5Δ yor1*
15 min	21.2%	14.4%
30 min	43.3%	23.9%

Figure 12. Bulk endocytosis is slowed in the *pdr5Δ yor1* strain. A. Wild-type and *pdr5Δ yor1* strains were grown to mid-log phase and chilled on ice. FM 4-64 dye was added to pre-chilled cells and cells were incubated at 4°C for 45 minutes. Samples were harvested and resuspended in pre-warmed YPD and incubated at 30°C for indicated time points. At designated time points, samples were washed with cold SC-Azide buffer and visualized by Nomarski optics (left panels) or fluorescence microscopy (right panels). B. Quantification of the percentage of pixels (fluorescence) on the vacuolar membrane as compared to the whole cell, determined as described in Experimental Procedures. Loss of Pdr5 and Yor1 causes a general endocytic defect.

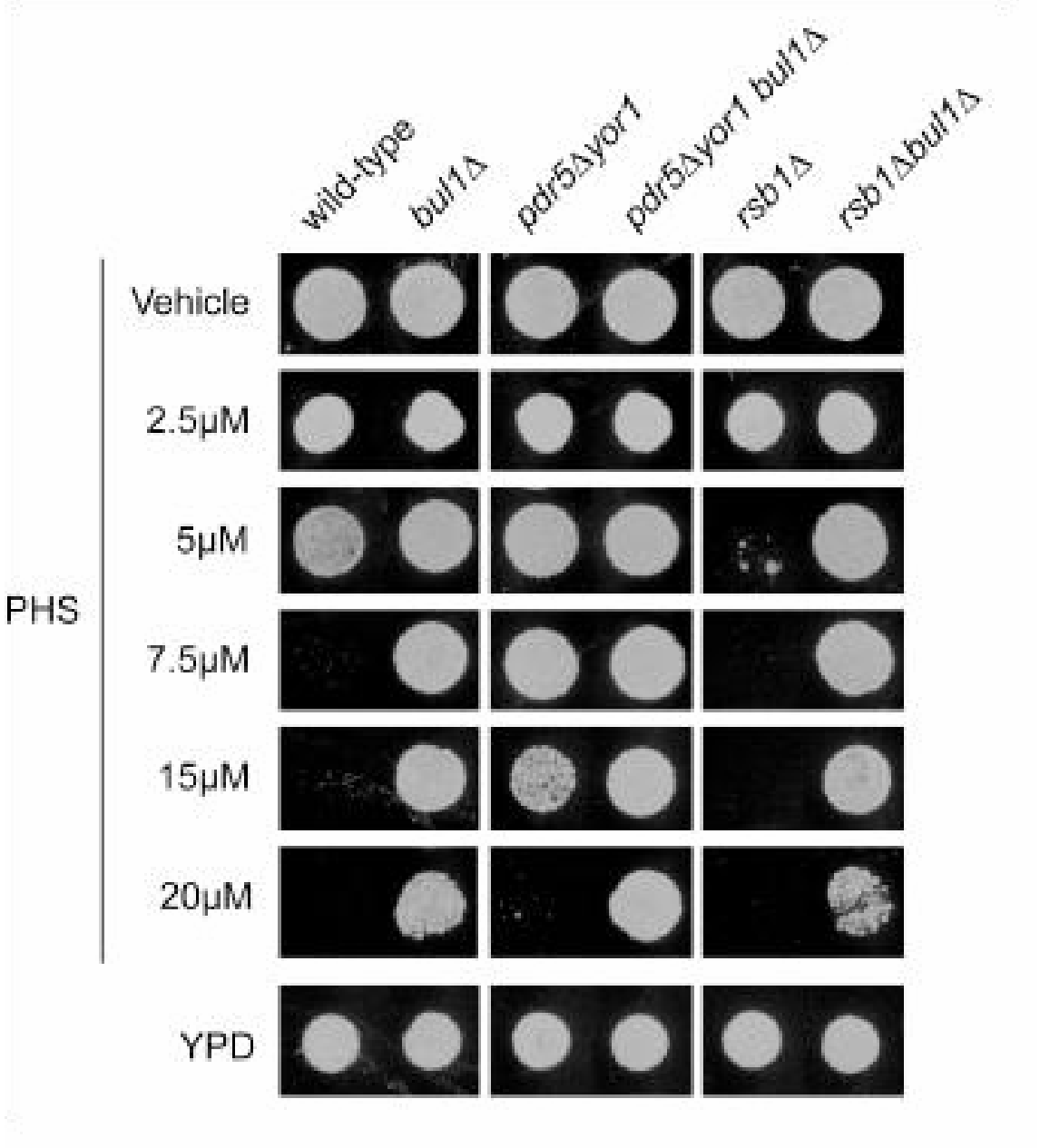

Figure 13. Interaction of Bul1 with Rsb1 and Pdr5/Yor1. A. Wild-type or isogenic mutants lacking the indicated genes were grown to mid-log phase and spotted onto YPD plates containing varying concentrations of PHS. Loss of Bul1 suppresses the PHS sensitivity of the *rsb1Δ* strain and has an additive effect of PHS resistance in the absence of Pdr5 and Yor1.

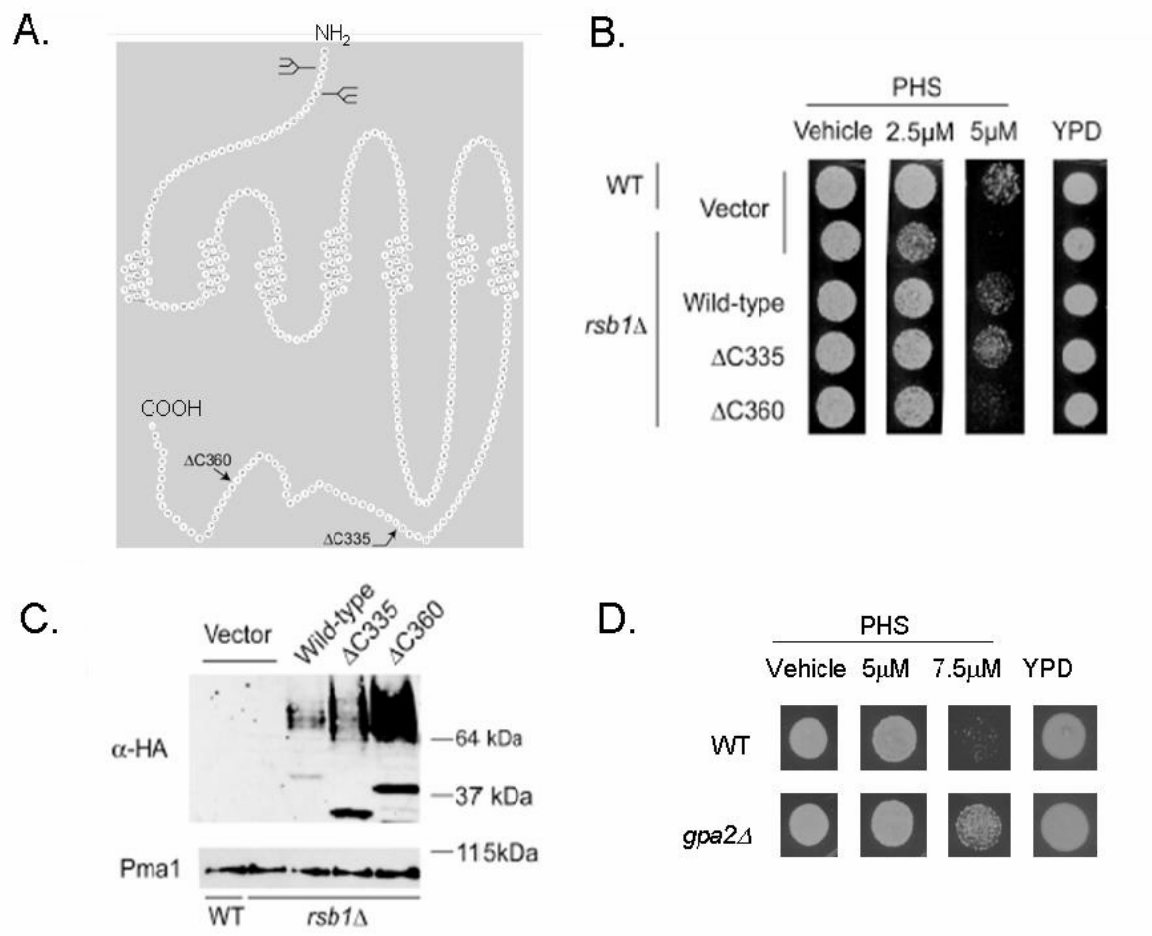

Figure 14. C-terminal truncations of Rsb1 show differential expression and PHS tolerance. A. Predicted topology of Rsb1. A prediction for the organization of Rsb1 made by the program RbDe (http://icb.med.cornell.edu/crt/RbDe/Rbde.xml) is shown. The locations of previously determined N-linked glycosylation sites in the luminal N-terminus (46) are graphically represented. The position of the C-terminal truncation mutations are indicated by arrows. B. Low-copy plasmids containing the above forms of Rsb1, along with an empty vector control, were transformed into wild-type and *rsb1*Δ strains. These transformants were grown to mid-log phase in selective minimal media and spotted onto YPD plates containing the concentrations of PHS indicated above. C. The same cultures from B were extracted as described in experimental procedures and equal amounts of total protein were run on SDS-PAGE, transferred to nitrocellulose and probed using an anti-HA epitope antibody. These membranes were stripped and re-probed for Pma1. D. Wild-type and *gpa2Δ* cells were grown to mid-log phase and spotted onto plates containing varying concentrations of PHS or YPD alone.

CHAPTER III

IDENTIFICATION AND ANALYSIS OF GENES INVOLVED IN THE AUREOBASIDIN A TOLERANCE OF STRAINS LACKING PDR5 AND YOR1

Introduction

As discussed in Chapter 2, previous work indicated that loss of the ABC transporters, Pdr5 and Yor1, increased tolerance to the long chain base, PHS (4). As we were unable to show an increase in Rsb1 transcription in a strain lacking these transporters, it was hypothesized that perhaps another gene, possibly a transporter, was induced to mediate PHS tolerance in this strain. To investigate this, the *pdr5Δ yor1* strain was mutagenized with ethyl methanesulfonate (EMS) and screened on PHS for susceptible colonies. Unfortunately, PHS was not ideal for screening, and the initial candidates from this screen did not display a consistent PHS sensitive phenotype. This led us to begin examining other compounds that target the sphingolipid pathway, such as Myriocin, an inhibitor of serine palmitoyl transferase and Aureobasidin A, an inhibitor of IPC synthase (Figure 2), as we considered that the phenotype of the *pdr5Δ yor1* strain might be due to sensing alterations in sphingolipid content. Aureobasidin A (AbA) was chosen as the compound with which to proceed, as the *pdr5Δ yor1* strain showed a remarkably robust resistance phenotype, similar to that seen on PHS, which was independent of Rsb1.

AbA is a cyclic depsipeptide and potent anti-fungal that targets Aur1, a subunit of the IPC synthase complex (80). If Aur1 is over-expressed, or mutated at specific residues (L137F, H157Y, or F158Y) the cell will become resistant to this compound (80,81). Interestingly, Yor1 was also demonstrated to mediate

tolerance to this compound (13). Since Yor1 is deleted in our strain of interest, it was ruled out as the mediator of resistance in this background. Another series of experiments ruled out Aur1 itself as the responsible gene as its expression, localization, and function do not appear to change in the absence of Pdr5 and Yor1.

Data from the EMS screening using AbA revealed seven mutant strains that maintained 2:2 segregation after three back-crosses. Of these, three were identified as Cyc8 (Ssn6), Gda1, and Mss4 by traditional methods. Three additional strains were sent to Iowa State University for genome sequencing and the mutations responsible for their phenotypes are still under investigation. The last mutant was tentatively identified as Ure2, a gene involved in nitrogen catabolite repression. Cyc8 (Ssn6) is a negative transcriptional regulator involved in multiple pathways including DNA damage response and glucose repression (82). Gda1 is a gene involved indirectly in movement of mannose into the Golgi, which is important for formation of mannosylated sphingolipids as well as proteins (83,84). Mss4 is the only PI_4P 5-kinase in yeast and it is localized to the plasma membrane where it functions in making $PI_{4,5}P_2$, a product that has several downstream effectors in multiple cellular processes such as actin cytoskeleton organization, exocytosis, cell wall integrity, and sphingolipid metabolism ((39-42,85,86)). These data, along with other mediators of AbA tolerance discovered indirectly from this screen or by other methods, will be discussed in further detail.

Experimental Procedures

Yeast strains and Media

The genotypes of yeast strains used in this study are listed in Table 2. Yeast transformations were performed using the lithium acetate procedure (51).

Cells were grown in YPD (1% yeast extract, 2% peptone, 2% glucose) under non-selective conditions or appropriate CSM media under selective conditions. Aureobasidin A (AbA) resistance was assessed by spot test assays on plates containing different concentrations of AbA. PHS resistance was also determined by spot test assays on plates containing varying concentrations of PHS as well as NP-40 as described previously (46).

To TAP tag AUR1, the TAP tag with the HIS3 marker was amplified from the AUR1-TAP BY4741 collection strain using primers AUR1 F 5'-CTATGATAT GCATGGCTCGC-3' from Open Biosystems and AUR1 (576st) R 5'-CATGGGC ATAAGGTATCTTC-3' which binds at 576bp downstream of the stop codon. This PCR product was transformed into SEY6210 wild-type cells and *pdr5Δ yor1* cells and the transformants were selected on –HIS plates. The strains were confirmed by PCR of genomic DNA. A similar approach was used to C-terminally GFP tag AUR1 in the SEY6210 wild-type, *pdr5Δ yor1* and EMS mutant strains. The GFP tag along with the HIS3 marker was amplified from the Invitrogen yeast GFP collection using the same primers used to amplify the TAP and HIS3 cassette above. These strains were also confirmed by PCR analysis of genomic DNA.

To introduce the *gda1Δ* allele, the corresponding region was amplified from the genomic DNA of BY4742 *gda1-Δ::KanMX4* with primers listed in Table 3 and transformed into the strains of interest. Transformants were selected on plates containing geneticin (200μg/ml) and confirmed by PCR analysis. CSG2, YPK1, YPK2, SJL1, PKH1, PKH2, BST1, PDR1, PDR3, were deleted in a similar manner as GDA1. SEC3 was deleted by amplifying the HIS3-MX6 cassette from the pFA6-HIS3MX6 plasmid with primers containing 20bp annealing to the HIS3 cassette and 50bp annealing to the flanking region of the SEC3 ORF (primers are listed in Table 3). The *sec3Δ* strains were confirmed by PCR. The *rsb1Δ* allele was constructed previously (46).

Plasmids

The pSR47 plasmid was constructed using pRS316 digested with Spe1 and a fragment containing all of the Mss4 5' and 3' regions as well as the ORF was digested with Nhe1 from a YCp50 library clone. The two pieces were ligated using standard procedures and confirmed by digestion. The Spe1 and Nhe1 sites were lost in this ligation.

The pSR97 plasmid was constructed using pRS426 digested with Kpn1 and Sac1. Ypk1 was amplified in two pieces with 200bp overlap for recombination. The promoter and N-terminal half of Ypk1 were amplified with primers Ypk1 500bp F1 5'- cggccagtgagcgcgcgtaatacgactcactatagggcgaattgg gtaccGATTTAAAGAAATTTTAGGA-3' and Ypk1 HA-R 5'- AGCGTAATCTGGG ACGTCGTATGGGTAtctaatgcttctaccttgca-3'. The C-terminal half of Ypk1 and 3'-UTR were amplified with primers Ypk1 HA-F 5'- TACCCATACGACGTCCCAG ATTACGCTACTTAGTGAATACATTATCAAC -3' and Ypk1 ds R4 5'- acgccaagc gcgcaattaaccctcactaaagggaacaaaagctggagctcCAAGGAGAAAATTTTCAACA-3'. The two amplicons and cut vector were transformed into yeast and cloned by recombination. Plasmids were isolated by standard procedures, electroporated into *E. coli*. Plasmids were confirmed by digestion and sequencing. Plasmids used in this study are listed in Table 4.

EMS mutagenesis

The EMS mutagenesis was completed using Linda Hoskins' protocol from the Hahn Lab at the Fred Hutchinson Cancer Research Center. The *pdr5Δ yor1* strain was treated with EMS for 40 minutes which gave approximately 50% survival. Fifteen thousand cells were plated on YPD plates at a density of 500 cells per plate and allowed to recover for 2 days. These were then replica plated onto YPD plates containing 75ng/ml Aureobasidin A (AbA) and back onto YPD.

After overnight incubation at 30°C, plates were screened for colonies that were sensitive to AbA. These colonies were streaked and rechecked for AbA sensitivity, grouped into 3 categories based on degree of AbA sensitivity (C = most sensitive, B = intermediate sensitivity, A = mildly sensitive). At this point the group C and group B colonies were back-crossed to the parent *pdr5Δ yor1* strain. Twenty independent colonies were subjected to tetrad analysis and tested for AbA sensitivity by replica plating. Only sensitive colonies from tetrads that segregated 2:2 were used in subsequent analysis. This procedure was repeated for a total of 3 back-crossings. The final strains were subjected to high efficiency transformation (87) with a genomic YCp50 library and were plated onto CSM -Ura plates and allowed to recover. These transformants were replica plated onto YPD plates containing 75ng/ml AbA as well as CSM -Ura and incubated overnight at 30°C. AbA plates were checked once a day for up to 5 days for colony formation on the YPD AbA plates. These colonies were streaked onto YPD 75ng/ml AbA and CSM -Ura. Plasmids were isolated from yeast using standard methods and electroporated into *E. coli*. Plasmids were retrieved from bacteria, digested to check for the presence of a large genomic insert and re-transformed into the mutant strain to verify that reversion of the AbA phenotype was plasmid-linked. Plasmids were sequenced on the ends with YCp50 specific primers, 5'- gccgcccagtcctgctcgcttcgct and 3'-tgatgtcggcgatataggcgccagc. The genomic region contained in the complementing plasmid was determined by BLAST searches in the Saccharomyces Genome Database (SGD). To determine the mutant gene, subclones lacking one or more genes from the complementing YCp50 plasmids were constructed, transformed into mutant strains and AbA phenotypes were assessed. Deletions of candidate genes were made by amplifying the KanMX4 deletion cassettes from the BY4742 collection and transforming into SEY6210 wild-type and the *pdr5Δ yor1* strains. These

deletions were phenotyped by spot test assay on YPD plates containing varying concentrations of AbA. To confirm mutant genes, EMS mutants were mated with the *pdr5Δ yor1* strains also containing the corresponding gene deletion and dissection of tetrads was performed to confirm 0:4 (resistant:sensitive) AbA sensitive segregation.

TLC of sphingolipids

Cells were grown overnight in CSM supplemented with 80mg/L serine. Cells were then subcultured to a starting OD A_{600} of 0.2 in CSM and ^{3H}Serine was added to a final concentration of 20μCi/ml (30). Cultures were grown at 30°C for 6 hours, pelleted and stored at -80°C overnight. Extraction was done as described previously (30). Briefly, cells were treated with 5% TCA on ice for 15 minutes and washed twice with water. Sphingolipids were extracted with solvent containing diethyl ether:95% EtOH:H_2O:pyridine:concentrated ammonia (5:15:15:1:0.018) at 60°C for 1 hour. Extracts were dried under a nitrogen stream and treated with monomethylamine reagent for 30 minutes at 50°C to deacylate phospholipids. Lipids were resuspended in $CHCl_3$:MeOH:H_2O (16:16:5) and run on Whatman Silica gel 60 TLC plates with solvent $CHCl_3$:MeOH:4.2N NH_4OH (9:7:2). TLC plates were exposed to film (Amersham Hyperfilm MP) for 3-5 days. After film exposure, TLC plates were sprayed with orcinol and H_2SO_4 to detect glycosylated lipid standards and $CuSO_4$ in H_3PO_4 to detect all lipid standards.

Western analysis

For analysis of Aur1, cells were grown to An A_{600} of 0.8-1.0 and whole cell extracts were prepared using the TWIRL buffer (8M urea, 5% SDS, 10% glycerol, 50mM Tris pH 6.8) extraction method. Briefly, 2 OD units of cells were resuspended in 60μl of TWIRL buffer and vortexed for 2 minutes with glass

beads at 4°C and centrifuged for 5 minutes at 12k rpm at 4°C. Samples were electrophoresed on SDS-PAGE, transferred to nitrocellulose, and Western blotted using monoclonal anti-HA (1:1000) (Covance). These membranes were stripped and re-probed with an antibody against the vacuolar membrane protein Vph1 (1:5000) antibodies (Molecular Probes).

For analysis of Ypk1, wild-type and *pdr5Δ yor1* strains were transformed with either YEp351 vector only or YEp351 vector carrying Gal driven N-terminally Myc-tagged Ypk1 (pAM54) (88). These transformants were grown and processed as described previously (16). In brief, cells were grown to an OD A_{600} of 0.3 in CSM –Leu media containing 2% raffinose and 0.2% sucrose. The cultures were then induced with 2% galactose for 3 hours. For samples that were drug treated, cells were induced with galactose for 1 hour and AbA was added for the remaining 2 hours of galactose induction. One OD A_{600} unit of cells were harvested at an OD A_{600} of approximately 0.6-0.8 and washed once with water. Cells were lysed by addition of 150μl of 1.85M NaOH, 7.4% β-mercaptoethanol. Protein was precipitated by addition of 150μl 50% TCA on ice for 10 minutes. Samples with centrifuged, washed once with acetone, and resuspended in 80μl of 0.1M Tris, 5% SDS, after which 20μl of a 5x stock of Laemmli sample buffer was added to each. Samples were boiled for 5 minutes and 20μl samples were resolved by SDS-PAGE (6% acrylamide, 75:1 acrylamide:bis ratio), transferred to nitrocellulose and incubated with anti-myc 9E10 antibody (Covance) and secondary HRP-conjugated anti-mouse antibody. Protein was detected by chemiluminescence.

Fluorescence Microscopy

Strains containing GFP-tagged AUR1 were grown to an A_{600} of 0.8-1.0. 1ml of cells was centrifuged and washed once with sterile water. Pellet was

resuspended in 25-50μl of sterile water. Cells were visualized for GFP fluorescence and Nomarski optics using an Olympus (Tokyo, Japan) BX-60 microscope with a 100X oil objective. Images were captured using a Hamamatsu (Shizuoka, Japan) ORCA charge-coupled device camera.

Aur1 Activity Assay

Wild-type and *pdr5Δ yor1* cells were subcultured to an A_{600} of 0.15 and grown to an A_{600} of 0.4-0.6. 10 OD units of cells were centrifuged and resuspended in CSM, fatty acid free BSA (5mg/ml), 20μM C6-NBD-ceramide and incubated for 20 minutes at 30°C. Samples that were pretreated with AbA were incubated with 10μg/ml AbA for 10 minutes at 30°C prior to addition of NBD-ceramide. Cells were pelleted and washed 4 times in ice-cold CSM containing 5mg/ml fatty acid free BSA. Lipids were extracted by adding 500μl $CHCl_3$:MeOH: 1M HCl (5:12:4) and small glass beads (425-600μm) and vortexing for 5 minutes at 4°C. Samples were centrifuged at 4°C for 5 minutes and the supernatant transferred to a fresh eppendorf. Lipid extract was mixed with 125μl $CHCl_3$ and centrifuged to separate phases. The lower organic phase was transferred to a glass tube and dried under a nitrogen stream. Dried lipids were resuspended in 25-50μl $CHCl_3$:MeOH:30mM KCl (11:9:2). Samples were normalized to fluorescence units and run on a Whatman Silica gel 60 TLC plate in $CHCl_3$:MeOH:30mM KCl. Samples were visualized and quantified using an IVIS Bioluminescence Imager (Xenogen). This protocol was adapted from a previously established assay (89).

Results

A strain lacking the ABC transporters Pdr5 and Yor1 increases resistance to the sphingolipid biosynthesis inhibitor, Aureobasidin A

To search for genetic determinants involved in the induced PHS resistance seen in a *pdr5Δ yor1* strain, I subjected this strain to ethyl methanesulfonate (EMS) mutagenesis with a goal of finding mutants that no longer exhibited elevated PHS tolerance. The screen was done using PHS initially, but the selection provided by this long chain base was insufficient and subsequent phenotyping to confirm sensitivity of the candidates was inconsistent. The *pdr5Δ yor1* strain was then assessed for other phenotypes related to inhibition of the sphingolipid biosynthetic pathway. Aureobasidin A (AbA), a potent inhibitor of the IPC synthase complex component Aur1 (26,80), was selected for further experiments after determining that the *pdr5Δ yor1* strain showed a robust resistance phenotype to this compound, which is independent of Rsb1 (Figure 15). Wild-type, *rsb1Δ*, *pdr5Δ yor1, pdr5Δ yor1 rsb1Δ* cells were grown to mid-log phase and spotted onto YPD plates containing varying concentrations of AbA. The *pdr5Δ yor1* cells were resistant at a concentration of 75ng/ml as compared to the wild-type, which grew to about 50ng/ml. Loss of Rsb1 did not show any effect on AbA in either background. The resistant phenotype of the *pdr5Δ yor1* strain may be due to slowed turnover of a previously unidentified transporter for AbA, reduced entrance of AbA into the cell, or a change in the target of AbA, AUR1.

Changes in AUR1 are not responsible for the AbA resistance of the *pdr5Δ yor1* strain

AbA inhibits Aur1, a subunit of the inositol phosphorylceramide (IPC) synthase, thereby blocking the synthesis of complex sphingolipids (26) . Aur1 itself is known to be a mediator of AbA tolerance when either mutated or over-expressed (80,90). Therefore I first examined the simple possibility that Aur1 was the mediator of AbA tolerance in the *pdr5Δ yor1* background. To determine if expression was altered, Aur1 was C-terminally TAP tagged in both the wild-type and *pdr5Δ yor1* strains. Expression of Aur1 in the TAP tagged strains appeared similar in both wild-type and *pdr5Δ yor1* as determined by Western blot (Figure 16A). Although expression was not altered, it was possible that localization of Aur1 might be affected in the absence of Pdr5 and Yor1 because loss of both of these transporters affects membrane lipid content as discussed earlier. Aur1 was C-terminally GFP tagged in wild-type and *pdr5Δ yor1* strains to examine localization by fluorescence microscopy (Figure 16B). Aur1 localization to the Golgi appeared to be normal in both strains. Changes in the lipid environment are well-known to affect not only localization but also activity of the proteins that reside there (91). Therefore Aur1 activity was examined to determine if it was altered in the absence of Pdr5 and Yor1. Aur1 activity was measured using the fluorescent ceramide derivative, NBD-ceramide, to assess conversion of ceramide to IPC, as described previously (89). The presence of a fluorescent species was detected in both the wild-type and *pdr5Δ yor1* samples (lanes 1, 3), the amount of which was similar between the two strains (Figure 16C). To show specificity of this species as the product of Aur1 (NBD-IPC in this case), two samples were pre-treated with AbA. This pretreatment prevented production of any detectable NBD-IPC (lanes 2, 4). To further confirm a lack of Aur1 activity changes, complex sphingolipids were extracted from cells labeled with ^{3}H-Serine

and equal counts were run on a TLC plate. The TLC plates were dried and exposed to film for several days (Figure 16D). The complex sphingolipid distribution appeared similar in the wild-type and *pdr5Δ yor1* strains. These data provide additional confirmation that Aur1 is probably not the major player in the AbA tolerance seen in the *pdr5Δ yor1* strain.

Mutations in genes involved in multiple pathways result in reversal of the *pdr5Δ yor1* AbA phenotype

As I was able to rule out any changes in Aur1 with the assays above, I repeated the ethyl methanesulfonate (EMS) mutagenesis on the *pdr5Δ yor1* strain to determine what gene(s) might be responsible for the AbA resistant phenotype. EMS mutagenesis and cloning was carried out as described in experimental procedures. After 3 back-crosses, seven mutants remained that showed 2:2 segregation of AbA sensitivity, suggesting a single gene in each mutant strain is responsible for the phenotype (Figure 17A). All mutants recovered from the screen were recessive, as determined by AbA phenotype of the diploid strains obtained by mating of the mutant haploid with the parent haploid strain (Figure 17B). The haploid strains were also cross-screened on PHS, as it was possible that determinants for AbA resistance and PHS could overlap (Figure 17C). Interestingly, several of the mutants displayed a PHS sensitive phenotype, indicating that there are some common determinants of PHS and AbA tolerance in the *pdr5Δ yor1* strain.

Of these seven mutants, three were amenable to cloning by standard methods (Table 2). To identify the remaining mutants, genomic DNA was isolated from the B19, C1, and C21 mutants and sent to Iowa State University for genome sequencing along with the wild-type strain. Several mutations for each of these strains were obtained from this analysis and further work is required to

determine the mutations responsible for the AbA phenotypes of these strains. The C17 mutant was not sequenced as it was tentatively identified at the time of sequencing as Ure2, a gene involved in nitrogen catabolite repression, which will be discussed later. The three strains identified by standard cloning, B27, B33, and C25, contained mutations in *CYC8* (*SSN6*), *GDA1*, and *MSS4*, respectively.

Cyc8 is a general negative transcriptional regulator, which functions in complex with Tup1 and is recruited to various DNA binding repressors (82,92). This complex is responsible for repression of genes involved in multiple cellular processes, including DNA damage response and glucose repression (82). As Cyc8 affects a multitude of pathways, there was no clear direction to pursue for this mutant and it has not been followed up to date.

URE2 is involved in AbA resistance

The AbA phenotype of the EMS mutant designated C17 was complemented by a low-copy clone containing several genes involved in a variety of functions. To first assess which gene might be important, these genes were deleted individually in the wild-type strain and in the corresponding *pdr5Δ yor1* strain. Interestingly, only loss of *URE2* was able to reverse the AbA phenotype of the *pdr5Δ yor1* strain (Figure 18A). *URE2* deletion in the *pdr5Δ yor1* strain lowered the AbA resistance to about 50ng/ml, as compared to the parent *pdr5Δ yor1* strain, which grew well beyond 75ng/ml. The effect of *URE2* deletion by itself in our wild-type strain background was variable, with one mutant barely growing at 25ng/ml, while the other behaved similarly to wild-type, growing to about 50ng/ml. The variability in phenotype precludes an understanding of whether or not the *ure2Δ* by itself shows a phenotype on AbA. Construction of the *URE2* single deletion strains was difficult and continued efforts were suspended when it was determined by linkage analysis that the responsible gene

in the C17 mutant strain was not *URE2*. *URE2* is involved in nitrogen catabolite repression (93). It is normally found in the cytoplasm, bound to phosphorylated forms of the transcription factor Gln3 (94,95). When the cells are grown in the presence of a poor nitrogen source, Gln3 is dephosphorylated, allowing its release from Ure2 and subsequent translocation to the nucleus to activate transcription of genes involved in dealing with this metabolic condition (94). One gene in particular that is induced in the absence of Ure2 is *GAP1*, the general amino acid permease (55). Typically induction of *GAP1* causes a down-regulation of other amino acid permeases, such as Tat2 (96). Strikingly, loss of Ure2 in the *pdr5Δ yor1* strain obliterated the resistance to low tryptophan that is usually seen in this strain, barely allowing growth at 20μg/ml tryptophan as compared to *pdr5Δ yor1 cells* that normally grow well even at 4μg/ml (Figure 18B). This data suggests that loss of Ure2 may trigger a response similar to that seen in nitrogen starvation, which will be discussed later.

Loss of Gda1 affects AbA resistance

Characterization of the mutant designated B33 indicated that the affected gene in this strain was *GDA1*. Gda1 is a guanosine diphosphatase that is localized to the Golgi and functions indirectly in movement of mannose into the Golgi lumen. This imported mannose is required for glycosylation of proteins and sphingolipids (83). Mutation in *GDA1* suppresses the AbA resistance of the *pdr5Δ yor1* strain (Figure 19A). However this phenotype could be due to changes in mannosylated proteins or sphingolipids. To determine if a block in only mannosylated sphingolipids would phenocopy the *GDA1* mutation, I made a deletion of the *CSG2* gene, encoding the regulatory subunit of the MIPC synthase complex. *CSG2* was deleted in both the wild-type and *pdr5Δ yor1* strains. Loss of Csg2 in the *pdr5Δ yor1* strain caused a dramatic decrease in

AbA resistance. Cells were only able to grow up to 50ng/ml AbA, compared to the *pdr5Δ yor1* strain, which was grew robustly beyond this same concentration. This *pdr5Δ yor1 csg2Δ* strain was remarkably similar in phenotype to the *pdr5Δ yor1 gda1Δ* strain, suggesting that the effects seen on AbA may be due to changes in sphingolipid content. However, TLC of the *gda1Δ* strains showed little or no effect on complex sphingolipid content as compared to the *csg2Δ* (Figure 19B). Figure 19C shows a schematic of the sphingolipid biosynthetic pathway and the steps at which each above protein functions. A recent study indicated that loss of Gda1 has also been implicated in defective anchoring of GPI-anchored cell wall proteins, presumably because they are underglycosylated (97). Interestingly, another gene involved in formation of GPI-anchored proteins, Bst1 (*B*ypass of *s*ec *t*hirteen) also has a phenotype on AbA, which suggests the possibility that loss of Gda1 may be contributing to a cell wall defect, rather than changes in sphingolipid content, that increase its susceptibility to AbA.

Loss of Bst1 causes a dramatic decrease in AbA tolerance

Bst1 is a GPI inositol deacylase that is localized to the ER and is required for discrimination of ER resident proteins and Golgi-bound cargo (98). It is necessary for GPI proteins to reach the Golgi because a lack of deacylation retains these proteins in the ER (98). A screen recently done by another member of our lab, Bernice Thommandru, indicated that loss of Bst1 severely impaired the cell's ability to deal with AbA stress. I was able to verify this phenotype in independently constructed strains and also discovered that loss of Bst1 profoundly affects the AbA phenotype of the *pdr5Δ yor1* strain (Figure 20). Strikingly, single *bst1Δ* strains were unable to grow at even 10ng/ml AbA as compared to the wild-type strain, which grew well until about 30ng/ml. The *pdr5Δ*

yor1 strains grew well beyond 30ng/ml, however the *pdr5Δ yor1 bst1Δ* strains were not able to grow at concentrations above 10ng/ml. These data indicate that changes in the GPI-anchored protein spectrum of the cell alter the cell's ability to deal with AbA.

Mutation of Mss4 reverses the AbA resistance of the *pdr5Δ yor1* strain

Mss4 is the only PI_4P 5-kinase in *Saccharomyces cerevisiae*. Its product, $PI_{4,5}P_2$ is known to function in multiple downstream signaling pathways, which regulate cellular processes including actin cytoskeleton organization, cell wall integrity, sphingolipid biosynthesis, and exocytosis (39-41,86). Mss4 was initially identified as a multicopy suppressor of a Stt4 mutant, which functions in making the substrate of Mss4, PI_4P (99). The gene responsible for the mutant phenotype in the strain designated C25 was identified by standard cloning methods and was shown to correspond to *MSS4*. Complementation of this mutant with a low-copy plasmid containing only *MSS4* is shown in Figure 21A. The *pdr5Δ yor1* strain containing this allele of *MSS4* showed markedly reduced AbA resistance, only growing to a concentration of 25ng/ml, as compared to the *pdr5Δ yor1* strain, which grew well to about 75ng/ml. The addition of a low-copy plasmid containing *MSS4* complements this AbA sensitive phenotype, suggesting it is specific to *MSS4*. No additional increase in AbA tolerance is seen in the wild-type or *pdr5Δyor1* transformants likely owing to the fact that this is a low-copy plasmid. Sequence analysis indicated that this mutant allele contains two mutations, T271I and T724M, which have not been described previously and cause a temperature sensitive growth phenotype at 37°C (Figure 21B). The above data suggest that Mss4 and its product, $PI_{4,5}P_2$ may be crucial for the AbA resistance of the *pdr5Δ yor1* strain.

Deletion of *SJL1* (*INP51*) partially suppresses the AbA sensitivity of the *pdr5Δ yor1 mss4* strain

Sjl family members are homologues of the mammalian synaptojanin proteins. Synaptojanins function as inositol 5' phosphatases and are involved in endocytosis of synaptic vesicles (100). The yeast, *S. cerevisiae*, contains three synaptojanin-like proteins (Sjl1-3), which function in cleavage of phosphoinositides (101). Sjl2 and 3 contain a polyphosphoinositide phosphatase domain in their N-terminus, allowing them to act on multiple phosphoinositides, while Sjl1 lacks this domain and specifically acts on $PI_{4,5}P_2$ (101). Based on the requirement of Mss4 in the *pdr5Δ yor1* strain for AbA tolerance, we hypothesized that Mss4 may be more active in this strain, thus having an increased amount of $PI_{4,5}P_2$. This idea suggests that the sensitivity of the *pdr5Δ yor1 mss4* strain is due to a decreased amount of $PI_{4,5}P_2$. I then hypothesized that loss of Sjl1, which would decrease breakdown of $PI_{4,5}P_2$, might restore AbA resistance in the *pdr5Δ yor1 mss4* strain. *SJL1* was deleted in wild-type, *pdr5Δ yor1*, and *pdr5Δ yor1 mss4* strains and AbA resistance was examined. The *pdr5Δ yor1 mss4 sjl1Δ* mutant showed partial suppression, growing reasonably well at 30ng/ml AbA, while the *pdr5Δ yor1 mss4* strain was almost unable to grow at the same concentration (Figure 22). Loss of Sjl1 in the *pdr5Δ yor1* strain showed a slight increase in AbA tolerance, as seen at 75ng/ml, while *sjl1Δ* by itself showed a similar slight increase in AbA tolerance at 30ng/ml as compared to the wild-type strain. These data support the idea that increasing $PI_{4,5}P_2$ enhances AbA resistance.

Mutation in Mss4 may decrease exocytosis, counteracting the endocytic defect of the *pdr5Δ yor1* strain

We have demonstrated previously that loss of both Pdr5 and Yor1 causes a decline in endocytosis. It is possible that this endocytic defect plays a role in AbA tolerance via an unspecified mechanism, possibly stabilization of an unidentified AbA exporter or decreased uptake of AbA itself. Mss4 has been implicated in control of exocytosis (85,86). Exo70, one component of the exocyst complex, interacts with $PI_{4,5}P_2$ and is important for recruitment of the exocyst complex (86). We hypothesized that mutation of Mss4, which may slow exocytosis may counteract the endocytic defect of the *pdr5Δ yor1* strain by possibly slowing outward trafficking of an AbA transporter or increasing uptake of AbA by the cell, thus reversing the phenotype.

To test the theory that a change in exocytosis may suppress the AbA resistance of the *pdr5Δ yor1* strain, Sec3 was deleted in both wild-type and *pdr5Δ yor1* cells. Sec3 is the only known non-essential late-acting secretory (sec) gene (41). Two other groups have demonstrated that strains deleted for Sec3 are viable and show an expected secretory defect (86,102). The above strains along with wild-type, *pdr5Δ yor1,* and *pdr5Δ yor1 mss4* controls were grown to mid-log phase and spotted onto CSM AbA plates. The *pdr5Δ yor1 sec3Δ* strains were unable to grow at a concentration of 25ng/ml AbA, comparable to the *pdr5Δ yor1 mss4* strain, while the *pdr5Δ yor1* strain grew robustly beyond 50ng/ml (Figure 23). Interestingly, the Sec3 deletion by itself also caused a severe defect in AbA tolerance, only able to grow at a concentration of AbA lower than 25ng/ml, as compared to the wild-type strain, which was viable to about 50ng/ml AbA. The reversal of the *pdr5Δ yor1* phenotype by deletion of Sec3 supports the hypothesis that an endocytic defect may play a role in AbA resistance, while the

phenotype of the Sec3 deletion by itself suggests that a change in exocytosis alone alters the cell's ability to deal with AbA.

Loss of Ypk1, but not Ypk2, causes a dramatic decrease in AbA resistance

In my efforts to identify genes that respond to the loss of Pdr5 and Yor1, I took a candidate gene approach and tested several loci that have been implicated in control of membrane trafficking and possess a link to sphingolipids. One of the genes I tested was *YPK1* (*Y*east *p*rotein *k*inase 1). Ypk1 is activated by complex sphingolipids and required for normal endocytosis (16,36). To determine if this protein kinase was involved in *pdr5Δ yor1*-induced AbA resistance, *YPK1* and its homologue, *YPK2*, were each deleted in either wild-type or *pdr5Δ yor1* cells. The resulting strains were grown to mid-log phase and assessed for a phenotype on AbA. Strikingly, loss of Ypk1 decreased tolerance to AbA (Figure 24). The *ypk1Δ* strain was completely inviable at 25ng/ml AbA as compared to wild-type which grew well until about 50ng/ml. The *pdr5Δ yor1* strain grew robustly beyond 50ng/ml, while the *pdr5Δ yor1 ypk1Δ* strain was sick around 25ng/ml. Loss of Ypk2 in either background had no effect on AbA tolerance. These data imply that Ypk1, but not Ypk2, plays an important part in AbA tolerance. It has been demonstrated previously that Ypk1 is regulated by multiple kinases, including Pkc1, which is a known downstream effector of the Mss4 product $PI_{4,5}P_2$ (37). This led to the hypothesis that perhaps Ypk1 is acting downstream of Mss4.

Over-expression of Ypk1 partially restores AbA tolerance in a *pdr5Δ yor1 mss4* strain

As mentioned above, Ypk1 is a target of the kinase Pkc1, which functions downstream of Mss4, amongst other pathways (37,88). To assess whether or

not Ypk1 functions downstream of Mss4 in regulation of AbA tolerance, wild-type, *pdr5Δ yor1*, and *pdr5Δ yor1 mss4* strains were transformed with either a high-copy vector alone or a high-copy vector carrying C-terminally HA tagged *YPK1*. Transformants were grown in selective media to mid-log phase and spotted onto YPD plates containing varying concentrations of AbA (Figure 25). Wild-type carrying vector only or high-copy Ypk1 grew well up to a concentration of 40ng/ml AbA. The *pdr5Δ yor1* strains transformed with either vector alone or vector containing Ypk1 grew similarly beyond 40ng/ml AbA. The *pdr5Δ yor1 mss4* mutant carrying vector alone was unable to grow at 30ng/ml, while the same strain carrying high-copy Ypk1 grew well to a concentration of 40ng/ml. This partial suppression of the AbA sensitive phenotype suggests that Ypk1 may function downstream of Mss4, though it does not appear to be the only downstream effector. This data does not rule out a possibility that Ypk1 is acting in a parallel pathway that has overlapping function with another downstream effector of Mss4.

Over-expression of Mss4 partially suppresses the *ypk1Δ* AbA sensitivity

The partial suppression of the *mss4* mutant strain by Ypk1 suggests that either Ypk1 functions downstream of Mss4 or that it functions in a parallel pathway. We hypothesized that if these proteins function in the same pathway, over-expression of Mss4 would have no effect in the absence of Ypk1. Surprisingly, over-expression of Mss4 caused a slight increase in AbA tolerance, even in the absence of Ypk1 (Figure 26). The *ypk1Δ* strain was very sick on AbA, even at the very low concentration of 5ng/ml, while this strain in the presence of multicopy Mss4 restored some growth at 5ng/ml, though not beyond. Over-expression of Mss4 showed a slight increase in AbA tolerance in both the

wild-type (40ng/ml) and *pdr5Δ yor1* (100ng/ml). These data do not clearly demonstrate a role for Ypk1 directly downstream of Mss4 signaling. However, it is possible that Ypk1 does function downstream of Mss4, but that a second pathway also controlled by Mss4 acts in parallel in AbA tolerance as well.

Pkh1, another regulator of Ypk1 activity, affects AbA tolerance

Ypk1 has more than one upstream effector that regulates its activity. Aside from Pkc1, as mentioned above, the protein kinases Pkh1 and Pkh2 (*P*kb-activating *k*inase *h*omologue) are also well-known upstream regulators of Ypk1 activity and cell wall integrity (88). Since the above data also do not rule out a pathway separate from Mss4 for regulation of Ypk1 in this case, we next sought to determine if Pkh1 or 2 might be involved. I hypothesized that Pkh1 or Pkh2 may be activated in the absence of Pdr5 and Yor1. Single deletions of *PKH1* and *PKH2* were constructed in both wild-type and *pdr5Δ yor1* strains. These strains were grown to mid-log phase and spotted onto YPD plates containing varying concentrations of AbA (Figure 27). The *pkh1Δ* cells were more sensitive to AbA, growing well until 25ngml, as compared to wild-type, which became sensitive around 40ng/ml. Loss of Pkh1 in the *pdr5Δ yor1* strain showed sensitivity at 75ng/ml AbA, while the *pdr5Δ yor1* strain grew well at this same concentration. Loss of Pkh2 did not phenocopy the strains lacking Pkh1, suggesting this is specific to Pkh1. These data argue for a role of Pkh1 in AbA tolerance, possibly via activation of Ypk1.

Ypk1 does not appear to have increased phosphorylation in the *pdr5Δ yor1* strain

The above data suggest that activation of Ypk1, either by Pkh1 or a downstream effector of Mss4, may be crucial to the cell's ability to maintain

resistance to AbA. Based on these data we hypothesized that perhaps Ypk1 gets activated in the *pdr5Δ yor1* strain, thus contributing to the strong resistance phenotype. To assess this, wild-type and *pdr5Δ yor1* strains were transformed with either vector alone or a galactose-inducible form of Ypk1 that is myc tagged. Cells were grown and processed as described in experimental procedures. Western blotting did not show a distinct change in the amount of phosphorylated Ypk1 between wild-type and the *pdr5Δ yor1* strains (Figure 28). In the case of Pkh1, activated Ypk1 would be indicated by an increase in phosphorylation of Ypk1. Although the amount of phosphorylation does not appear to be different, this was not assessed directly and it is possible that the specific residues that get phosphorylated differ between these strains. It is also possible that there may only be a phosphorylation difference triggered by the presence of AbA.

Low AbA concentrations increase levels of Ypk1 in the *pdr5Δ yor1* strain

It was shown by the Thorner group that Ypk1 phosphorylation is obliterated by the addition of an exceedingly high concentration of AbA (500ng/ml) (16). This was indicated to be due to AbA preventing formation of MIPC, which in turn stimulates Fpk1 phosphorylation and activity (16). Fpk1 is a protein kinase that phosphorylates and inhibits Ypk1. I repeated this same experiment in our wild-type and *pdr5Δ yor1* strains and found a similar result (Figure 29A). In the absence of AbA treatment, multiple phosphorylation species for Ypk1 were detected in both wild-type and *pdr5Δ yor1* strains. However, in the lanes treated with AbA, no phosphorylated forms of Ypk1 are present. Although a very high level of AbA blocks Ypk1 phosphorylation, this amount of AbA far exceeds the amount necessary to inhibit growth of either the wild-type strain or the *pdr5Δ yor1* strain in a plate assay. To determine if there might be a drug-

dependent change in Ypk1 phosphorylation at a more relevant concentration of AbA, this was re-assessed using concentrations similar to those used in the plate assays above. Wild-type and *pdr5Δ yor1* strains were grown and processed as above, except that cultures were treated with either 50ng/ml or 100ng/ml concentrations of AbA instead of 500ng/ml. Western blotting indicated that as the amount of AbA increased, the number of phosphorylated species of Ypk1 decreased in both strains (Figure 29B). However, it appeared that the total amount of Ypk1 increased as the concentration of AbA was increased in the *pdr5Δ yor1* strain, which was not seen in the wild-type strain. These data suggest that treatment with low levels of AbA alter the amount of Ypk1 in the *pdr5Δ yor1* strain, possibly contributing to the resistance phenotype of this strain.

EMS Mutant B19 is suppressed by over-expression of Sfk1

The EMS mutant designated B19 is currently unknown as it was not amenable to standard cloning techniques and has not been identified from the sequencing analysis as yet. However, one gene of interest in the list of candidates from this mutant was Sfk1. Sfk1 is known to interact and recruit Stt4, the enzyme that makes PI_4P, the substrate for Mss4, to the plasma membrane (103). Loss of Sfk1 has been shown to decrease the amount of Stt4 at the plasma membrane by about 30-40% (103). Furthermore, Sfk1 is regulated, in part, by the Yrr1 transcription factor, which is regulated by Pdr1 (69). To determine if Sfk1 could suppress the AbA sensitivity of the B19 mutant, wild-type, *pdr5Δ yor1*, and the B19 strains were transformed with either high-copy vector only or vector expressing Sfk1. Surprisingly, the B19 mutant strain was suppressed by the plasmid over-expressing Sfk1 (Figure 30). The B19 strain, carrying vector alone, was unable to grow at 25ng/ml while the B19 mutant

carrying the Sfk1 over-expressing plasmid grew to about 50ng/ml AbA. This construct did not appear to increase AbA tolerance in wild-type or *pdr5Δ yor1* cells. One caveat to the high-copy plasmid used here is that it contains multiple genes from a chromosomal region, so it was possible the suppression was not specific to Sfk1. To test whether or not Sfk1 by itself could affect the B19 mutant AbA phenotype, a low-copy plasmid containing Sfk1 under control of its own promoter was constructed. This low-copy clone of Sfk1 was able to slightly suppress the AbA phenotype of the B19 mutant, allowing growth at 10ng/ml AbA, while the mutant strain carrying vector only was unable to grow at this concentration (data not shown). Unfortunately, deletion of Sfk1 in either wild-type or *pdr5Δ yor1* strains showed no change in AbA tolerance (Figure 31) and the B19 mutant was complemented by a *pdr5Δ yor1 sfk1Δ* strain (data not shown). These data suggest that the mutation responsible for the AbA phenotype of B19 is not Sfk1. However, the suppression by Sfk1 supplies yet another link between the cell wall integrity pathway and AbA, suggesting that AbA may be affecting this pathway in a novel way. Possibly the mutation in B19 is in a gene that interacts with Sfk1, however this has not yet been determined.

Over-expression of the transcription factor, Yrr1, increases AbA tolerance

As mentioned above, Sfk1 is a target of Yrr1 (*Y*east *R*everomycin-A *R*esistance, aka Pdr2) (69). Yrr1 is a transcription factor that contains PDREs in its promoter and is both activated by Pdr1/Pdr3 and is also positively auto-regulated (5). Intriguingly, I found that a hyperactive form of Yrr1 increases tolerance to AbA (Figure 32). Wild-type cells carrying vector alone were able to grow to 50ng/ml AbA, while a wild-type strain carrying the hyperactive allele of Yrr1 was growing robustly at 100ng/ml AbA (and beyond). As Yor1 is a known

target of Yrr1, as well as a known mediator of resistance to AbA, we next asked whether the effect seen by Yrr1 is solely from Yor1. Cells deleted for Yor1 and carrying vector alone grew similarly to wild-type cells. Strikingly, loss of Yor1 blunted the effect of Yrr1 on AbA, but did not abolish it, suggesting that there is more than one Yrr1-regulated target that confers resistance to AbA. As mentioned above, Sfk1 is also a target of Yrr1. Deletion of Sfk1 did not suppress the robust AbA resistance phenotype of the hyperactive Yrr1 allele and was comparable to wild-type cells carrying the same plasmid. This suggests that the role of Sfk1 here is less than that of Yor1, however it is possible that deletion of Sfk1 along with Yor1 would blunt the phenotype further. It is also possible that another target of Yrr1 has a novel role in AbA tolerance. Deletion of Yrr1 in either the wild-type or *pdr5Δ yor1* strains did not show any defect in the AbA tolerance of these strains (data not shown). However, another related transcription factor, Yrm1, may be compensating for loss of Yrr1 in these strains and double mutants of these factors may be necessary to discern a phenotype, if one exists.

Pdr1, but not Pdr3 is important for the AbA phenotype of the *pdr5Δ yor1* strain

Since Pdr5 and Yor1 are regulated by the PDR transcription factors Pdr1 and Pdr3, we considered the idea that there might be feedback to the PDR network in the absence of these ABC transporters. Deletions of Pdr1 and Pdr3 were constructed in the *pdr5Δ yor1* strains and tested on AbA with wild-type and *pdr5Δ yor1* strains, along with *pdr1Δ* and *pdr3Δ* strains that were constructed previously (Figure 33). Neither the *pdr1Δ* or *pdr3Δ* strains showed any difference compared to wild-type, all growing to less than 75ng/ml AbA. However, loss of Pdr1 specifically affected the resistance of the *pdr5Δ yor1* strain. The *pdr5Δ yor1*

and *pdr5Δ yor1 pdr3Δ* strains grew well at 75ng/ml while the *pdr5Δ yor1 pdr1Δ* strain behaved similarly to the wild-type strain. This data indicates that Pdr1 specifically plays a role downstream of the *pdr5Δ yor1* strain in AbA tolerance. The target of Pdr1 in this background has not yet been determined.

Discussion

This genetic screen was aimed at determining the nature of the genes involved in triggering the enhanced AbA resistance I observed in a *pdr5Δ yor1* strain. My interest in this phenotype was prompted by previous observations that loss of these two ABC transporters typically led to pronounced drug sensitivity (7,10,12). The finding that mutations in a range of genes can reverse the AbA resistance phenotype, coupled with data in the previous chapter demonstrating a likely endocytic defect in the *pdr5Δ yor1* strain suggests that this genetic background has a defect in the plasma membrane that triggers a pleiotropic response to maintain cellular integrity. It is important to note that the presence of AbA is not required to cause the plasma membrane defect in the *pdr5Δ yor1* strain since I was able to demonstrate endocytic defects in this strain in the absence of any drug. However, early studies of AbA treatment demonstrated that these cells had delocalized chitin and problems with actin assembly (104). These data correlate nicely with the genes involved in cell wall integrity, GPI-anchored protein trafficking, exocytosis, and actin cytoskeleton organization that were identified in the EMS screen.

Gda1 was isolated from the EMS screen as a suppressor of the AbA resistance of the *pdr5Δ yor1* strain. Since Gda1 is involved in mannosylation of sphingolipids and proteins, the first obvious question we asked was if the AbA phenotype was due to changes in sphingolipids or proteins. The similarity in AbA sensitivity of the strains lacking Gda1 or Csg2 suggested initially that the effect

was due to changes in sphingolipid content. Evidence from the Conzelmann lab has demonstrated that changes in N-glycosylation affect IPC levels in the cell (105). Cells lacking Cwh8, a dolichyl pyrophosphate phosphatase that is important for normal N-glycosylation, show a decrease in IPC levels that is independent of sphingolipid enzyme activity (105). Since Gda1 is involved in N-mannosylation, it is possible that loss of this protein causes a chronic decrease in IPC levels, which sensitizes the cell to AbA. However, wild-type and *gda1Δ* strains did not show obvious differences in IPC levels as measured by TLC (Figure 19B). This is in contrast to the sphingolipid content of a *csg2Δ* strain which shows complete loss of MIPC and $M(IP)_2C$. These data suggested that perhaps this phenotype was not dependent on chronic sphingolipid content changes.

Surprisingly, Gda1 was recently implicated in localization and anchoring of GPI-anchored cell wall proteins (97). The outer cell wall layer is composed of glycosylated mannoproteins, which protect the glucan layer from the degradative activity of glucanases (106). About half of all GPI-anchored proteins in the cell are found at the cell wall and are linked to β1-3 glucans via β1-6 glucan chains (106). This group demonstrated that loss of Gda1 caused a decrease in the amount of GPI-anchored proteins localized to the cell wall and suggested that this decrease was caused by a diminished amount of glycosylation, which may exclude these proteins from the cell wall (97). Studies in *Candida albicans* also demonstrated that loss of Gda1 causes the cells to become more susceptible to β1-3 glucanase activity, possibly due to a decreased outer layer of protective cell wall proteins (107,108). These data suggest that loss of Gda1 may cause cells to become more susceptible to AbA due to effects on cell wall composition. Remarkably, we also demonstrated that loss of Bst1, a gene involved in deacylating GPI-anchors and allowing trafficking of these GPI-anchored proteins

to the Golgi (98), causes a dramatic decrease in AbA tolerance. These data provide support for the idea that cell wall composition and integrity may be crucial for AbA tolerance.

Mss4 is the only PI_4P 5-kinase in the yeast, *Saccharomyces cerevisiae*. Its product, $PI_{4,5}P_2$, plays a crucial role in multiple downstream signaling pathways, including those involved in exocytosis and cell wall integrity (39,41,86). Reversal of the *pdr5Δ yor1* phenotype by mutation in Mss4 was an intriguing result. It suggested that levels of $PI_{4,5}P_2$ are important for AbA tolerance and led to the idea that perhaps Mss4 is more active in the absence of Pdr5 and Yor1. The suppression of the *pdr5Δ yor1 mss4* mutant strain by deletion of *SJL1*, a specific $PI_{4,5}P_2$ phosphatase, provided further support for the idea that levels of $PI_{4,5}P_2$ may be important for this phenotype.

One downstream effect of Mss4 involves regulation of exocytosis. Exo70, a component of the exocyst complex, has been shown to be recruited to the plasma membrane via interaction with $PI_{4,5}P_2$, which mediates targeting of the exocyst complex to the plasma membrane (41). Exo70 and Sec3 have been suggested to act together in recruitment of the exocyst and double mutants show a more severe decrease in exocyst targeting than either single mutant (41). As was discussed in Chapter 2, the *pdr5Δ yor1* strain has a defect in normal endocytosis, which affects turnover of Tat2 and probably other proteins. One hypothesis regarding *pdr5Δ yor1* resistance to AbA was that decreased endocytosis may be slowing either entry of AbA into the cell or slowing turnover of an unknown AbA exporter protein. We considered the possibility that mutation in Mss4 reverses the AbA resistance of the *pdr5Δ yor1* strain because it was slowing exocytosis, thus counteracting the endocytic defect of the *pdr5Δ yor1* strain and enhancing susceptibility to this drug. Strikingly, deletion of Sec3, the only non-essential secretory gene, in the *pdr5Δ yor1* strain showed a dramatic

decrease in AbA tolerance that was similar to that of the *pdr5Δ yor1 mss4* mutant. This suggests that changes in exocytosis due to alteration of $PI_{4,5}P_2$ levels, and possibly decreased recruitment of Exo70, may account at least in part for the AbA sensitivity of the *pdr5Δ yor1 mss4* mutant strain. Deletion of Sec3 on its own showed a comparable AbA sensitivity, suggesting that an exocytic defect, regardless of background, affects the cell's ability to deal with AbA. One intriguing idea as to why exocytic changes might affect AbA tolerance is that GPI-anchored proteins, or other components of the cell wall, are delayed in trafficking, leading to similar defects as are seen in the absence of Gda1 or Bst1.

The ability of Ypk1 over-expression to partially suppress the AbA phenotype of the *pdr5Δ yor1 mss4* mutant strain suggests two possibilities, either Ypk1 has a role directly downstream of Mss4 or that it functions in parallel with another downstream effector of Mss4 in tolerance to AbA. The AbA sensitive phenotype of the *pkh1Δ* strain provides further support for the idea that Ypk1 may be functioning in parallel with Mss4. Pkh1 activates not only Ypk1, but also Pkc1, which is regulated by downstream effectors of Mss4 as well (109). Work from other groups has indicated that the Ypk proteins may act in parallel with the Pkc1-mediated signaling pathway to maintain cell wall integrity, possibly via independent activation of the MAP kinase, Mpk1 (37,88). Ypk mutant strains have decreased Mpk1 activity and loss of Ypk1, Ypk2, and Mpk1 results in inviability (37,88). It is interesting that single deletions of either Pkh1 or Ypk1 specifically affect AbA tolerance, while their counterparts, Pkh2 and Ypk2 do not, as it has been demonstrated previously that Pkh1 appears to prefer Ypk1 as a substrate, while Pkh2 prefers Ypk2 (88). This result suggests that *pkh1Δ* strains may be sensitive to AbA due to a lack of activation of Ypk1. The implication of Pkh1 and Ypk1 in cell wall integrity signaling is interesting, as it may be that loss

of these proteins disrupts the cell wall and thereby allows easier entry of AbA into the cell.

More recent work from the Thorner lab indicated that one downstream target of Ypk1 is Fpk1, a kinase that activates flippases, but also phosphorylates Ypk1 at N-terminal residues, S51 and S71, thereby inactivating it (16). Their work indicated that when Fpk1 was active, Ypk1 appeared to have an increased number of slower migrating (phosphorylated) species as compared to strains lacking Fpk1 in which this was severely decreased (16). Fpk1 appears to be modulated in two different ways, either by phosphorylation by Ypk1 or by stimulation via the complex sphingolipid MIPC, although it has not been determined if modulation of Fpk1 via MIPC is a direct effect or if the signal from MIPC may be acting through Ypk1 (16). The above evidence suggests that the decrease in slower migrating bands seen in the *pdr5Δ yor1* strain may be due to decreased Fpk1 activity, and therefore increased Ypk1 activity. Since loss of Pdr5 and Yor1 decreases outer movement of phospholipids, it seems reasonable to suggest that the cell may compensate for this loss and down regulate an activator of flippase activity in an attempt to modulate the membrane composition.

This same group also showed that treatment with very high levels of AbA, which causes a decrease in MIPC, also decreases Fpk1 activity (16). This would then decrease Fpk1-mediated phosphorylation of Ypk1 and presumably increase Ypk1 activity. Surprisingly, treatment with lower concentrations of AbA shows a different result as compared to strains treated with high AbA concentrations (Figure 29B). In wild-type cells, there are multiple phosphorylation bands in the absence of drug, which disappear even with low dose AbA treatment, behaving somewhat like the cells treated with very high levels of AbA. The *pdr5Δ yor1* strain shows a decrease in the slowest migrating (more phosphorylated) bands,

as well as an accumulation of less phosphorylated species of Ypk1, both of which are directly correlated with an increase in AbA treatment. This accumulation appears to be more dramatic than what one might expect to see if the normally phosphorylated forms of Ypk1 were de-phosphorylated and collapsed into a single band. This suggests that perhaps activated Ypk1 accumulates in this background due to enhanced Pkh1 activity and decreased Fpk1 activity. In the future, mass spectrometry analysis would be useful in order to gain better insight into which kinases might be modifying Ypk1 by determining which residues are phosphorylated. A better understanding of how Ypk1 is being modified may give some insight into the effects of AbA and loss of Pdr5 and Yor1 on Ypk1 function.

As mentioned earlier, Ure2 plays a role in regulating nitrogen catabolite repression. Under normal conditions, Ure2 is bound to the transcription factor, Gln3, sequestering it in the cytoplasm. In order for Gln3 to be bound to Ure2, it is phosphorylated by TOR, a subunit of the Target of Rapamycin Complex 1 (TORC1) (94). In the absence of Ure2, a majority of Gln3 moves to the nucleus, and presumably induces transcription of its target genes (94). Under conditions of nitrogen starvation, the general amino acid permease, Gap1, is induced and stabilized by Npr1 kinase-mediated phosphorylation, which prevents ubiquitination and subsequent degradation (55). Conversely, specific amino acid permeases such as Tat2, are degraded during conditions of nitrogen starvation, possibly via negative regulation by Npr1, although how Npr1 negatively regulates Tat2 is unknown (96). The data above demonstrating that deletion of Ure2 dramatically decreased the ability of the *pdr5Δ yor1* strain to tolerate low levels of tryptophan suggests that loss of Ure2 causes aberrant induction of genes such as Npr1 and/or Gap1, thus mimicking the cell's response to nitrogen starvation.

Remarkably, new evidence has demonstrated that Ypk1 is degraded upon nitrogen starvation and that this effect appears to be specific as treatment with rapamycin or glucose starvation did not show similar results (110). These associations are intriguing in light of the evidence presented above that loss of either Ure2 or Ypk1 causes a decrease in tolerance to AbA. This leads to the question of whether or not Ypk1 may be degraded upon loss of Ure2, since Ure2 deletion appears to mimic nitrogen starvation. If Ypk1 gets degraded in the absence of Ure2, this may explain why loss of Ure2 causes AbA sensitivity, although how Ypk1 itself fits into AbA tolerance is still under investigation.

The data indicating that loss of Pdr1 specifically affected AbA tolerance in the absence of Pdr5 and Yor1 suggests that there may be some sort of feedback through the PDR network that is at least in part responsible for the resistance phenotype. It is intriguing that a hyperactive form of the PDR transcription factor, Yrr1, increases resistance to AbA. These data suggest that perhaps Yrr1 gets induced by Pdr1 in the absence of Pdr5 and Yor1, however, the target of Yrr1 is unknown. In a wild-type cell it does appear that a majority of the effect of the hyperactive Yrr1 is coming through Yor1, though there is still some AbA resistance even in the absence of Yor1. Loss of Sfk1 alone does not appear to decrease the robust AbA resistance phenotype of the hyperactive Yrr1 protein, although it is still possible that this is the other gene important in this phenotype but that its effect is masked by the presence of Yor1. A *yor1 skf1Δ* double mutant strain would be necessary to examine this idea. It is also possible that another downstream target of Yrr1 is responsible for the remaining AbA tolerance.

The PDR pathway has been known to play an important part in maintenance of sphingolipid biosynthesis and plasma membrane asymmetry for some time (14,44). Several groups have also demonstrated that sphingolipid

signals are important in modulating activation of Pkh1 and Ypk1, which in turn activate Pkc1 and Mpk1, respectively (35,37,88). It seems reasonable to suggest that perhaps one role of the PDR pathway in AbA resistance stems from regulation of sphingolipids, which in turn are important in trafficking of GPI-anchored proteins to the cell surface and are also important in modulating downstream effectors involved in the cell wall integrity pathways.

One attractive notion suggested by the data above is that the cell wall integrity pathway is activated in the *pdr5Δ yor1* background (Figure 34). If this is true, then the *pdr5Δ yor1* strain may have an altered cell wall structure, thus making it more difficult for AbA to get into the cell if it targets the cell wall for entry, as has been suggested previously (104). This idea is supported by the decrease in resistance of the *pdr5Δ yor1* strain in the absence of genes known to be involved in cell wall integrity (Mss4, Ypk1, indirectly Gda1 and Bst1), however many more experiments are needed to substantiate this theory.

Table 2. Strains used in this study

Strain	Genotype	Ref.
SEY6210	MATα *leu2-3-112 ura3-52 lys2-801 trp1-901 his3-200 suc2-9 Mel-*	Scott Emr
SEY6210 pdr5Δyor1	SEY6210 *pdr5::hisG yor1::hisG*	Moye-Rowley Lab Collection
SEY6210 Δrsb1	SEY6210 *rsb1::natMX4*	(46)
SRY5	SEY6210 *pdr5::hisG yor1::hisG rsb1:natMX4*	This study
SRY31	SEY6210 *AUR1*-TAP:HIS3	This study
SRY33	SEY6210 *pdr5::hisG yor1::hisG* AUR1-TAP HIS3	This study
SRY88	SEY6210 *AUR1*-GFP HIS3	This study
SRY89	SEY6210 *pdr5::hisG yor1::hisG* AUR1-GFP HIS3	This study
SRY71	SEY6210 *gda1::natMX4*	This study
SRY73	SEY6210 *pdr5::hisG yor1::hisG gda1::kanMX4*	This study
SRY82	SEY6210 *csg2::natMX4*	This study
SRY117	SEY6210 *pdr5::hisG yor1::hisG csg2::kanMX4*	This study
B33	SEY6210 *pdr5::hisG yor1::hisG gda1*	This study
B27	SEY6210 *pdr5::hisG yor1::hisG cyc8G337D*	This study
C25	SEY6210 *pdr5::hisG yor1::hisG mss4_T271I, T724M*	This study
C17	Unknown EMS mutant	This study
C21	Unknown EMS mutant	This study
C1	Unknown EMS mutant	This study
B19	Unknown EMS mutant	This study
SRY120	SEY6210 *ure2::kanMX4*	This study
SRY116	SEY6210 *pdr5::hisG yor1::hisG ure2::kanMX4*	This study
SRY202	SEY6210 *sjl1::kanMX4*	This study
SRY203	SEY6210 *pdr5::hisG yor1::hisG sjl1::kanMX4*	This study
SRY204	SEY6210 *pdr5::hisG yor1::hisG mss4_T271I, T724M sjl1::kanMX4*	This study
SRY213	SEY6210 *sec3::HIS3-MX6*	This study
SRY214	SEY6210 *pdr5::hisG yor1::hisG sec3::HIS3-MX6*	This study
SRY175	SEY6210 *ypk1::kanMX4*	This study
SRY172	SEY6210 *pdr5::hisG yor1::hisG ypk1::kanMX4*	This study
SRY179	SEY6210 *ypk2::kanMX4*	This study

Table 2 continued

SRY180	SEY6210 *pdr5::hisG yor1::hisG ypk2::kanMX4*	This study
SRY183	SEY6210 *pkh1::kanMX4*	This study
SRY184	SEY6210 *pkh2::kanMX4*	This study
SRY185	SEY6210 *pdr5::hisG yor1::hisG pkh1::kanMX4*	This study
SRY186	SEY6210 *pdr5::hisG yor1::hisG pkh2::kanMX4*	This study
PB3	SEY6210 *pdr1::hisG*	Moye-Rowley Lab Collection
PB2	SEY6210 *pdr3::hisG*	Moye-Rowley Lab Collection
SRY187	SEY6210 *pdr5::hisG yor1::hisG pdr1::kanMX4*	This study
SRY188	SEY6210 *pdr5::hisG yor1::hisG pdr3::kanMX4*	This study
SRY215	SEY6210 *bst1::kanMX4*	This study
SRY216	SEY6210 *pdr5::hisG yor1::hisG bst1::kanMX4*	This study

Table 3. Primer list

Gene	Used for	Primers 5'-3' orientation
GDA1	Amplification of gda1::kanMX4 cassette	F - GCGGTAGAAGAATGTCAAAAC R - CGACCTGAAATGCAGTTTCTTC
GDA1	PCR confirmation of deletion	F - GCAGCATTTCTTCTGCATGG R - GGTACATGTCTCCGGGGAAG
CSG2	Amplification of csg2::kanMX4 cassette	F - GGTGAAGAACGCATGCAAGAAG R - CCAAGCGGAAGGAACCGTGTGT
CSG2	PCR confirmation of deletion	F - CTTGTGATCCAGCAAGAGAC R - TTGCGGGCGATCAGTAACTG
URE2	Amplification of ure2::kanMX4 cassette	F - GCAGGGCATGCGGCAGTGAA R - GGGACATTACTCACAGATTG
URE2	PCR confirmation of deletion	F - GCACTCCGTCCTTGTCGACT R -CATTAGTCGGGAAATCTTGCC
YPK1	Amplification of ypk1::kanMX4 cassette	F - ACAGACGAACCAACAGTCCG R - GGTGGTCGTTTACTTGTATT
YPK1	PCR confirmation of deletion	F - GCACAGGCAGTTCTGGTGCA R - CATCTAGGGCAGATTTCACGA
YPK2	Amplification of ypk2::kanMX4 cassette	F - CGGTCATCAAGTTCTTGAACT R - GGTAAGGCTCCCCATGGCTG
YPK2	PCR confirmation of deletion	F - GATTGTCAGGTACAGGTTCTT R - GGACTAGGCATCACCCAGACT
SJL1	Amplification of sjl1::kanMX4 cassette	F - GCCAAAGGTCGTTTTCAAGT R - GATCCTTGGGCCTAGAAATA
SJL1	PCR confirmation of deletion	F - GTGGCGAATTGTCAAACTTG R - GACACTACAACCCCTGTTGT
SEC3	Amplification of HIS3-MX6 cassette (upper case indicates 50bp of SEC3 sequence flanking the ORF, lower case indicates 20bp annealing to HIS3-MX6 cassette)	F - GTGCCAGATATCTCCAGCTA GGTAACAAGGCTACGCAATTTATT CTATATTcggatccccgggttaattaa R - TTACTTAATTAGTCTAAATATGT AATATGAAGCGACAATGCAGAGG TTACgaattcgagctcgtttaaac
SEC3	PCR confirmation of deletion	F - GACTATGTCACCCGGTATTA R - CGTATTTCCCGTGCATAAGGA
PKH1	Amplification of pkh1::kanMX4 cassette	F - CAGAAGGGTGCCAACATGTA R - CATACGATGTAGGCTAAGCA
PKH1	PCR confirmation of deletion	F - GTTAGGAACCAGAATCACTT R - AATGGGATTCCTCGATATGC

Table 3 continued

PKH2	Amplification of pkh2::kanMX4 cassette	F - GACAGATGGTTAACGATCGA R - CTGTTTGCAAAGGGGGAACA
PKH2	PCR confirmation of deletion	F - GCCATTTCCGACTAGCTCTA R - CAGGTGCCTTGGAATTTGAT
PDR1	Amplification of pdr1::kanMX4 cassette	F - CATTCCTACGTTATTACCAC R -CAAGAGCCATCGAACTTTCT
PDR1	PCR confirmation of deletion	F - GCTTCAGCCATTTACCCTGA R - GATAAGTTGCTAGCCCTTGT
PDR3	Amplification of pdr3::kanMX4 cassette	F - CTATTCTCACTGCCCTCTAT R - GGAATCGGTGTTTCTACACA
PDR3	PCR confirmation of deletion	F - TGAATGGCCTACTTCATACT R - AACTATTAGTTGATAGACGA
BST1	Amplification of bst1::kanMX4 cassette	F - ATACTCTTATATAGACAATT R - TCAAAATTTACGGCTTTGAA
BST1	PCR confirmation of deletion	F - CACCGAAATGAACACCGATA R - GAAGGAAGGAAACAACATCG

Table 4. Plasmids used in this study

Plasmid Name	Description	Ref.
pSR47	pRS316 Mss4	This Study
YGPM11g15	pGP564 Chromosome IV coordinates 863637-874941 (contains complete Mss4)	2μm tiling collection
pSR97	pRS426 Ypk1 HA	This Study
pAM54	pYEp351 Gal Ypk1 Myc	(101)
YGPM7h13	pGP564 Chromosome XI coordinates 340089-349629 (contains complete Sfk1)	2μm tiling collection
pXTZ121	pYEp352 Yrr1-1	Moye-Rowley Lab Collection

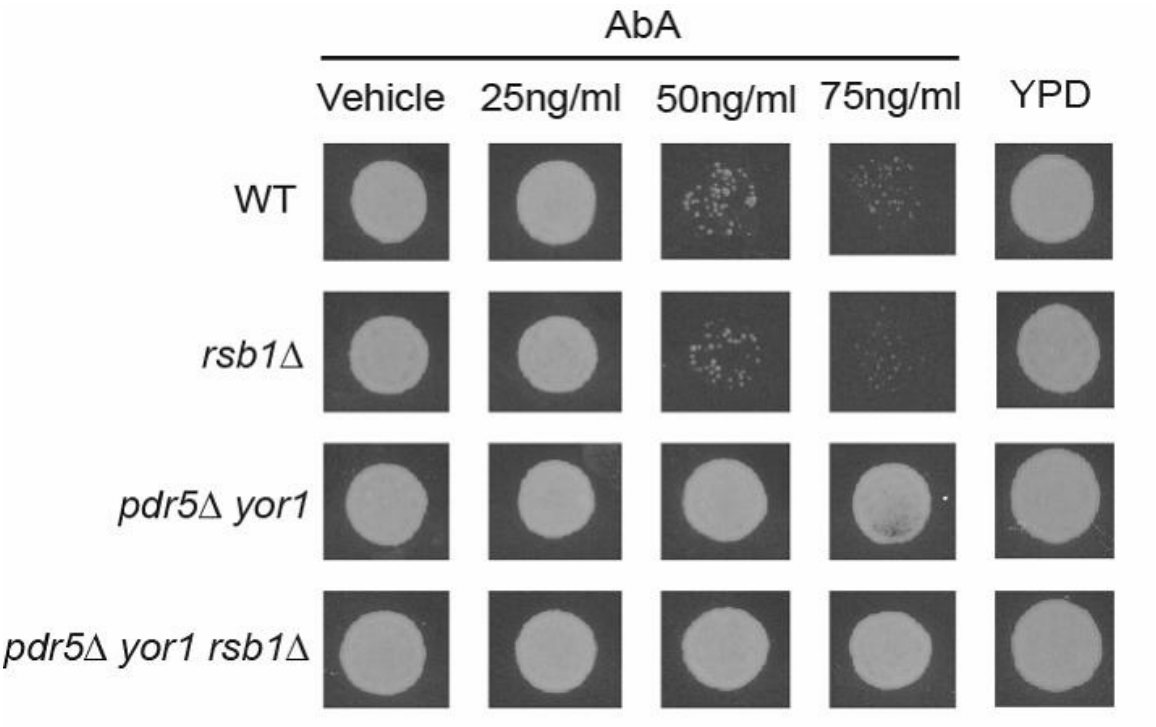

Figure 15. Loss of Pdr5 and Yor1 increases resistance to AbA, independent of Rsb1. Wild-type*, rsb1Δ, pdr5Δ yor1*, and *pdr5Δ yor1 rsb1Δ* strains were grown to mid-log phase in YPD and spotted onto YPD plates containing the indicated concentrations of AbA and YPD alone. Strains lacking Rsb1 show no effect on AbA, while strains lacking Pdr5 and Yor1 are robustly resistant, indicating that this phenotype is independent of Rsb1.

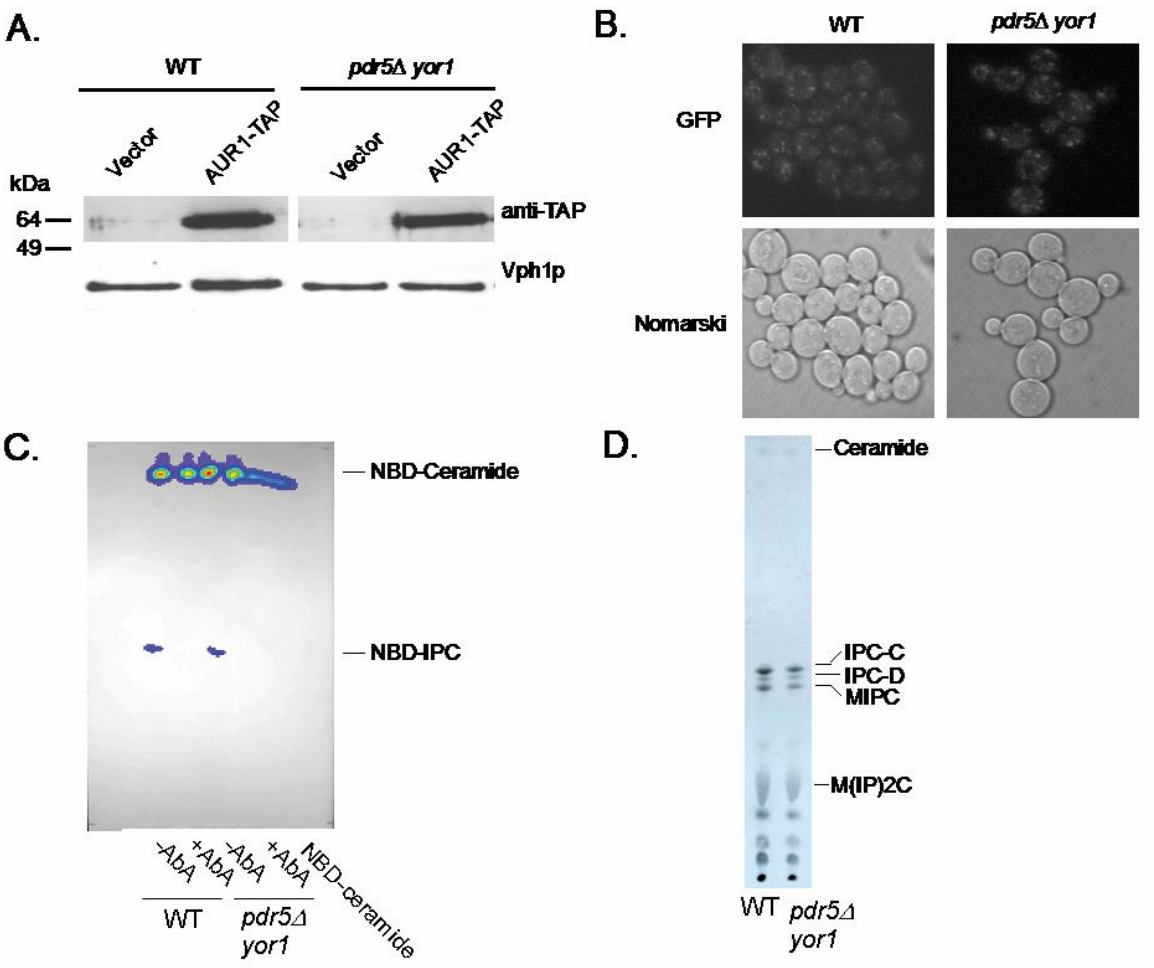

Figure 16. Changes in Aur1 are not responsible for the AbA resistant phenotype of the *pdr5Δ yor1* strain. (A) Aur1 was C-terminally TAP tagged in both wild-type and *pdr5Δ yor1* strains. Cells were grown to mid-log phase and protein extracts were run on SDS-PAGE and Western blotted with anti-TAP. The membrane was stripped and re-probed for Vph1 as a loading control. (B) Aur1 was C-terminally GFP tagged in the same strains as in (A) and strains were grown to mid-log phase and visualized by fluorescence microscopy. (C) Wild-type and *pdr5Δ yor1* strains were grown to an OD_{A600} of approximately 0.4. Cells pretreated with AbA were resuspended in medium containing fatty acid free BSA and treated with 10μg/ml AbA for 10 min at 30°C prior to addition of NBD-ceramide for 20 minutes. Lipids were extracted, normalized for fluorescence units and equal amounts were spotted onto TLC plates and visualized with an IVIS bioluminescence imager. (D) The same strains as above were labeled with ^{3}H-Serine for 6 hours and lipids were extracted as described in experimental procedures. Equal counts were spotted onto TLC plates and were exposed to film for 3-5 days. All of these assays indicated no change in Aur1 expression, localization, or activity, suggesting that Aur1 itself is not responsible for the AbA resistance of the *pdr5Δ yor1* strain.

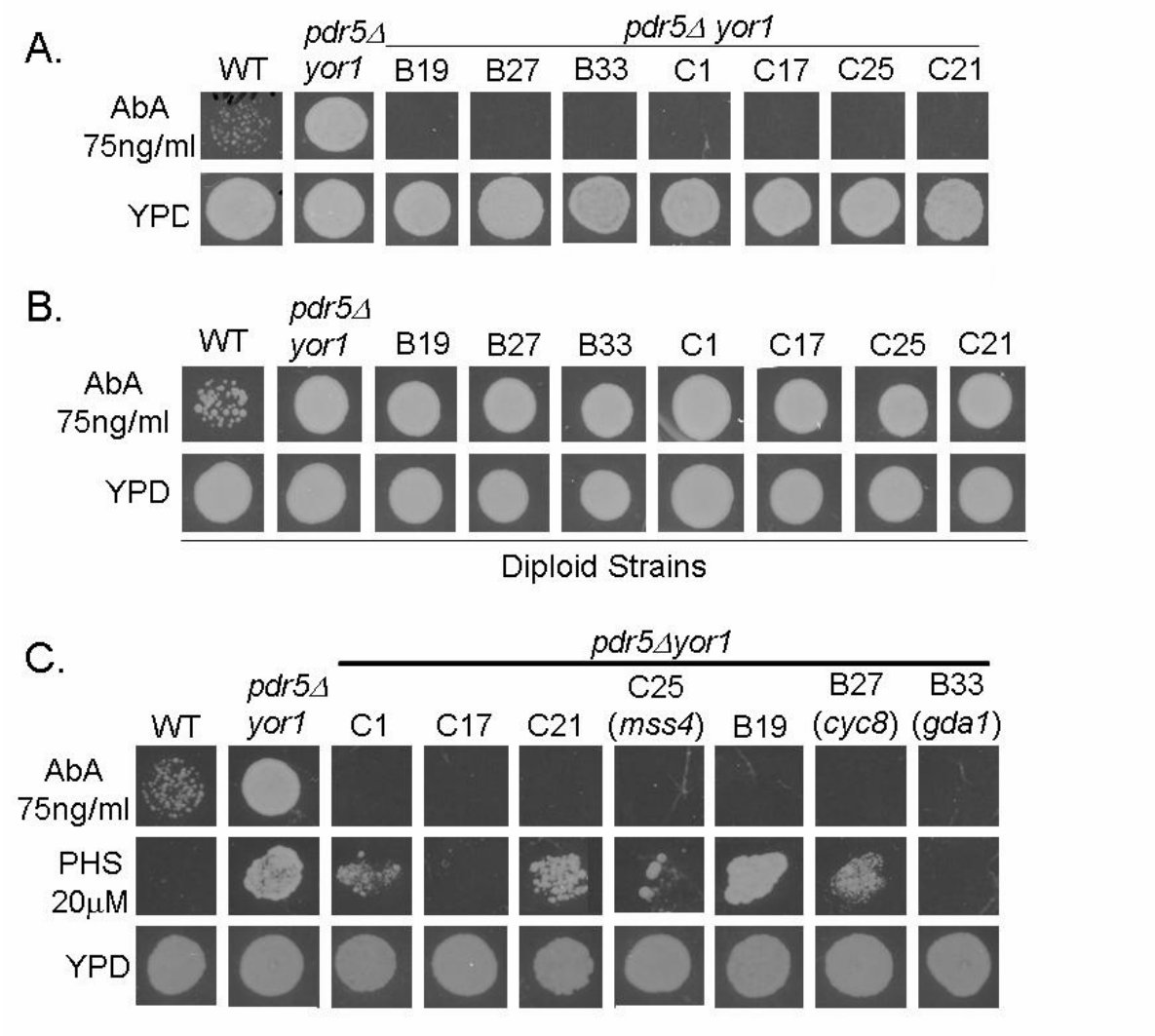

Figure 17. Mutants obtained from EMS screening are sensitive to AbA, recessive, and show variable phenotypes on PHS. (A) Wild-type, *pdr5Δ yor1*, and 7 EMS mutant strains obtained after 3 back-crossings were grown to mid-log phase in YPD and spotted onto YPD plates containing 75ng/ml AbA and YPD alone. (B) The wild-type strain was mated to an isogenic wild-type strain of opposite mating type, while all EMS mutant strains and the *pdr5Δ yor1* strain were mated to the parent *pdr5Δ yor1* strain of opposite mating type to form diploids and were assessed for an AbA phenotype as described in (A). (C) The same strains as above were grown to mid-log phase and spotted onto YPD alone or YPD plates containing 75ng/ml AbA or 20μM PHS. All strains were sensitive to AbA and recessive as determined by a reversal of the AbA sensitive phenotype when mated to the parent strain. The mutant haploid strains showed a diverse range of sensitivity to PHS, indicating that there are two classes of mutations, some that are important for both AbA and PHS resistance, and others that are specific for AbA tolerance alone.

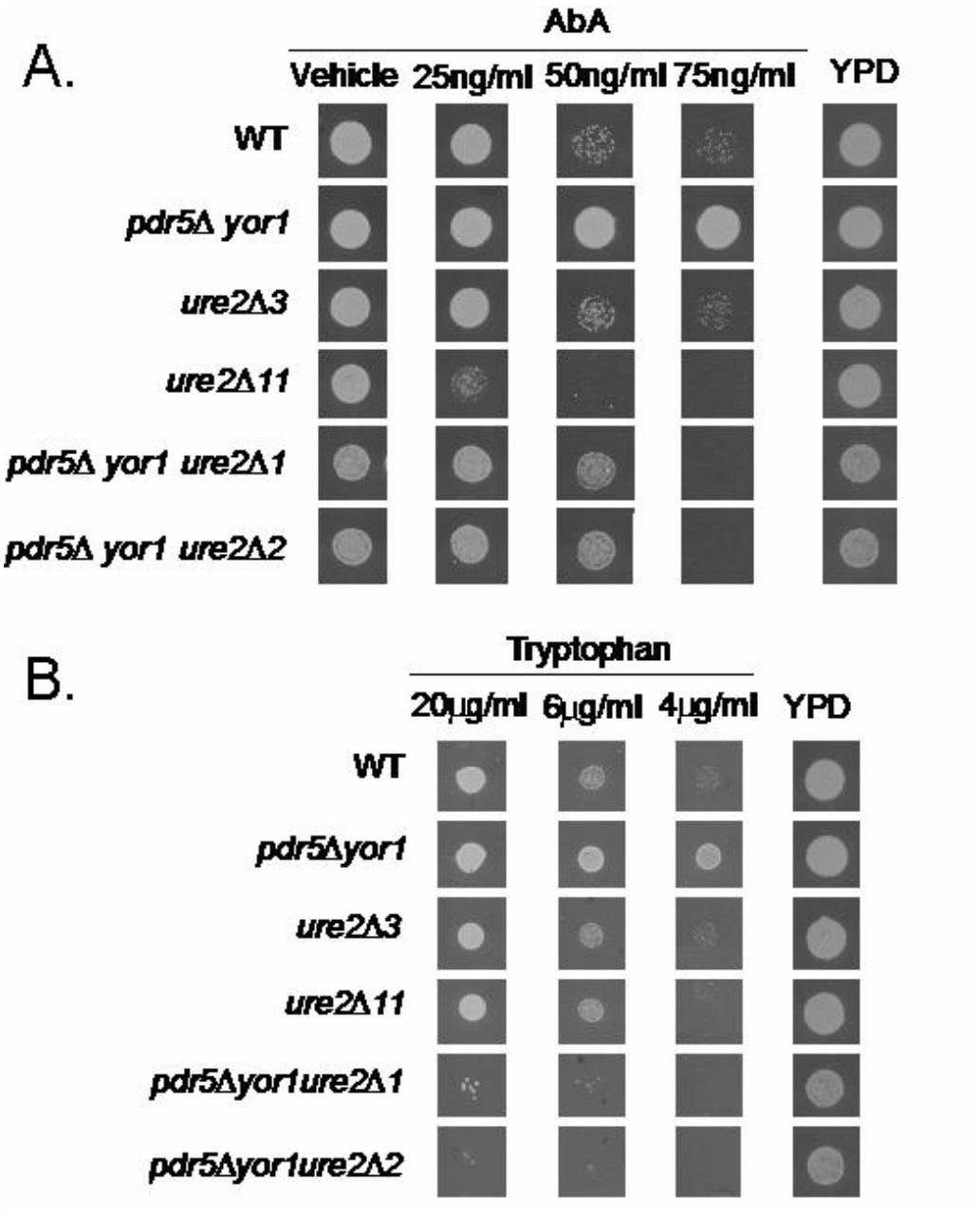

Figure 18. Loss of Ure2 reverses the AbA and low tryptophan tolerance of the *pdr5Δ yor1* strain. (A) Wild-type, *pdr5Δ yor1*, *ure2Δ*, and *pdr5Δ yor1 ure2Δ* strains were grown to mid-log phase and spotted onto YPD plates containing the indicated concentrations of AbA and YPD alone. Two different isolates of each strain lacking *URE2* are represented (B) The same strains as in (A) were grown in YPD and spotted onto minimal media plates containing the indicated concentrations of tryptophan. Loss of Ure2 sensitizes the *pdr5Δ yor1* strain to AbA and low tryptophan, indicating not only that Ure2 plays a role in AbA tolerance but that loss of this gene may phenocopy the cell's response to nitrogen starvation.

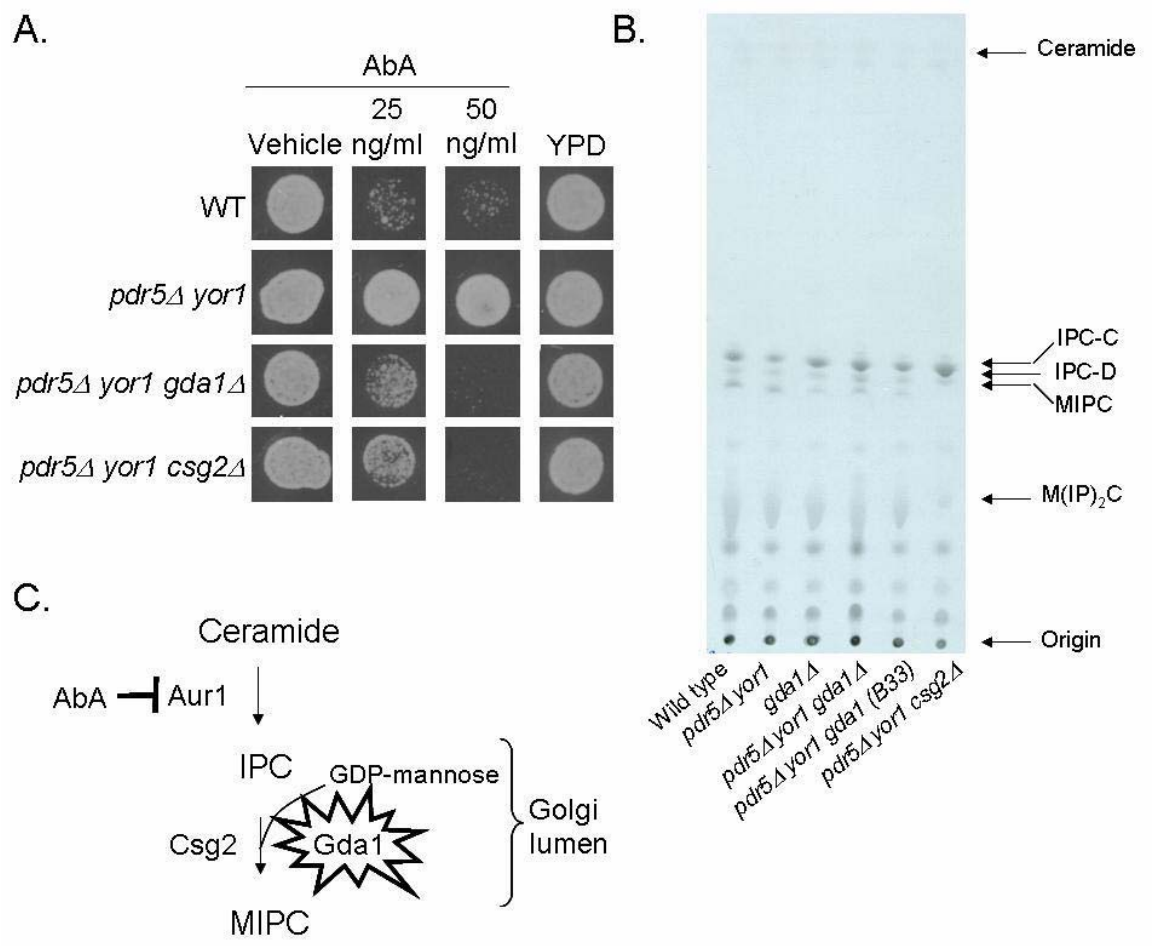

Figure 19. Gda1 is important for AbA tolerance, possibly independent of its role in sphingolipid biosynthesis. (A) Wild-type, *pdr5Δ yor1*, *pdr5Δ yor1 gda1Δ*, and *pdr5Δ yor1 csg2Δ* strains were grown in YPD to mid-log phase and spotted on to YPD alone or YPD plates containing the indicated concentrations of AbA. (B) The same strains from A, along with the B33 *pdr5Δ yor1 gda1* strain and *gda1Δ* alone were labeled with ^{3H}Serine and processed as described in experimental procedures. Equal amounts of radiolabeled lipids were run on TLC plates and exposed to film. Interestingly, although loss of either Gda1 or Csg2 in the absence of Pdr5 and Yor1 decreases the AbA resistance to a similar degree, lipid analysis shows that loss of complex sphingolipids is more severe in the absence of Csg2 as compared to Gda1. C. Schematic of sphingolipid pathway indicating where Gda1 acts and where AbA inhibits the pathway. This suggests that although complex sphingolipid formation may not be completely normal in the absence of Gda1, that there is another effect from loss of this gene that is contributing to its AbA phenotype, possibly a decrease in GPI-anchored proteins at the cell wall.

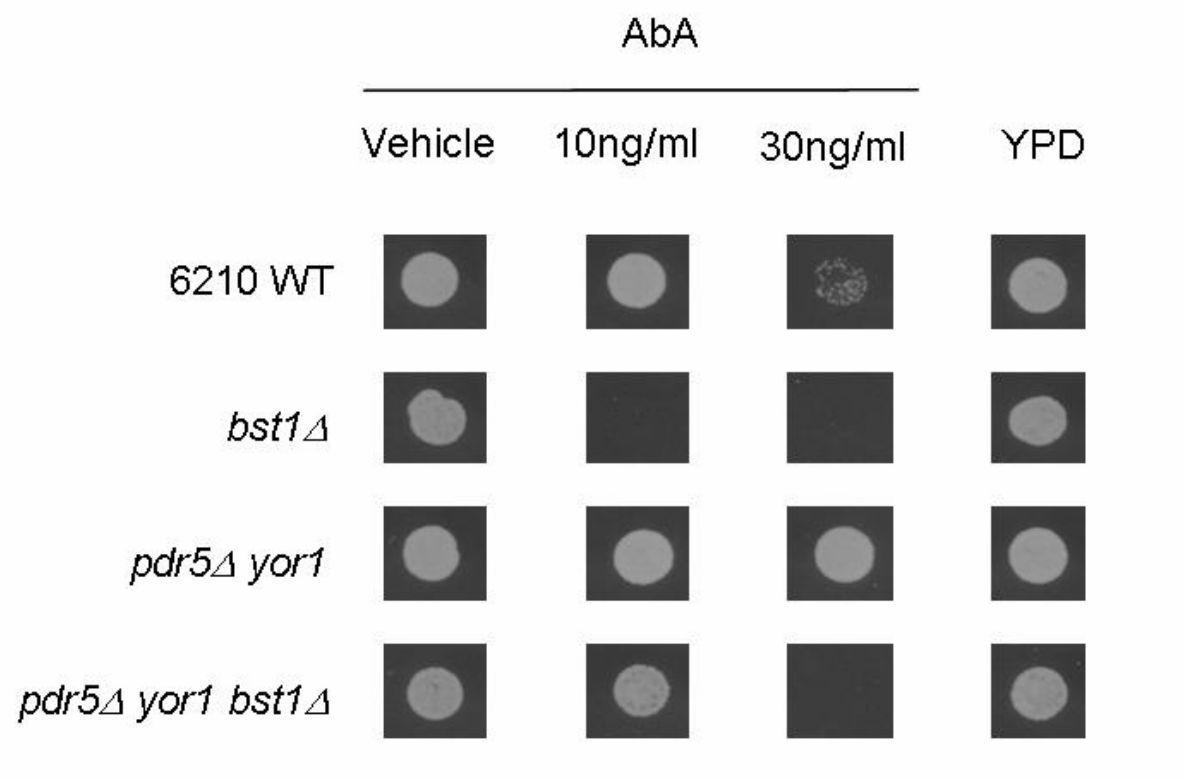

Figure 20. Loss of Bst1 profoundly increases AbA sensitivity. Wild-type, *bst1Δ, pdr5Δ yor1,* and *pdr5Δ yor1 bst1Δ* strains were grown in YPD to mid-log phase and spotted onto plates containing the indicated concentrations of AbA or YPD alone. Loss of Bst1 severely impacts AbA resistance on its own and greatly reduces the resistance of the *pdr5Δ yor1* strain. As Bst1 is known to be necessary for movement of GPI-anchored proteins out of the ER, this data suggests that there is a requirement for normal GPI-anchored protein processing in AbA tolerance

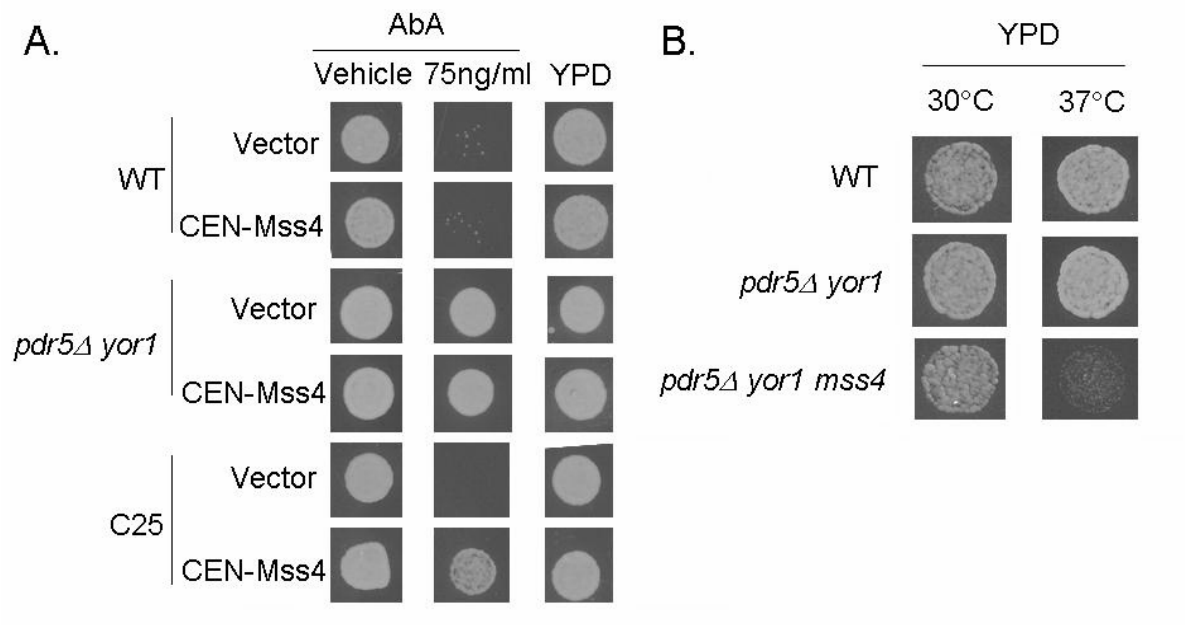

Figure 21. The EMS mutant designated C25 can be complemented by Mss4 and is temperature sensitive. (A) Wild-type, *pdr5Δ yor1*, and the C25 mutant strain were transformed with either a low-copy vector or the same low-copy vector carrying Mss4 under control of its own promoter. These strains were grown in selective minimal media to mid-log phase and spotted onto YPD AbA plates containing the indicated concentrations as well as YPD alone. The single copy of Mss4 was able to fully complement the C25 mutant, bringing AbA resistance back to that of the parent strain. (B) The same strains as above were grown in YPD to mid-log phase and spotted on two YPD plates, one incubated at 30°C and one incubated at 37°C for 2 days. The *pdr5Δ yor1 mss4* (C25 mutant) strain was also sensitive at 37°C.

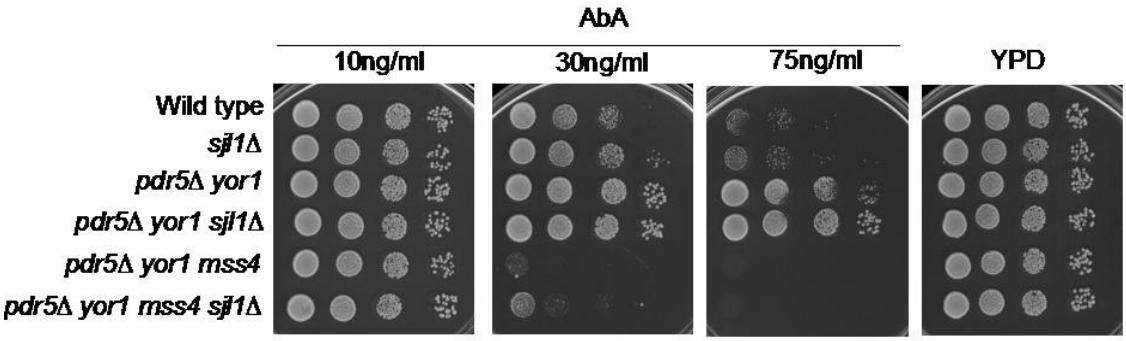

Figure 22. The AbA sensitivity of the *pdr5Δ yor1 mss4* strain can be suppressed by deletion of *SJL1*. Wild-type, *pdr5Δ yor1*, and *pdr5Δ yor1 mss4* strains along with their isogenic counterparts deleted for *SJL1* were grown to mid-log phase and 10-fold dilutions were spotted onto YPD plates containing the indicated concentrations of AbA as well as YPD only. The loss of Sjl1 was able to partially suppress the *pdr5Δ yor1 mss4* AbA sensitivity, suggesting that elevating $PI_{4,5}P_2$ levels will increase tolerance to AbA.

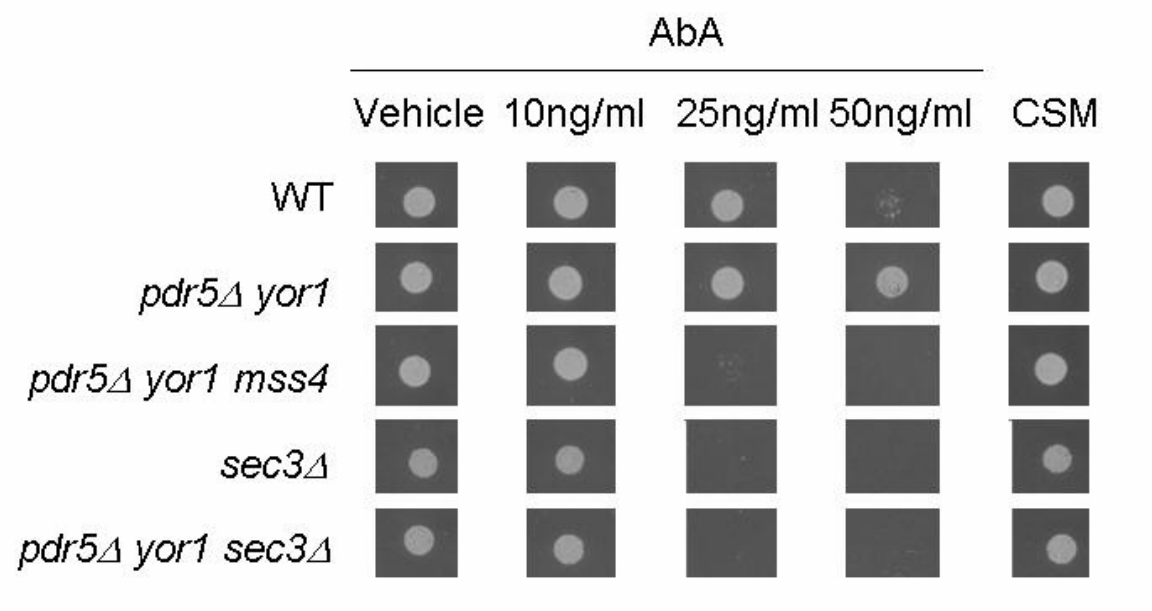

Figure 23. A decrease in exocytosis by deletion of Sec3 dramatically decreases AbA resistance. Wild-type, *sec3Δ*, *pdr5Δ yor1*, *pdr5Δ yor1 mss4,* and *pdr5Δ yor1 sec3Δ* strains were grown in minimal media to mid-log phase and spotted onto CSM plates containing the indicated concentrations of AbA and CSM alone. Strikingly, the Sec3 deletion by itself was sufficient to cause a severe decrease in AbA tolerance and was also able to phenocopy the Mss4 mutant. This data suggests that normal exocytosis is vital for dealing with AbA stress.

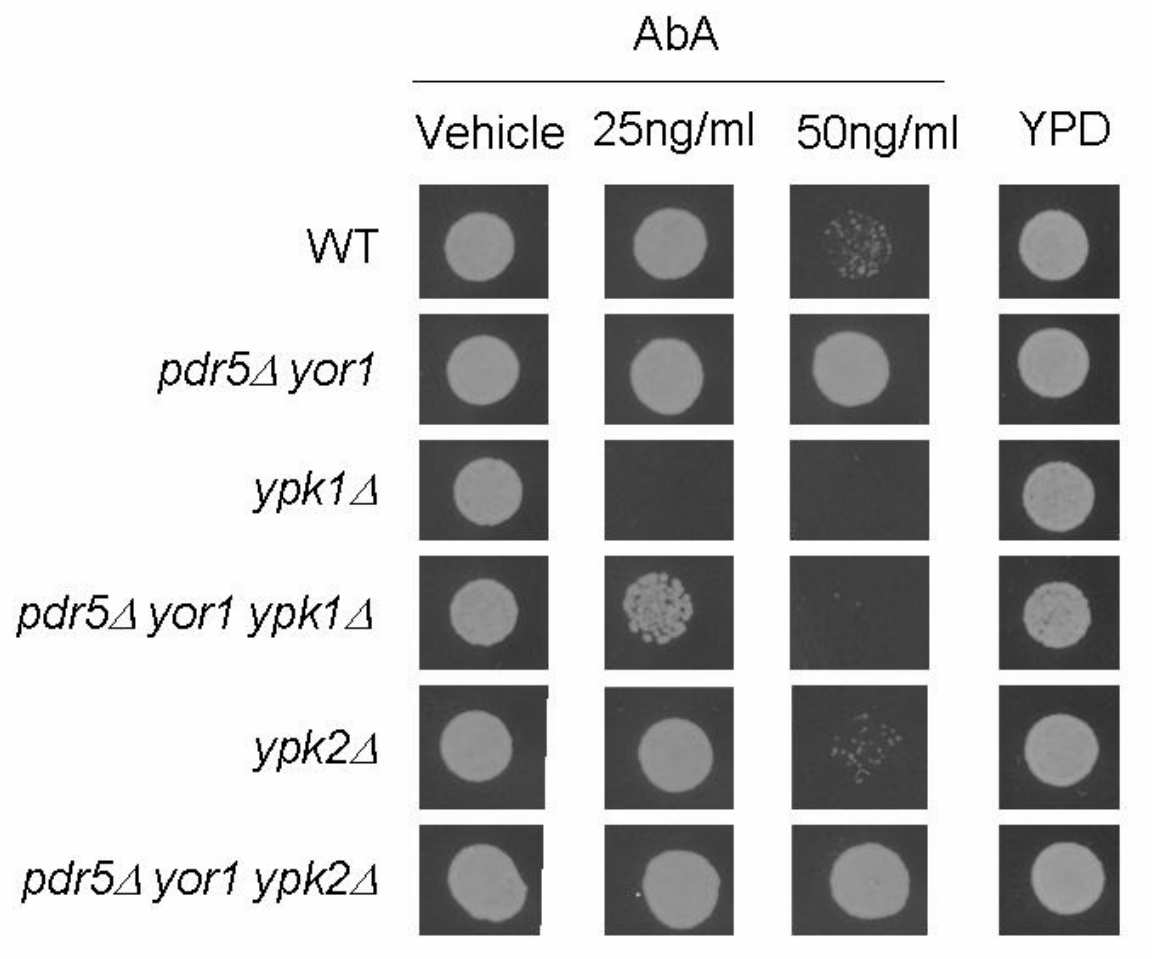

Figure 24. Ypk1, but not Ypk2, affects AbA tolerance. Wild-type, *ypk1Δ*, *ypk2Δ* *pdr5Δ yor1*, *pdr5Δ yor1 ypk1Δ,* and *pdr5Δ yor1 ypk2Δ* strains were grown in YPD and spotted onto plates containing the indicated concentrations of AbA. Loss of Ypk1 in both the wild-type and the *pdr5Δ yor1* strains showed dramatic decreases in AbA tolerance, while loss of Ypk2 had no effect, suggesting that there is a specific requirement for Ypk1.

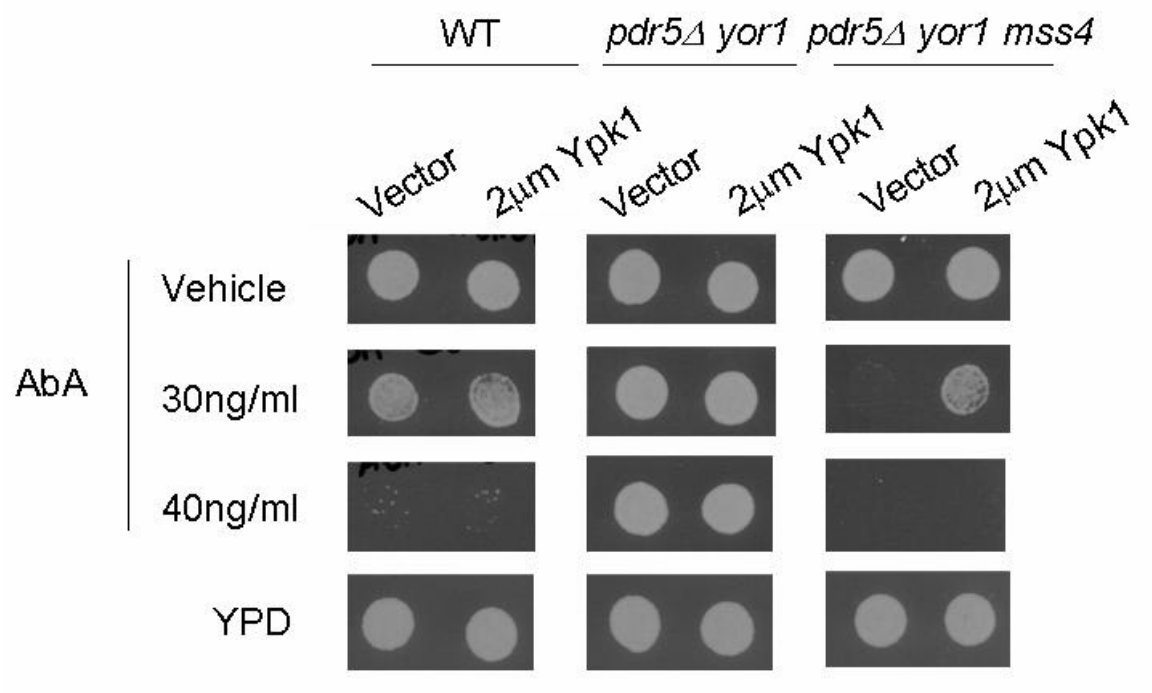

Figure 25. Over-expression of Ypk1 partially suppresses the AbA sensitivity of the *pdr5Δ yor1 mss4* strain. Wild-type, *pdr5Δ yor1*, and *pdr5Δ yor1 mss4* strains were transformed with a high-copy vector or a high-copy vector carrying C-terminally HA tagged Ypk1. These transformants were grown to mid-log phase in minimal selective media and spotted on to YPD plates containing the indicated concentrations of AbA. Interestingly, increased Ypk1 was able to moderately suppress the AbA sensitivity of the *pdr5Δ yor1 mss4* strain back to wild-type levels, though not to that of the parent strain, suggesting that Ypk1 may act downstream of Mss4, but that there may be other downstream effectors of Mss4 that are required for AbA tolerance in the *pdr5Δ yor1* strain.

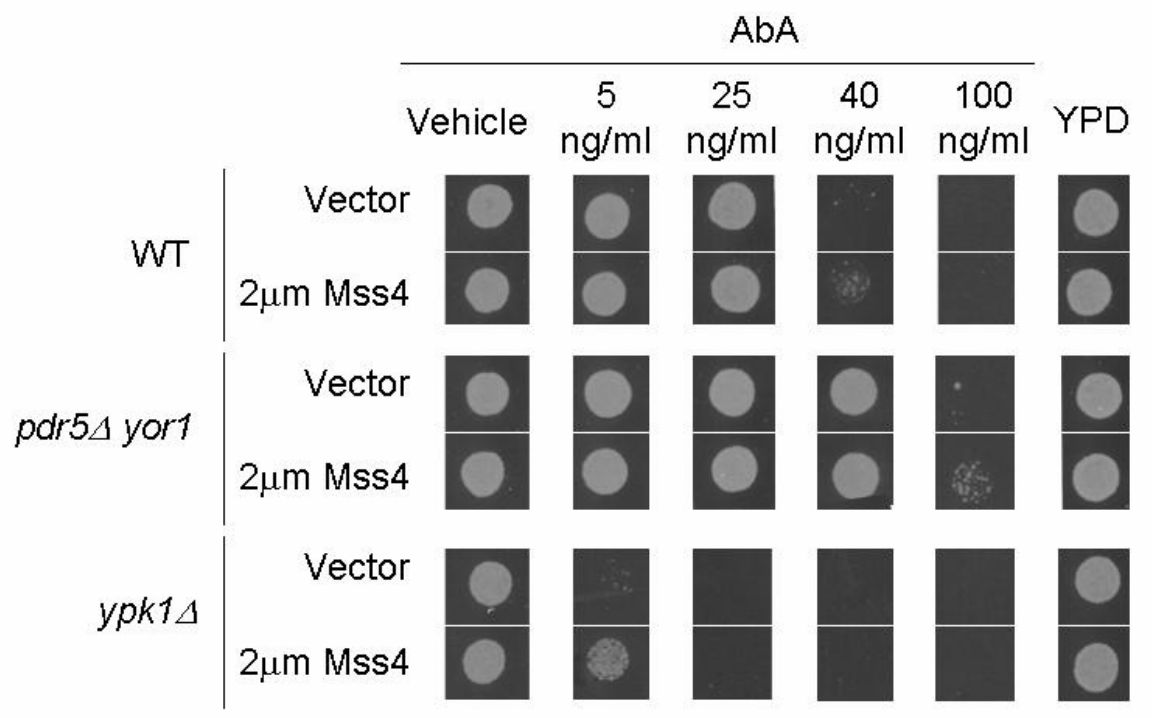

Figure 26. Mss4 over-expression partially suppresses *ypk1Δ* AbA sensitivity. Wild-type, *pdr5Δ yor1*, and *ypk1Δ* strains were transformed with either high-copy vector only or high-copy vector containing Mss4. Transformants were grown in minimal selective media to mid-log phase and spotted on to AbA plates. Surprisingly, the 2μm Mss4 did somewhat restore AbA resistance in the absence of Ypk1, suggesting that although Ypk1 plays an important role in AbA, possibly downstream of Mss4, that there is most likely another downstream target crucial for this phenotype.

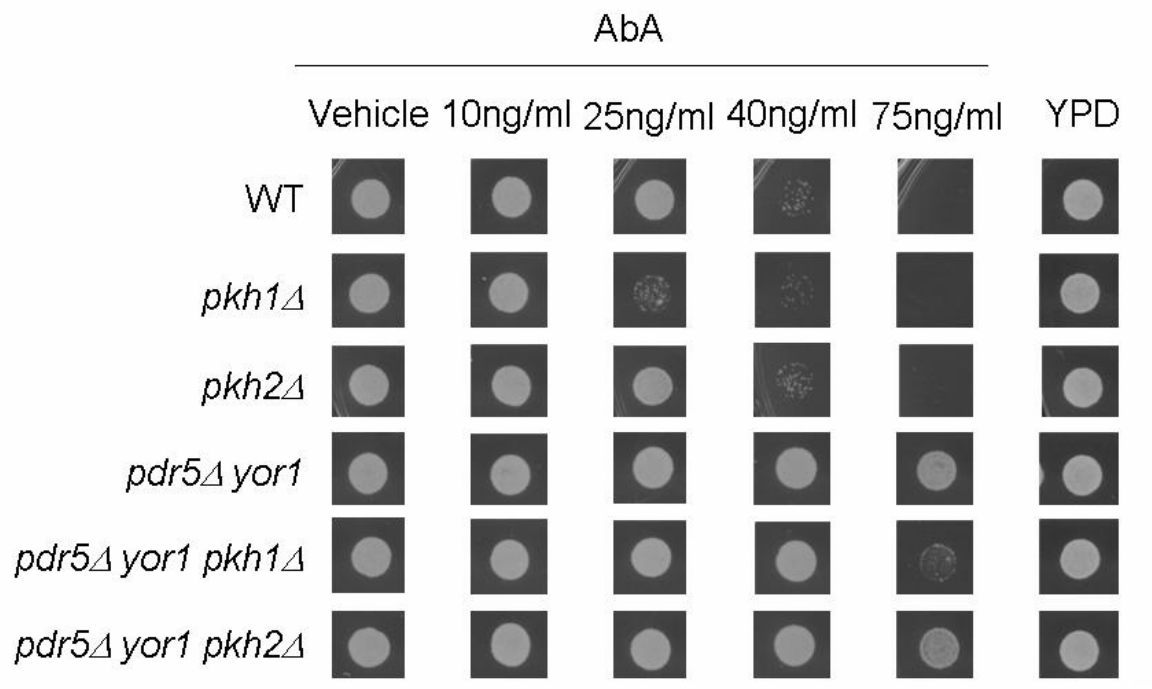

Figure 27. Loss of Pkh1 decreases AbA tolerance. Wild-type, *pdr5Δ yor1*, and their *PKH1*- or *PKH2*-deleted derivatives were grown in YPD and spotted onto AbA plates. Interestingly, Pkh1, which can activate Ypk1, caused a drop in AbA resistance in both wild-type and *pdr5Δ yor1* strains whereas loss of Pkh2 had no effect in either background. This suggests that Pkh1 is important in AbA tolerance, probably via its role in activation of Ypk1.

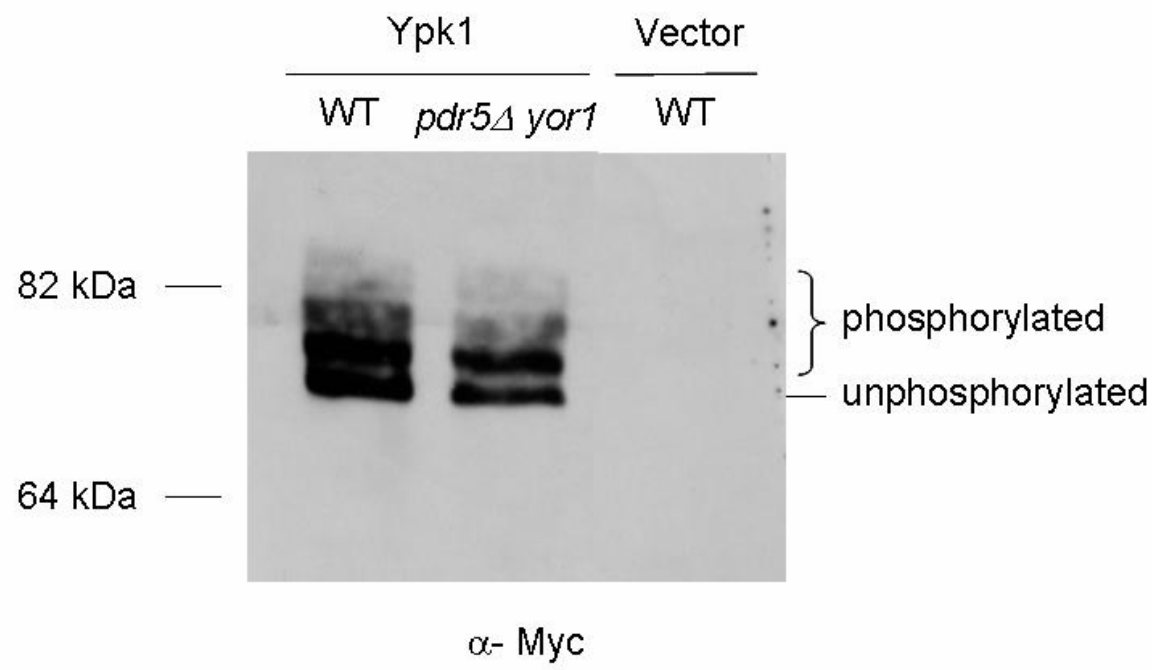

Figure 28. Ypk1 does not appear to have increased phosphorylation in the absence of Pdr5 and Yor1. Wild-type and *pdr5Δ yor1* strains were transformed with Gal-myc-Ypk1 or vector alone, grown and induced with galactose as described in experimental procedures. Total protein was extracted and run on an SDS-PAGE gel, transferred to nitrocellulose and probed with an anti-myc antibody. Loss of Pdr5 and Yor1 does not appear to have increased phosphorylation as measured by reduced migration on the gel. However, determining if this indicates Ypk1 is more or less active would require further analyses.

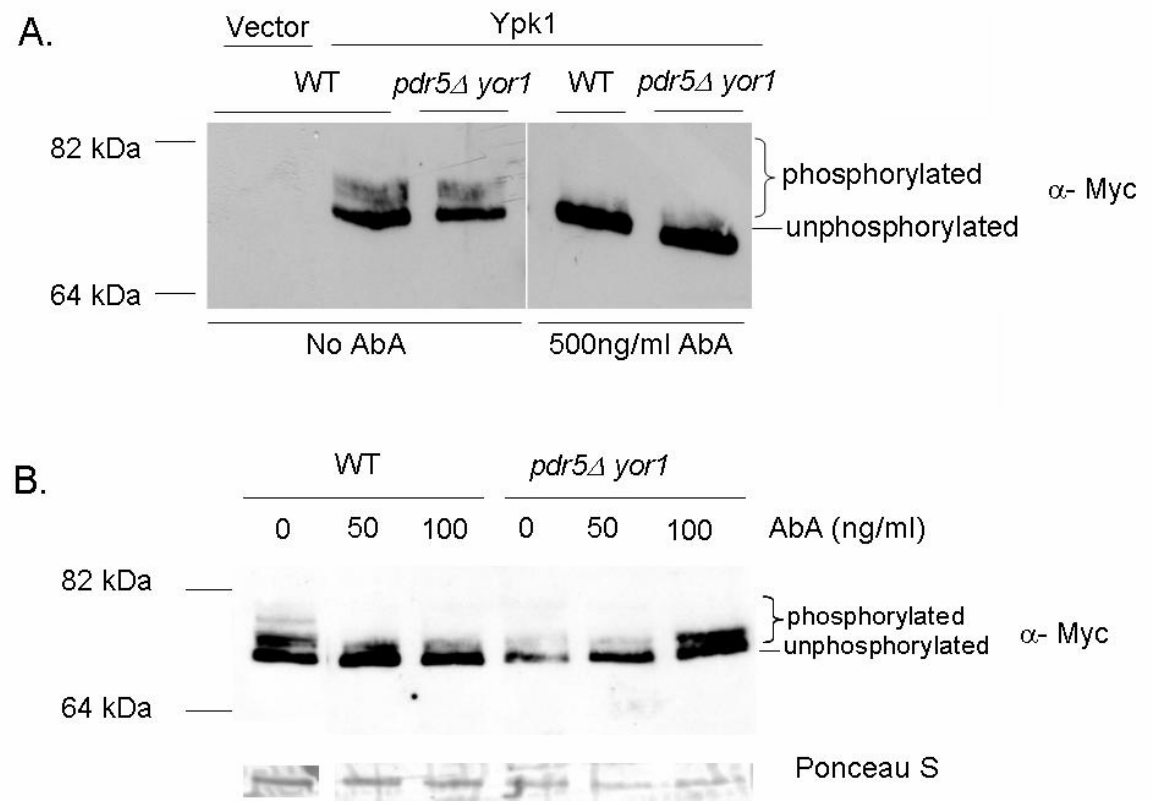

Figure 29. Low concentrations of AbA increase fast migrating species of Ypk1 in the *pdr5Δ yor1* strain. (A) Wild-type and *pdr5Δ yor1* cells were transformed with pAM54. Transformants were grown to early log phase and induced with galactose for one hour after which 500ng/ml AbA was added for the remaining two hours of galactose induction. Protein was extracted as described in experimental procedures, run on SDS-PAGE, transferred to nitrocellulose and probed for myc. (B) The same transformants as in (A) were processed the same as described above except that samples were treated with 50ng/ml and 100ng/ml AbA instead of 500ng/ml. Membrane was stained for Ponceau S to assess general protein levels. High levels of AbA (500ng/ml) blocked Ypk1 phosphorylation. Lower concentrations also showed a decrease in Ypk1 phosphorylation, however the total amount of fast migrating species of Ypk1 appears to increase in a dose-dependent manner in the *pdr5Δ yor1* strain, suggesting that Ypk1 expression or turnover may be affected in this strain, or that Fpk1 may have decreased activity leading to a decrease in inhibitory Ypk1 phosphorylation.

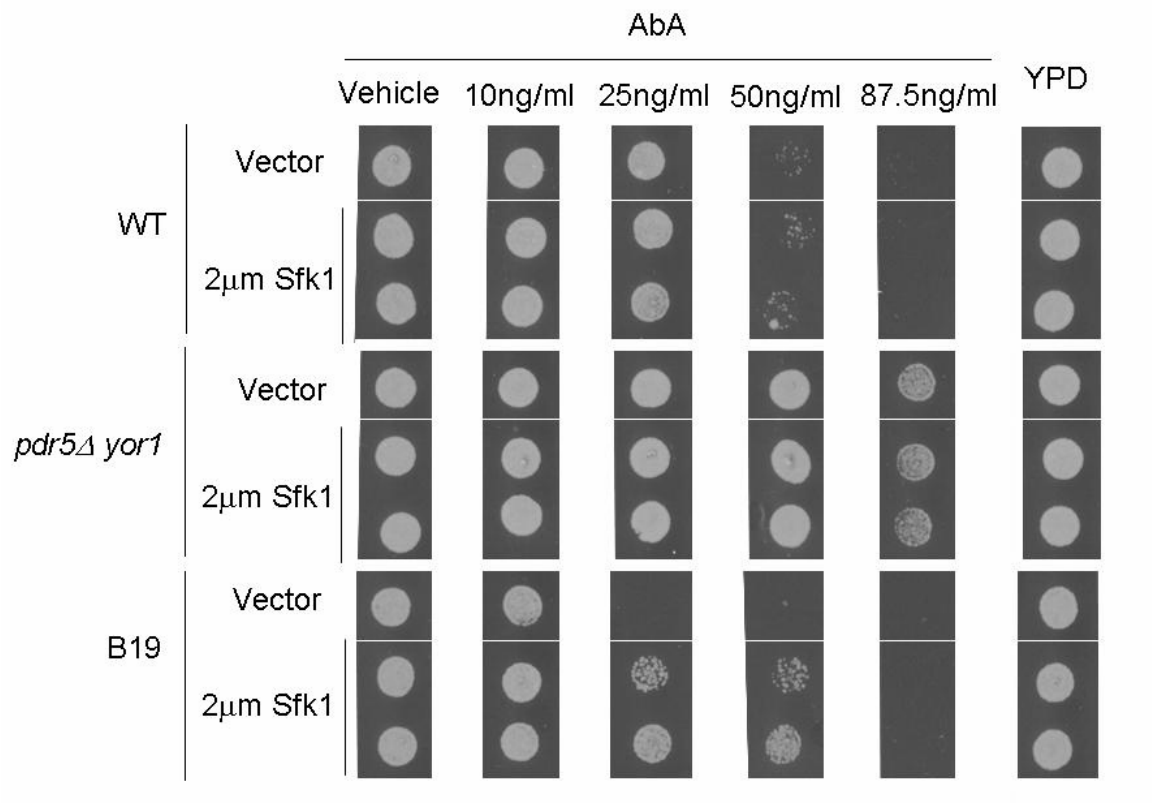

Figure 30. The AbA sensitivity of the EMS mutant designated B19 is suppressed by over-expression of Sfk1. Wild-type, *pdr5Δ yor1*, and the B19 EMS mutant were transformed with high-copy vector alone or high-copy vector carrying Sfk1. Transformants were grown in minimal selective media and spotted onto YPD plates containing the indicated concentrations of AbA. Intriguingly, over-expression of Sfk1 restored some resistance to the B19 mutant, allowing growth at a concentration comparable to wild-type. This suggests that the mutation responsible for the B19 mutant may be Sfk1 or a protein which acts upstream of Sfk1.

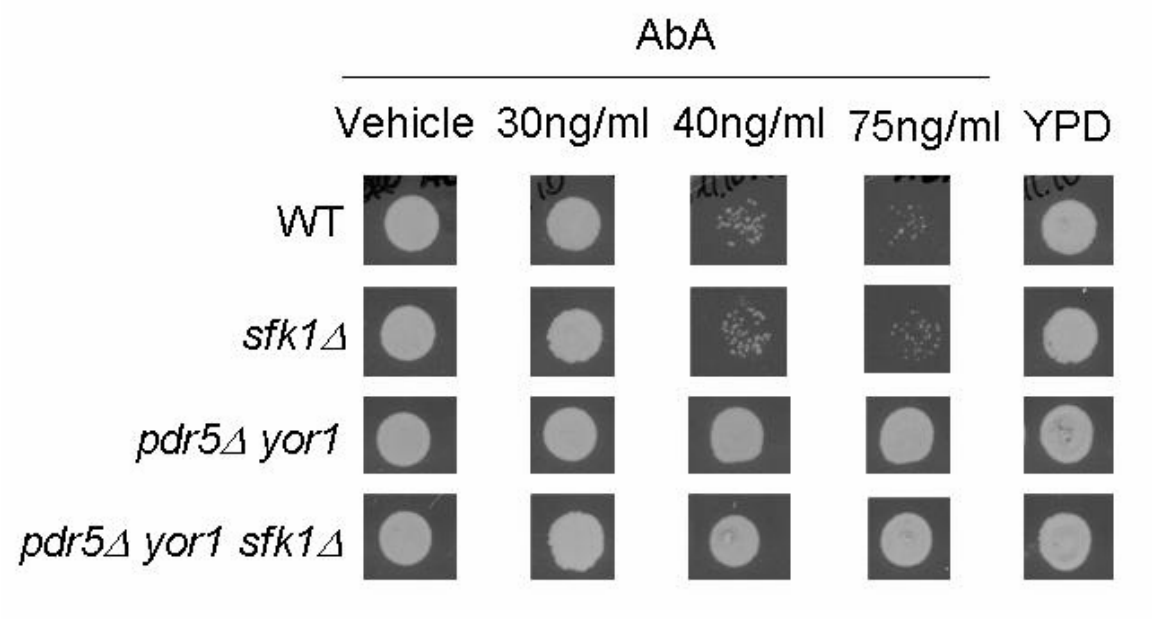

Figure 31. Deletion of Sfk1 does not affect AbA resistance. Wild-type and *pdr5Δ yor1* strains deleted for *SFK1* along with their isogenic counterparts were grown to mid-log phase and spotted onto YPD plates containing the indicated concentrations of AbA. Surprisingly, loss of Sfk1 did not affect AbA tolerance in either the wild-type or the *pdr5Δ yor1* strain, suggesting that the B19 mutant may not be Sfk1, but this does not rule out the mutation as being a protein upstream of Sfk1 or an Sfk1 interacting partner.

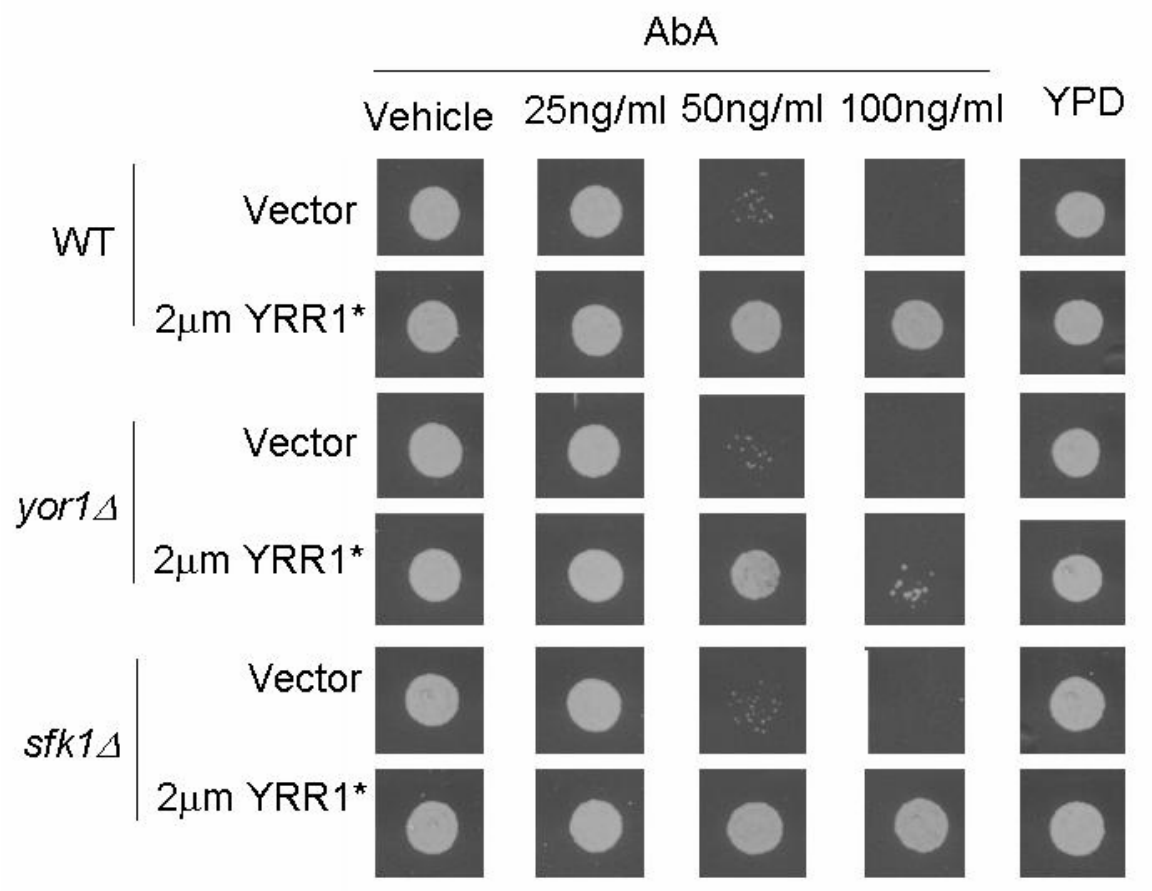

Figure 32. Hyperactive Yrr1 dramatically increases AbA tolerance. Wild-type, *yor1Δ*, and *sfk1Δ* strains were transformed with high-copy vector alone or high-copy vector containing a hyperactive allele of Yrr1 (* indicates hyperactive allele). These transformants were grown to mid-log phase in minimal selective media and spotted onto YPD plates containing the indicated concentrations of AbA. Strikingly, Yrr1 just in the wild-type strain was robustly resistant to AbA, which was partially blocked by deletion of Yor1. Loss of Sfk1 had no discernible effect on the resistance from Yrr1. The lack of a complete block of the Yrr1 effect by loss of Yor1 suggests that there is more than one target of Yrr1 that is responsible for AbA resistance.

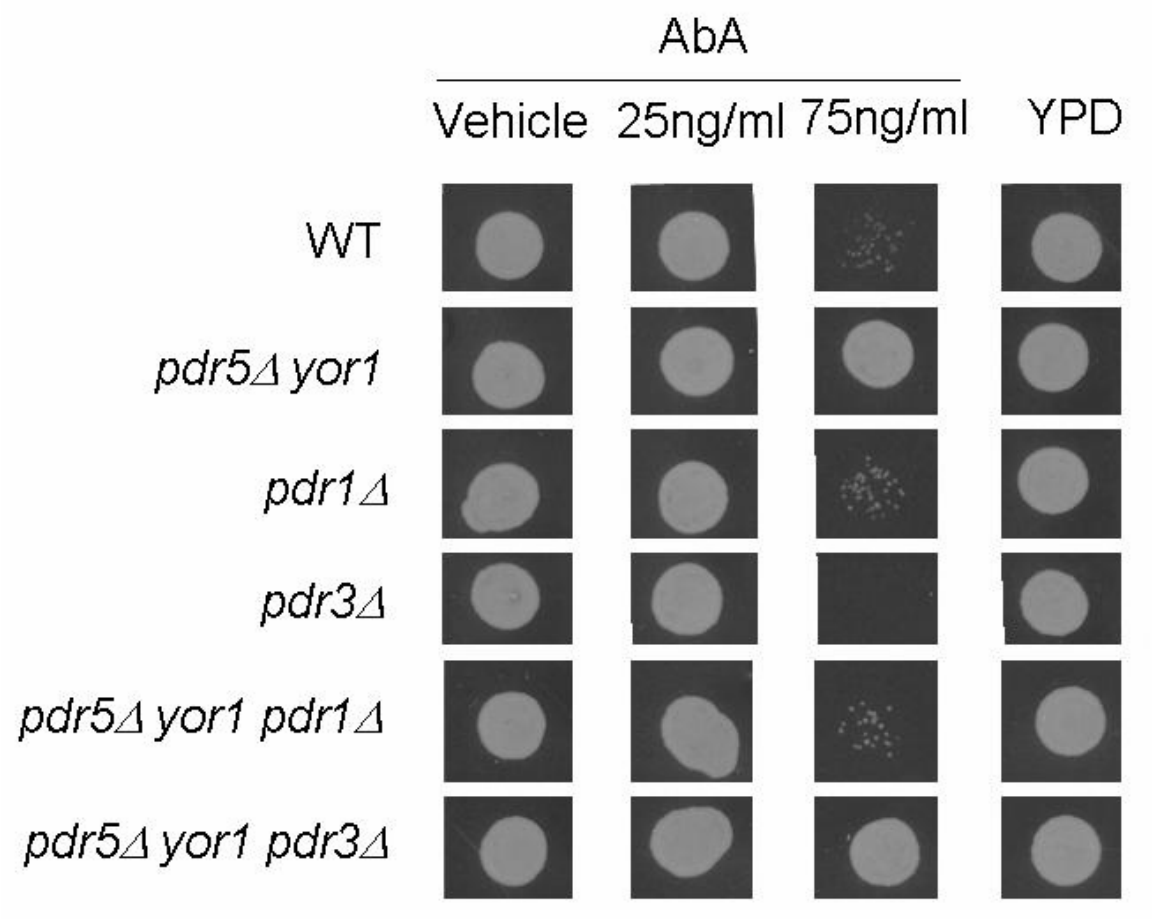

Figure 33. Pdr1 is significant for AbA tolerance in the *pdr5Δ yor1* strain. Wild-type, *pdr5Δ yor1*, *pdr1Δ*, *pdr3Δ, pdr5Δ yor1 pdr1Δ*, and *pdr5Δ yor1 pdr3Δ* strains were grown in YPD to mid-log phase and spotted onto YPD plates containing the indicated concentrations of AbA. Surprisingly, loss of Pdr1, but not Pdr3, severely diminished the AbA tolerance of the *pdr5Δ yor1* strain, suggesting that there may be a feedback loop to Pdr1 from loss of Pdr5 and Yor1 and that Yor1 is probably not the only PDR-regulated transporter required for this function.

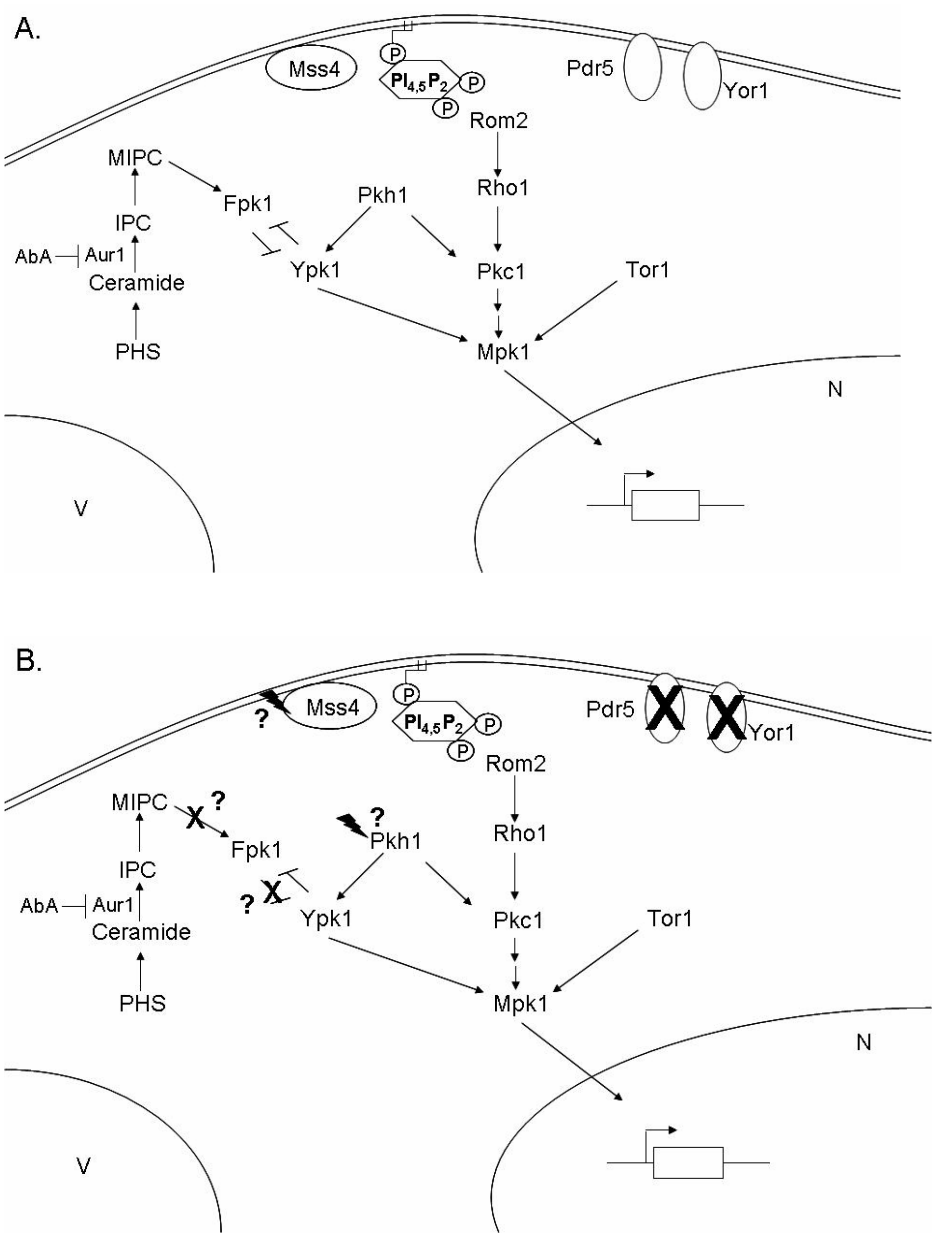

Figure 34. Models of cell wall integrity pathways in wild-type and *pdr5Δ yor1* cells. (A) Figure depicts the sphingolipid pathway, Pkh signaling and Mss4 signaling in a wild-type cell indicating interplay between these pathways. Arrows indicate activation while T-bars indicate inactivation. (B) Same pathway as (A) but in the absence of Pdr5 and Yor1. It is speculated that Mss4 and/or Pkh1 (and in turn Ypk1) may be activated in this strain. It is also considered that Fpk1 may be down regulated in the absence of Pdr5 and Yor1 possibly by decreased MIPC-mediated activation. Xs indicate loss of the protein or loss of that step in the signal cascade. Question marks (?) indicate unknown, but speculated alterations in these signaling pathways in the absence of Pdr5 and Yor1. Lightening bolts indicate potential activation.

CHAPTER IV

CONCLUSIONS

This work demonstrated that the plasma membrane protein Rsb1 not only plays a role in PHS tolerance, but also resistance to several other compounds, all of which can be affected by tryptophan status. An examination of the predicted topology of Rsb1 also indicated that this protein is more likely to function as a receptor or signaling molecule than a transporter, which is supported by the fact that Rsb1 affects the cell's ability to tolerate multiple compounds. Loss of the ABC transporters Pdr5 and Yor1 play an important role in regulation of endocytosis of the plasma membrane localized amino acid permease, Tat2, and possibly other membrane proteins as well. Not only do Pdr5 and Yor1 affect endocytosis, but they also appear to have a role in maintenance of the composition of the cell wall. Experiments to identify the determinants for AbA resistance in the *pdr5Δ yor1* strain led to the identification of several genes involved in cell wall integrity pathways.

The first half of this work demonstrated that the ABC transporters Pdr5 and Yor1 as well as the 7 transmembrane receptor-like protein, Rsb1 play a role in control of nutrient transporter endocytosis. Strains lacking Pdr5 and Yor1 displayed slower turnover of the Tat2 tryptophan permease and a corresponding increase in tryptophan uptake. Fluorescence microscopy also indicated that this strain shows slower movement of the dye FM4-64, which was interpreted to mean that endocytosis is delayed in the absence of Pdr5 and Yor1 presumably due to the defect in phospholipid flop leading to perturbed plasma membrane asymmetry. Although the FM4-64 experiment does not conclusively identify internalization as the trafficking step which is affected in this strain, the increased residence time of Tat2 at the plasma membrane and the increased uptake of

tryptophan support the idea that the defect is indeed at the internalization step. Tat2 is important in explaining the PHS resistance observed in the absence of Pdr5 and Yor1, however it is suggested by the FM4-64 data that turnover of other proteins is likely affected in this strain. It may be that Pdr5 and Yor1 affect a specific pool of proteins that are found in isolated regions of the plasma membrane. Tat2 is localized to areas of the plasma membrane known as the membrane compartment of Can1 (MCC) (110). Along with Can1, the argenine permease, and Tat2, the uracil permease Fur4 is also localized to the MCC (110). It is possible that Fur4 and Can1 may also be modulated by Pdr5 and Yor1, which could be determined by pulse-chase analysis and fluorescence microscopy as was done for Tat2.

Rsb1 has long been purported to be a long chain base transporter or translocase (31). However the data presented here indicate an alternative role for Rsb1 as that of a potential signaling molecule which controls turnover of Tat2 and possibly other proteins. Although loss of Rsb1 shows increased sensitivity to PHS, this can be explained by a decrease in Tat2 at the plasma membrane, which is independent of endogenous PHS levels as indicated by HPLC analysis. Further support for the idea that Rsb1 does not function as a transporter protein is its predicted topology, which indicates that Rsb1 has 7 transmembrane domains, suggesting that it is part of the 7 transmembrane (7 TM) family of proteins. This family of proteins is normally involved in signaling cascades, though none are speculated to act as transporters. Although this work did not indicate that Rsb1 affects proteins other than Tat2, it also does not rule out a more global role for Rsb1 in regulation of endocytosis of membrane proteins.

Several questions remain regarding the physiological role of Rsb1. The initial experiments to determine what regions of the C-terminus of Rsb1 are important for its function led to observation that loss of the C-terminal 22 amino

acids (ΔC360 mutant) led to a remarkable increase in the amount of Rsb1 protein, however this did not correlate with a dramatic increase in PHS tolerance. The ΔC335 Rsb1 mutant, lacking the C-terminal 47 residues was able to restore PHS resistance back to almost that of wild-type. Its expression was also elevated as compared to the wild-type Rsb1, though not to the same extent as the ΔC360 mutant. These data suggest that these regions may be important for interaction with downstream signaling effectors and possibly turnover of Rsb1 itself. In order to determine interacting partners for Rsb1, co-immunoprecipitation and mass spectrometry experiments could be performed. It is also possible that Rsb1 interacts transiently with another protein, which may impede identification.

One family of proteins that may act downstream of Rsb1 is the arrestins. Arrestins are adapter proteins that bind to a variety of plasma membrane localized proteins and mediate ubiquitination and endocytosis (64). Bul1 and its homologue Bul2 are considered arrestin-like adapter proteins and appear to function in a manner similar to arrestins (64). The data demonstrating that loss of Bul1 bypasses the PHS sensitivity of the *rsb1Δ* strain indicates that Bul1 may act downstream of Rsb1 in regulation of turnover of Tat2 and possibly other proteins. Bul1 has been shown to be necessary for turnover of Tat2, as loss of all arrestins did not completely block endocytosis of Tat2 without the additional deletion of Bul1, which was also true for Fur4 (64). The data above along with the work presented here indicate that Rsb1 may have a negative effect on Bul1-mediated endocytosis of Tat2. β-arrestin1 in mammals is itself regulated by phosphorylation (111). This protein remains in a phosphorylated state when in the cytoplasm and gets de-phosphorylated after recruitment to the plasma membrane, which is required for its interaction with protein complexes necessary for its function in endocytosis (111). A mutant form of β-arrestin1 (S412D), which mimics the normal phosphorylated state was shown to act as a dominant

negative and block internalization of its target protein, β_2AR (111). These data indicate that changes in the phosphorylation state of arrestin proteins can have negative effects on their ability to mediate endocytosis. One possible role of Rsb1 is to signal via a currently unknown protein to regulate phosphorylation of Bul1 and/or other arrestin proteins necessary for Tat2 ubiquitination and internalization. In the absence of Rsb1, Bul1 may be in a de-phosphorylated state, therefore able to bind and recruit the E3 ubiquitin ligase, Rsp5 to Tat2, thus increasing endocytosis.

The second half of this work demonstrated that the AbA tolerance of the *pdr5Δ yor1* strain could be abolished by mutation or deletion of several different genes involved in a variety of cellular processes, many of which affect cell wall integrity. Mutation in Mss4 and its subsequent suppression by loss of the $PI_{4,5}P_2$ 5-phosphatase Sjl1 indicate that changes in $PI_{4,5}P_2$ levels may be crucial for AbA tolerance in the *pdr5Δ yor1* strain, however this has not been tested directly. Lipid extraction and HPLC analysis of $PI_{4,5}P_2$ levels in the wild-type, *pdr5Δ yor1*, and *pdr5Δ yor1 mss4* strains is currently underway in a collaboration with Lois Weisman's lab at the University of Michigan. If these analyses indicate that there is no difference in $PI_{4,5}P_2$ in these strains, this may be attributable to the absence of treatment with AbA, in which case it would be important to repeat these analyses in the presence of AbA treatment. If $PI_{4,5}P_2$ levels are increased in the *pdr5Δ yor1* strain this could suggest that Mss4 is activated and leading to enhanced cell wall signaling in the *pdr5Δ yor1* strain. However, there is a possibility that $PI_{4,5}P_2$ levels are not increased either in the absence of presence of AbA treatment in the *pdr5Δ yor1* strain, which would indicate that Mss4 itself plays an important role in AbA tolerance independent of loss of Pdr5 and Yor1. One way to examine effects of this Mss4 mutant allele alone would be to mate the *pdr5Δ yor1 mss4* strain back to the wild-type strain and dissect tetrads to get

the Mss4 allele by itself and examine effects on AbA resistance. The ability of a *sec3Δ* strain alone to increase AbA sensitivity indicates that normal exocytosis is important for tolerance to this drug. This leads to the idea that perhaps the crucial role for Mss4 in AbA tolerance is due to the role of $PI_{4,5}P_2$ in recruitment of Exo70 and regulation of exocytosis.

Ypk1 deletion has a dramatic effect on the AbA tolerance of the *pdr5Δ yor1* strain, severely decreasing resistance. While the bypass of the AbA sensitivity of the *pdr5Δ yor1 mss4* strain with over-expression of Ypk1 indicated that perhaps Ypk1 functions downstream of Mss4 in AbA tolerance, it is also possible that Ypk1 functions in a separate but parallel pathway, which is an idea supported by the observation that loss of Pkh1, a known activator of Ypk1, also decreases AbA tolerance. However because Pkh1 also activates Pkc1, a known downstream effector of the Mss4 signaling cascade, additional analysis is necessary to identify the pathways involved. The Western blot analyses of Ypk1 indicate that there appears to be a decrease in phosphorylated forms of Ypk1 in the *pdr5Δ yor1* strain. There also appears to be an increase in faster migrating forms of Ypk1 at lower concentrations of AbA treatment. These data indicate that Fpk1, a kinase which inactivates Ypk1 by phosphorylation, might be down regulated in the absence of Pdr5 and Yor1. In this case, less phosphorylated forms of Ypk1 would be considered more active. The increase in total Ypk1 after treatment with 100ng/ml AbA suggests that turnover of Ypk1 may be decreased. Mass spectrometry analysis to determine which residues of Ypk1 are phosphorylated would help to shed some light on which pathways may be active or inactive regarding regulation of Ypk1 in the absence of Pdr5 and Yor1.

Bst1 and Gda1 both affect GPI-anchored protein content of the cell (97,98,112). Bst1 affects the GPI anchor and trafficking of these proteins, while Gda1 affects the glycosylation status. Both of these genes are important in AbA

resistance, as deletion or mutation greatly diminishes the tolerance of wild-type and *pdr5Δ yor1* cells to AbA. To determine if the GPI-anchored protein content of the cell wall is altered in the absence of Pdr5 and Yor1, cell walls can be separated by extraction and GPI-anchored protein content assessed by Western blotting as described previously (113). Since changes in the GPI-anchored content of the cell alter the composition of the cell wall, this indicates yet another link between AbA tolerance and cell wall integrity.

Although this screen was carried out using AbA as the screening agent, this project was initiated with the intent to determine novel mediators of PHS tolerance in the *pdr5Δ yor1* strain. Two of the genes identified from this screen, Mss4 and Gda1, also showed a sensitive phenotype on PHS when deleted in the context of the *pdr5Δ yor1* strain. The *pdr5Δ yor1 sec3Δ* strain, which mimicked the *pdr5Δ yor1 mss4* phenotype on AbA, suggests that a decrease in exocytosis may counteract the decrease in endocytosis that occurs in the *pdr5Δ yor1* strain thus leading to AbA sensitivity. This same argument could also explain the PHS sensitivity of the *pdr5Δ yor1 mss4* strain. It was demonstrated in Chapter 2 that loss of Pdr5 and Yor1 slows turnover of Tat2, which increases PHS tolerance. Therefore it is possible that the Mss4 mutation may decrease exocytosis of Tat2, thus not allowing as much Tat2 to get to the plasma membrane and subsequently increasing sensitivity to PHS. To test this idea, the wild-type, *pdr5Δ yor1*, and *pdr5Δ yor1 mss4* strains should be examined for a phenotype on limiting concentrations of tryptophan and/or radio-labeled to follow trafficking of Tat2.

Loss or mutation of Gda1 in the *pdr5Δ yor1* strain decreased not only the AbA tolerance but also the PHS resistance of this strain. Rsb1 does have an important function in PHS tolerance, though the data presented here indicate that it is not likely to be due to direct removal of sphingolipid intermediates. Rsb1 has

two N-glycosylation sites at its N-terminus which are required for normal PHS tolerance (46). Since Gda1 affects glycosylation status, it is possible that dysfunctional Gda1 may have a detrimental affect on Rsb1 protein structure, leading to enhanced PHS sensitivity. It would be interesting to test whether over-expression of Rsb1 could bypass the sensitivity of the *gda1Δ* strains and also to examine expression of Rsb1 by Western blot in the presence and absence of Gda1. If Gda1 affects glycosylation of Rsb1, then there may be a visible decrease in the amount of the glycosylated form of Rsb1 in the strains lacking Gda1.

The above data still does not fully explain why the *pdr5Δ yor1* strain is resistant to AbA, although it does offer some intriguing ideas. As many of the mutations identified to reverse the *pdr5Δ yor1* phenotype are involved in cell wall integrity, this suggests the possibility that this strain may have aberrant cell wall structure. As mentioned in Chapter 3, it was suggested previously (104) that AbA may target the cell wall in an unknown way to gain access to the cell. It is possible that the *pdr5Δ yor1* strain has an altered cell wall structure limiting AbA access to the inside of the cell. As it is unknown exactly how AbA gets into the cell, it is also possible that the delay in endocytosis seen in the *pdr5Δ yor1* strain could also be the reason for the increased resistance.

Although this work has investigated effects of loss of ABC transporters, cancers which have increased expression of ABC transporters likely also have altered phospholipid asymmetry which could lead to similar cellular responses. Mss4 homologues, PIP5-kinases, are activated in the context of hepatocellular carcinoma (114). SGK protein kinases, the mammalian counterparts of Ypk1, have been shown to be over-expressed in hepatocellular carcinomas as well as breast ductal carcinomas (115). Interestingly, PIP5-kinases as well as lipid rafts play important roles in the formation of invadopodia in breast cancer, suggesting

that dysregulation of phosphoinositides, as well as sterols and sphingolipids, contributes to cancer metastasis (116,117).

The implication of multiple different pathways in the response to the loss of Pdr5 and Yor1 indicates that these ABC transporters play an important role in controlling normal cell integrity. Work in mammalian cells provided the first evidence that ABC transporters were involved in movement of lipids from the cell (118). Given that mammalian homologues of Mss4 and Ypk1 exist, it is reasonable to suggest that similar response pathways are evolutionarily conserved. The work described here provides the important illumination of the functional connections between phospholipid asymmetry in the plasma membrane and the mechanisms that act to maintain cell integrity when these lipid gradients are disturbed.

REFERENCES

1. Ostrosky-Zeichner, L., Rex, J. H., Pappas, P. G., Hamill, R. J., Larsen, R. A., Horowitz, H. W., Powderly, W. G., Hyslop, N., Kauffman, C. A., Cleary, J., Mangino, J. E., and Lee, J. (2003) *Antimicrob Agents Chemother* **47**, 3149-3154

2. Klein, I., Sarkadi, B., and Varadi, A. (1999) *Biochim Biophys Acta* **1461**, 237-262

3. Moye-Rowley, W. S. (2003) *Prog Nucleic Acid Res Mol Biol* **73**, 251-279

4. Kihara, A., and Igarashi, Y. (2004) *Mol Biol Cell* **15**, 4949-4959

5. Zhang, X., Cui, Z., Miyakawa, T., and Moye-Rowley, W. S. (2001) *J Biol Chem* **276**, 8812-8819

6. Hinrichs, J. W., Klappe, K., and Kok, J. W. (2005) *J Membr Biol* **203**, 57-64

7. Leppert, G., McDevitt, R., Falco, S. C., Van Dyk, T. K., Ficke, M. B., and Golin, J. (1990) *Genetics* **125**, 13-20

8. Bissinger, P. H., and Kuchler, K. (1994) *J Biol Chem* **269**, 4180-4186

9. Hirata, D., Yano, K., Miyahara, K., and Miyakawa, T. (1994) *Curr Genet* **26**, 285-294

10. Kolaczkowski, M., van der Rest, M., Cybularz-Kolaczkowska, A., Soumillion, J. P., Konings, W. N., and Goffeau, A. (1996) *J Biol Chem* **271**, 31543-31548

11. Meyers, S., Schauer, W., Balzi, E., Wagner, M., Goffeau, A., and Golin, J. (1992) *Curr Genet* **21**, 431-436

12. Katzmann, D. J., Hallstrom, T. C., Voet, M., Wysock, W., Golin, J., Volckaert, G., and Moye-Rowley, W. S. (1995) *Mol Cell Biol* **15**, 6875-6883

13. Ogawa, A., Hashida-Okado, T., Endo, M., Yoshioka, H., Tsuruo, T., Takesako, K., and Kato, I. (1998) *Antimicrob Agents Chemother* **42**, 755-761

14. Decottignies, A., Grant, A. M., Nichols, J. W., de Wet, H., McIntosh, D. B., and Goffeau, A. (1998) *J Biol Chem* **273**, 12612-12622

15. Nagao, K., Kimura, Y., Mastuo, M., and Ueda, K. *FEBS Lett* **584**, 2717-2723

16. Roelants, F. M., Baltz, A. G., Trott, A. E., Fereres, S., and Thorner, J. *Proc Natl Acad Sci U S A* **107**, 34-39

17. Bagnat, M., Keranen, S., Shevchenko, A., and Simons, K. (2000) *Proc Natl Acad Sci U S A* **97**, 3254-3259

18. Souza, C. M., and Pichler, H. (2007) *Biochim Biophys Acta* **1771**, 442-454

19. Dickson, R. C. (2008) *J Lipid Res* **49**, 909-921

20. Nagiec, M. M., Baltisberger, J. A., Wells, G. B., Lester, R. L., and Dickson, R. C. (1994) *Proc Natl Acad Sci U S A* **91**, 7899-7902

21. Beeler, T., Bacikova, D., Gable, K., Hopkins, L., Johnson, C., Slife, H., and Dunn, T. (1998) *J Biol Chem* **273**, 30688-30694

22. Grilley, M. M., Stock, S. D., Dickson, R. C., Lester, R. L., and Takemoto, J. Y. (1998) *J Biol Chem* **273**, 11062-11068

23. Nagiec, M. M., Skrzypek, M., Nagiec, E. E., Lester, R. L., and Dickson, R. C. (1998) *J Biol Chem* **273**, 19437-19442

24. Oh, C. S., Toke, D. A., Mandala, S., and Martin, C. E. (1997) *J Biol Chem* **272**, 17376-17384

25. Saba, J. D., Nara, F., Bielawska, A., Garrett, S., and Hannun, Y. A. (1997) *J Biol Chem* **272**, 26087-26090

26. Nagiec, M. M., Nagiec, E. E., Baltisberger, J. A., Wells, G. B., Lester, R. L., and Dickson, R. C. (1997) *J Biol Chem* **272**, 9809-9817

27. Sato, K., Noda, Y., and Yoda, K. (2009) *Mol Biol Cell* **20**, 4444-4457

28. Beeler, T. J., Fu, D., Rivera, J., Monaghan, E., Gable, K., and Dunn, T. M. (1997) *Mol Gen Genet* **255**, 570-579

29. Uemura, S., Kihara, A., Iwaki, S., Inokuchi, J., and Igarashi, Y. (2007) *J Biol Chem* **282**, 8613-8621

30. Dickson, R. C., Nagiec, E. E., Wells, G. B., Nagiec, M. M., and Lester, R. L. (1997) *J Biol Chem* **272**, 29620-29625

31. Kihara, A., and Igarashi, Y. (2002) *J Biol Chem* **277**, 30048-30054

32. Chung, N., Mao, C., Heitman, J., Hannun, Y. A., and Obeid, L. M. (2001) *J Biol Chem* **276**, 35614-35621

33. Skrzypek, M. S., Nagiec, M. M., Lester, R. L., and Dickson, R. C. (1998) *J Biol Chem* **273**, 2829-2834

34. Schmidt, A., Hall, M. N., and Koller, A. (1994) *Mol Cell Biol* **14**, 6597-6606

35. Liu, K., Zhang, X., Sumanasekera, C., Lester, R. L., and Dickson, R. C. (2005) *Biochem Soc Trans* **33**, 1170-1173

36. deHart, A. K., Schnell, J. D., Allen, D. A., and Hicke, L. (2002) *J Cell Biol* **156**, 241-248

37. Schmelzle, T., Helliwell, S. B., and Hall, M. N. (2002) *Mol Cell Biol* **22**, 1329-1339

38. Tabuchi, M., Audhya, A., Parsons, A. B., Boone, C., and Emr, S. D. (2006) *Mol Cell Biol* **26**, 5861-5875

39. Audhya, A., Loewith, R., Parsons, A. B., Gao, L., Tabuchi, M., Zhou, H., Boone, C., Hall, M. N., and Emr, S. D. (2004) *EMBO J* **23**, 3747-3757

40. Desrivieres, S., Cooke, F. T., Parker, P. J., and Hall, M. N. (1998) *J Biol Chem* **273**, 15787-15793

41. He, B., Xi, F., Zhang, X., Zhang, J., and Guo, W. (2007) *EMBO J* **26**, 4053-4065

42. Santarius, M., Lee, C. H., and Anderson, R. A. (2006) *Biochem J* **398**, 1-13

43. Kobayashi, T., Takematsu, H., Yamaji, T., Hiramoto, S., and Kozutsumi, Y. (2005) *J Biol Chem* **280**, 18087-18094

44. Hallstrom, T. C., Lambert, L., Schorling, S., Balzi, E., Goffeau, A., and Moye-Rowley, W. S. (2001) *J Biol Chem* **276**, 23674-23680

45. Kolaczkowski, M., Kolaczkowska, A., Gaigg, B., Schneiter, R., and Moye-Rowley, W. S. (2004) *Eukaryot Cell* **3**, 880-892

46. Panwar, S. L., and Moye-Rowley, W. S. (2006) *J Biol Chem* **281**, 6376-6384

47. Cowart, L. A., and Obeid, L. M. (2007) *Biochim Biophys Acta* **1771**, 421-431

48. Dickson, R. C., Sumanasekera, C., and Lester, R. L. (2006) *Prog Lipid Res* **45**, 447-465

49. Rosenbaum, D. M., Rasmussen, S. G., and Kobilka, B. K. (2009) *Nature* **459**, 356-363

50. Welsch, C. A., Roth, L. W., Goetschy, J. F., and Movva, N. R. (2004) *J Biol Chem* **279**, 36720-36731

51. Ito, H., Fukuda, Y., Murata, K., and Kimura, A. (1983) *J Bacteriol* **153**, 163-168

52. Bligh, E. G., and Dyer, W. J. (1959) *Can J Biochem Physiol* **37**, 911-917

53. Merrill, A. H., Jr., Wang, E., Mullins, R. E., Jamison, W. C., Nimkar, S., and Liotta, D. C. (1988) *Anal Biochem* **171**, 373-381

54. Abe, F., and Horikoshi, K. (2000) *Mol Cell Biol* **20**, 8093-8102

55. Beck, T., Schmidt, A., and Hall, M. N. (1999) *J Cell Biol* **146**, 1227-1238

56. Khozoie, C., Pleass, R. J., and Avery, S. V. (2009) *J Biol Chem* **284**, 17968-17974

57. Hanson, P. K., Malone, L., Birchmore, J. L., and Nichols, J. W. (2003) *J Biol Chem* **278**, 36041-36050

58. Didion, T., Regenberg, B., Jorgensen, M. U., Kielland-Brandt, M. C., and Andersen, H. A. (1998) *Mol Microbiol* **27**, 643-650

59. Umebayashi, K., and Nakano, A. (2003) *J Cell Biol* **161**, 1117-1131

60. Vida, T. A., and Emr, S. D. (1995) *J Cell Biol* **128**, 779-792

61. Abe, F., and Iida, H. (2003) *Mol Cell Biol* **23**, 7566-7584

62. Helliwell, S. B., Losko, S., and Kaiser, C. A. (2001) *J Cell Biol* **153**, 649-662

63. DeWire, S. M., Ahn, S., Lefkowitz, R. J., and Shenoy, S. K. (2007) *Annu Rev Physiol* **69**, 483-510

64. Nikko, E., and Pelham, H. R. (2009) *Traffic* **10**, 1856-1867

65. Abe, F. (2007). in *International Congress Series*

66. Protchenko, O., Shakoury-Elizeh, M., Keane, P., Storey, J., Androphy, R., and Philpott, C. C. (2008) *Eukaryot Cell* **7**, 859-871

67. Soustre, I., Letourneux, Y., and Karst, F. (1996) *Curr Genet* **30**, 121-125

68. Manente, M., and Ghislain, M. (2009) *FEMS Yeast Res* **9**, 673-687

69. Le Crom, S., Devaux, F., Marc, P., Zhang, X., Moye-Rowley, W. S., and Jacq, C. (2002) *Mol Cell Biol* **22**, 2642-2649

70. Gilman, A. G. (1987) *Annu Rev Biochem* **56**, 615-649

71. Dohlman, H. G., and Thorner, J. W. (2001) *Annu Rev Biochem* **70**, 703-754

72. Gancedo, J. M. (2008) *FEMS Microbiol Rev* **32**, 673-704

73. Heenan, E. J., Vanhooke, J. L., Temple, B. R., Betts, L., Sondek, J. E., and Dohlman, H. G. (2009) *Biochemistry* **48**, 6390-6401

74. Slessareva, J. E., Routt, S. M., Temple, B., Bankaitis, V. A., and Dohlman, H. G. (2006) *Cell* **126**, 191-203

75. Leon, S., and Haguenauer-Tsapis, R. (2009) *Exp Cell Res* **315**, 1574-1583

76. Sun, Y., McGarrigle, D., and Huang, X. Y. (2007) *Mol Biosyst* **3**, 849-854

77. Barthet, G., Framery, B., Gaven, F., Pellissier, L., Reiter, E., Claeysen, S., Bockaert, J., and Dumuis, A. (2007) *Mol Biol Cell* **18**, 1979-1991

78. Labasque, M., Reiter, E., Becamel, C., Bockaert, J., and Marin, P. (2008) *Mol Biol Cell* **19**, 4640-4650

79. Lefkowitz, R. J., and Shenoy, S. K. (2005) *Science* **308**, 512-517

80. Heidler, S. A., and Radding, J. A. (1995) *Antimicrob Agents Chemother* **39**, 2765-2769

81. Hashida-Okado, T., Ogawa, A., Endo, M., Yasumoto, R., Takesako, K., and Kato, I. (1996) *Mol Gen Genet* **251**, 236-244

82. Smith, R. L., and Johnson, A. D. (2000) *Trends Biochem Sci* **25**, 325-330

83. Abeijon, C., Yanagisawa, K., Mandon, E. C., Hausler, A., Moremen, K., Hirschberg, C. B., and Robbins, P. W. (1993) *J Cell Biol* **122**, 307-323

84. Berninsone, P., Miret, J. J., and Hirschberg, C. B. (1994) *J Biol Chem* **269**, 207-211

85. Yakir-Tamang, L., and Gerst, J. E. (2009) *Mol Biol Cell* **20**, 3583-3597

86. Zhang, X., Orlando, K., He, B., Xi, F., Zhang, J., Zajac, A., and Guo, W. (2008) *J Cell Biol* **180**, 145-158

87. Gietz, R. D., and Woods, R. A. (2002) *Methods Enzymol* **350**, 87-96

88. Roelants, F. M., Torrance, P. D., Bezman, N., and Thorner, J. (2002) *Mol Biol Cell* **13**, 3005-3028

89. Levine, T. P., Wiggins, C. A., and Munro, S. (2000) *Mol Biol Cell* **11**, 2267-2281

90. Hashida-Okado, T., Yasumoto, R., Endo, M., Takesako, K., and Kato, I. (1998) *Curr Genet* **33**, 38-45

91. Maxfield, F. R., and Tabas, I. (2005) *Nature* **438**, 612-621

92. Malave, T. M., and Dent, S. Y. (2006) *Biochem Cell Biol* **84**, 437-443

93. Coffman, J. A., el Berry, H. M., and Cooper, T. G. (1994) *J Bacteriol* **176**, 7476-7483

94. Beck, T., and Hall, M. N. (1999) *Nature* **402**, 689-692

95. Blinder, D., Coschigano, P. W., and Magasanik, B. (1996) *J Bacteriol* **178**, 4734-4736

96. Crespo, J. L., and Hall, M. N. (2002) *Microbiol Mol Biol Rev* **66**, 579-591, table of contents

97. Gonzalez, M., Goddard, N., Hicks, C., Ovalle, R., Rauceo, J. M., Jue, C. K., and Lipke, P. N. *Yeast* **27**, 583-596

98. Fujita, M., Yoko, O. T., and Jigami, Y. (2006) *Mol Biol Cell* **17**, 834-850

99. Yoshida, S., Ohya, Y., Nakano, A., and Anraku, Y. (1994) *Mol Gen Genet* **242**, 631-640

100. Singer-Kruger, B., Nemoto, Y., Daniell, L., Ferro-Novick, S., and De Camilli, P. (1998) *J Cell Sci* **111 (Pt 22)**, 3347-3356

101. Stefan, C. J., Audhya, A., and Emr, S. D. (2002) *Mol Biol Cell* **13**, 542-557

102. Wiederkehr, A., Du, Y., Pypaert, M., Ferro-Novick, S., and Novick, P. (2003) *Mol Biol Cell* **14**, 4770-4782

103. Audhya, A., and Emr, S. D. (2002) *Dev Cell* **2**, 593-605

104. Endo, M., Takesako, K., Kato, I., and Yamaguchi, H. (1997) *Antimicrob Agents Chemother* **41**, 672-676

105. Pittet, M., Uldry, D., Aebi, M., and Conzelmann, A. (2006) *Glycobiology* **16**, 155-164

106. Levin, D. E. (2005) *Microbiol Mol Biol Rev* **69**, 262-291

107. De Nobel, J. G., Klis, F. M., Ram, A., Van Unen, H., Priem, J., Munnik, T., and Van Den Ende, H. (1991) *Yeast* **7**, 589-598

108. Ellerton SS, L. A., Gonzalez M, Jue, CK. (2008) *Journal of Biological Science* **8**, 1211-1215

109. Roelants, F. M., Torrance, P. D., and Thorner, J. (2004) *Microbiology* **150**, 3289-3304

110. Shimobayashi, M., Takematsu, H., Eiho, K., Yamane, Y., and Kozutsumi, Y. *J Biol Chem*

111. Lin, F. T., Krueger, K. M., Kendall, H. E., Daaka, Y., Fredericks, Z. L., Pitcher, J. A., and Lefkowitz, R. J. (1997) *J Biol Chem* **272**, 31051-31057

112. Fujita, M., and Jigami, Y. (2008) *Biochim Biophys Acta* **1780**, 410-420

113. Vossen, J. H., Muller, W. H., Lipke, P. N., and Klis, F. M. (1997) *J Bacteriol* **179**, 2202-2209

114. Singhal, R. L., Prajda, N., Yeh, Y. A., and Weber, G. (1994) *Cancer Res* **54**, 5574-5578

115. Tessier, M., and Woodgett, J. R. (2006) *J Cell Biochem* **98**, 1391-1407

116. Yamaguchi, H., Takeo, Y., Yoshida, S., Kouchi, Z., Nakamura, Y., and Fukami, K. (2009) *Cancer Res* **69**, 8594-8602

117. Yamaguchi, H., Yoshida, S., Muroi, E., Kawamura, M., Kouchi, Z., Nakamura, Y., Sakai, R., and Fukami, K. (2010) *Cancer Sci* **101**, 1632-1638

118. Dekkers, D. W., Comfurius, P., Schroit, A. J., Bevers, E. M., and Zwaal, R. F. (1998) *Biochemistry* **37**, 14833-14837